Republic of Iraq

Ministry of Higher Education and Scientific Research

University of Misan/Collage of Engineering

Department of Civil Engineering

NONLINEAR ANALYSIS OF SOLID AND HOLLOW SLENDER RC COLUMNS STRENGTHENED BY SFR SUBJECTED TO CONCENTRIC AND ECCENTRIC LOADS

By

Wameedh Issa Braidi

B.Sc. civil engineering, 2009

A THESIS

Submitted in Partial Fulfillment of the

Requirements for the Degree of

Master of Science/Master of Structural Engineering

(in Civil Engineering)

Advisor: Professor Dr. Mohammed Salih Abed Ali

بسم الله الرحمن الرحيم

وَوَصَّيْنَا الْإِنْسَانَ بِوَالِدَيْهِ إِحْسَانًا حَمَلَتْهُ أُمُّهُ كُرْهًا وَوَضَعَتْهُ كُرْهًا وَحَمْلُهُ وَفِصَالُهُ ثَلَاثُونَ شَهْرًا حَتَّى إِذَا بَلَغَ أَشُدَّهُ وَبَلَغَ أَرْبَعِينَ سَنَةً قَالَ رَبِّ أَوْزِعْنِي أَنْ أَشْكُرَ نِعْمَتَكَ الَّتِي أَنْعَمْتَ عَلَيَّ وَعَلَى وَالِدَيَّ وَأَنْ أَعْمَلَ صَالِحًا تَرْضَاهُ وَأَصْلِحْ لِي فِي ذُرِّيَّتِي إِنِّي تُبْتُ إِلَيْكَ وَإِنِّي مِنَ الْمُسْلِمِينَ

صدق الله العلي العظيم

الاحقاف 15

The University of Misan

October/2022

ABSTRACT

Column is one of the fundamental structural components in a building. The usage of slender columns is becoming more and more prevalent as a result of increased interest in space utilization. The objective of this study is on the numerical analysis of solid and hollow slender reinforced concrete columns behavior under various parameters. Solid columns with dimension of (120×60×2000) mm concentrically loaded and strengthened using SFR at the middle of different columns length L, L/2, and L/3 in addition to the reference strengthened column, while hollow columns with dimension of (140×80×2000) mm concentrically and eccentrically loaded with different opening shapes.

This work is done on nine tested specimens (four solid, five hollow) columns using ABAQUS 2020 software as a 3D finite element analysis procedure. The results collected clearly show that the slender column simulated using ABAQUS program without selecting a specify imperfection value to the modeling data will show more load resistance than the experimental test result so it's considered to be perfect, and this does not exist in real life. According to Eurocode this value depends on columns length, constant length means constant factor, but this work showed that the use of SFR will change the value of this factor despite of the length of columns are constant. Also, from these results an equation could be suggested to represents the relationship

between imperfection factor and the change in SFR distribution through the column length. Some of important parameters, such as the slenderness ratio, concrete compressive strength, section shapes, load eccentricity, and SFR strengthening distribution, are assessed using the validated models.

From the obtained results of solid column, it is evident that the decreasing columns length by 25% will decrease slenderness ratio and led to increase the ultimate load by 7%, in the other hand the increasing in columns length by 25% and 50% will increase the slenderness ratio and led to decrease the ultimate load by 5% and 7% respectively. When the concrete compressive strength of the column decreased to 25MPa the ultimate load will decreased by 12%, in the other hand when the concrete compressive strength increased to 32MPa that will increase the ultimate load by 5%, also when the concrete compressive strength increased to 36MPa that will increase the ultimate load by 26%. Square and circular columns buckling strength increased by 5% and 2% respectively, while elliptical column buckling strength decreased by 6%. Increasing solid column load eccentricity to 20mm, 30mm, and 40mm decreasing the ultimate load by 69%, 82%, and 89% respectively.

In the other hand the obtained results of hollow column showed that decreasing columns length by 25% will decrease slenderness ratio and led to increase the ultimate load by 9%, while the increasing in columns length by 25% and 50%

will increase the slenderness ratio and led to decrease the ultimate load by 6% and 10% respectively. When the concrete compressive strength of the column decreased to 25MPa the ultimate load will decreased by 21%, while when the concrete compressive strength increased to 40MPa and 45MPa that will increase the ultimate load by 9% and 20% respectively. Square and circular columns buckling strength increased by 12%, while elliptical column buckling strength decreased by 1%. Using the SFR to strengthening the whole, half, or third columns length increases the ultimate load by 20%, 30%, and 12%.

SUPERVISOR CERTIFICATION

I certify that the preparation of this thesis entitled "**Nonlinear Analysis of Solid and hollow Slender RC Columns Strengthened by SFR Subjected to Concentric and Eccentric loads**" was presented by "**Wameedh Issa Braidi**", and prepared under my supervision at The University of Misan, Department of Civil Engineering, College of Engineering, as a partial fulfillment of the requirements for the degree of Master of Science in Civil Engineering (Structural Engineering).

Signature:

Prof. Dr. Mohammed Salih Abd Ali

Date:

In view of the available recommendations, I forward this thesis for discussion by the examining committee.

Signature:

Assist. Prof. Dr. Samir M Chassib

(Head of Civil Eng. Department)

Date:

EXAMINING COMMITTTEE'S REPORT

We certify that we, the examining committee, have read the thesis titled **(Nonlinear Analysis of Solid and hollow Slender RC Columns Strengthened by SFR Subjected to Concentric and Eccentric Loads)** which is being submitted by (**Wameedh Issa Braidi**), and examined the student in its content and in what is concerned with it, and that in our opinion, it meets the standard of a thesis for the degree of Master of Science in Civil Engineering (Structures).

Signature:
Name:
(Supervisor)
Date: / /2022

Signature:
Name:
(Co-supervisor)
Date: / /2022

Signature:
Name:
(Chairman)
Date: / /2022

Signature:
Name:
(Member)
Date: / /2022

Signature:
Name:
(Member)
Date: / /2022

Approval of the College of Engineering:

Signature:
Name:
Dean, College of Engineering
Date: / /2022

DEDICATION

To all my dear family and friends in my heart for their support, standing by my side and encouraging me. I present my effort to them with all my respect and appreciation.

ACKNOWLEDGEMENTS

Praise and thanks to my GOD for enabling me to achieve this study.

Cordial thanks to my supervisor Prof. Dr. Mohammed Salih Abd Ali for his continued valuable suggestions and guidance throughout preparation of this work.

Thanks, and gratitude to Prof. Dr. Abbas Oda Dawood Dean of the college of engineering, Assist Prof. Dr. Samir Mohamed Chassib, the Head of Civil Engineering Department.

Deep thanks to my friends, for their interest and support during this study.

Great thanks to my family especially my wife for their support and prayers.

TABLE OF CONTENTS

LIST OF TABLES

LIST OF FIGURES

LIST OF SYMBOLES

A Sectional are

b Width of a column (dimension of cross-section perpendicular to h)

e Load eccentricity

e_o Initial eccentricity (imperfection)

f′c Cylinder concrete compressive strength

f_{b0}/f_{c0} Strength ratio in the biaxial state to uniaxial strength state

f_{cu} Cube compressive strength

h Depth of cross-section measured in the plane under consideration

I Moment of inertia of the section

K Effective length factor

l_{ex} Effective height in respect of the major axis

l_{ey} Effective height in respect of the minor axis

l_o Effective height

l_u Unsupported column length

m Number of members to be restrained

r Radius of gyration

μ Viscosity

λ Slenderness ratio according to Eurocode 2

LIST OF ABBREVIATIONS

ASCE	American Society of Civil Engineers
ACI	American concrete institute
BS	British Standards Institution
CDP	Concrete damaged plasticity
CFRP	Carbon fiber reinforced polymers
EC	Euro code Institution
FEA	Finite element analysis
FEM	Finite element method
HC	Hollow column
HP	Hollow parametric column
NSM	Near surface mounted
$P_{Ana.}$	Finite element analysis ultimate load
$P_{Exp.}$	Experimental ultimate load
RC	Reinforced concrete
SC	Solid column
SFR	Steel fiber reinforcement
SFRC	Steel fiber reinforced concrete
SIFCON	Slurry infiltrated fiber concrete
SP	Solid parametric column
SSRC	Special shaped reinforced concrete

CHAPTER ONE: INTRODUCTION

1.1 General

Structural parts that carry loads under compression are referred to as columns, they usually carry loads in compression and bending moments along one or both of the cross sections' axes. There are three categories of columns: short, intermediate, and long (slender) columns. Short columns are those that have large cross sections in comparison to their lengths. Short column is one whose ultimate load at a particular eccentricity is determined only by the materials' strength and cross-sectional dimensions. Intermediate column is one that some of the fibers will reach the yield stress and some will note, also the column is failed by both yielding and buckling, and its behavior is said to be inelastic. Slender columns are those that have small cross sections in comparison to their lengths. Slender column is one in which the ultimate load is determined not only by the strength of the materials and the dimensions of the cross section but also by its slenderness, which produces additional bending moment due to lateral deformations. In general, slender columns have lower strength than short columns, and increasing the length reduces the

strength for a constant cross section [1]. Slender column usually fails elastically. Figure 1-1 shows short and slender columns.

Figure 1-1 Classification of Columns[2, 3].

Slender columns are preferred over short columns for a variety of architectural and structural reasons When the cost of concrete excessive, or the weight of concrete members must be maintained to a minimum, hollow reinforced concrete columns may be the most cost-effective option. Also, transverse openings and longitudinal holes are frequently included to give access for utilities like as plumbing and electrical wiring [4]. Furthermore, slender columns are used especially in high-rise

buildings, the ongoing need to enhance materials and lower the dimensions and sizes necessary in structural systems became critical [5]. Figure 1-2 illustrates some of precast hollow columns.

Figure 1-2 Precast hollow columns[6].

1.2 Slenderness Ratio

Buckling, elastic shortening, and secondary moment related to lateral deflection are expected to have minor effect on the ultimate strength of short columns in analysis and design; consequently, these parameters will not be considered in the design. When the column is slender, however, these parameters must be taken into account.

The extra length reduces column strength, which varies depending on the column effective height, section width, slenderness ratio, and column end conditions. The slenderness ratio of the reinforced concrete column is significant in determining its strength and failure mode. The slenderness ratio is the ratio of the column height, l, to the radius of gyration, r, where $r = \sqrt{\frac{I}{A}}$, I being the moment of inertia of the section and A the sectional area [7]. Table 1-1 summarizes the limitations of the slenderness ratio specified by different codes [8], [9], [10].

Table 1-1 Lower Slenderness Ratio According to Different Codes.

Code	ACI 318-2014 Section 6.2.5 $\frac{Kl_u}{r}$		BS 8110 Part 1, Section 3.8.1.3 $\frac{l_{ex}}{h}$ & $\frac{l_{ey}}{b}$		EC2 Part1, Section 5.8.3.1 $\frac{l_o}{r}$
Frame system	Braced	Unbraced	Braced	Unbraced	Braced & unbraced
Slenderness ratio	40	22	15	10	$\lambda = \frac{20.A.B.C}{\sqrt{n}}$ (Refer code for A,B,C and n)

British and American standards for column classification displayed a limit that was somewhat resemblant. However, classification for edge columns based on EC 2 has differed somewhat from that established using BS 8110 and ACI 318. In fact, for edge columns in braced frames with little axial compression, the variation is considerable[11].

1.3 Types of Columns

Depending upon several conditions, there are different column types used in structures, based on shape, type of reinforcement and type of loading. Short, intermediate, and slender column could be one or more of the flowing types.

1.3.1 Column Cross-section

In most buildings, square or rectangular columns are used in the construction of buildings as shown in Figure 1-3. Because to the flexibility of shuttering and reinforcement placement, these types of columns are both cost-effective and easy to constructs.

Figure 1-3 Square and Rectangular Column[12].

For aesthetic reasons, circular columns are commonly used in piling and construction elevation as shown in Figure 1-4. Due to their high deflection resistance, circular columns are also used as bridge pillars.

Figure 1-4 Circular Columns[13].

It is common for two walls to be crossed, forming T shapes, L shapes, or Cross shapes at any point or at the building's corners. Specially shaped columns in a room eliminate noticeable corners, allowing for more usable floor space [14]. Ductility, deformation capacity, and energy dissipation capacity of the specially shaped column with appropriate design are good. Structural safety and an affordable construction cost are the realistic goals of structural design. To accomplish this, a

specially shaped column optimization design should be carried out based on the overall structural design [15]. Figure 1-5 shows the specially shaped columns.

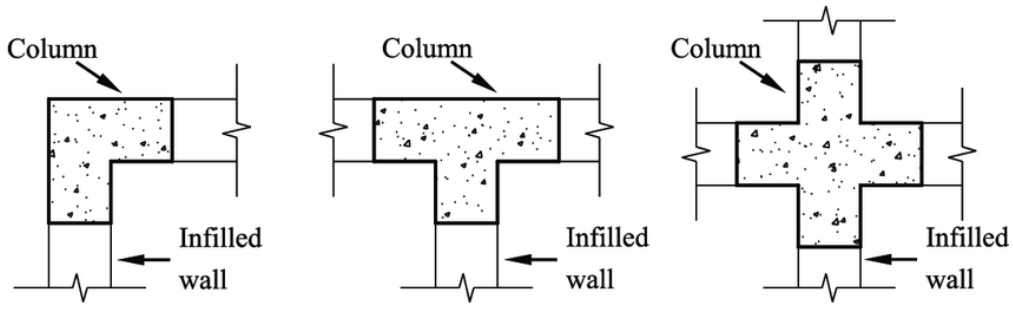

Figure 1-5 L- Shape, T- Shape, and Cross - Shape Columns[16].

In addition to the previous shapes of column, there is also elliptical, hexagonal, octagonal and Y shape columns.

1.3.2 Type of Reinforcement

Reinforced concrete columns normally contain longitudinal steel bars and are designed by the type of lateral bracing provided for those bars. The bars in tied columns are braced or tied at intervals by closed loops known as ties, Figure 1-6. The bars of spiral columns are wrapped in a tightly spaced helix or spiral of small diameter wire or rod. A steel or cast-iron structural element is encased in concrete and reinforced with both spiral and longitudinal reinforcement in composite columns. Concrete-filled steel pipe columns are also used. Tied and spiral are the most common forms [17].

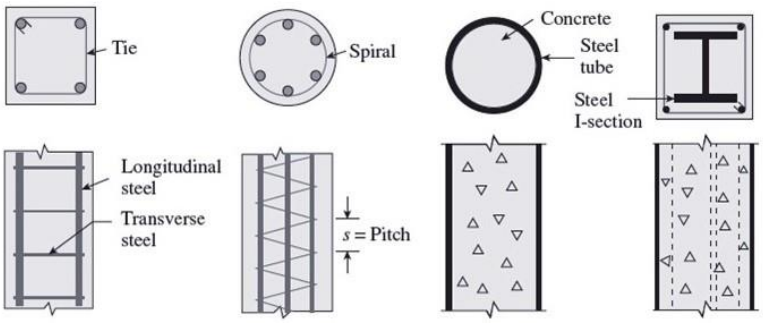

Figure 1-6 Concrete Column Types of Reinforcement[18].

1.3.3 Type of loading

The type of loading on columns can be categorized as follows [19], Figure 1-7:

1- Axially loaded columns: Loads are considered to act at the center of the column section in axially loaded columns.

2- Uniaxially eccentrically loaded columns: Loads act at a distance e from the center of the column section in eccentrically loaded columns. The distance (e) could be on the (x) or (y) axis, resulting in moments on either axis.

3- Biaxially eccentrically loaded columns: Biaxially loaded columns are those in which the load is applied anywhere on the column section, creating moments in both the x and y axes at the same time.

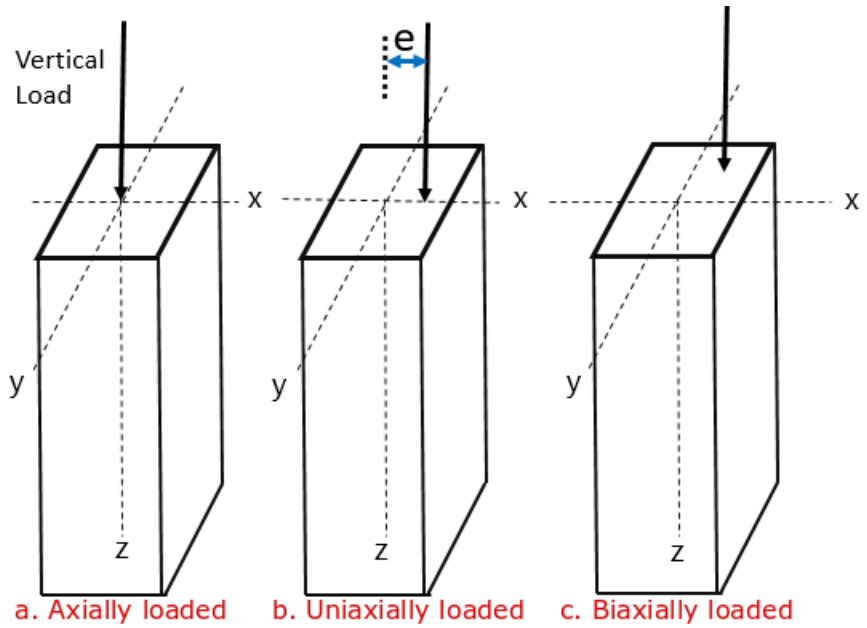

Figure 1-7 Concrete Column Types of Loading[20].

1.4 Column Failure Patterns

Short column failure patterns differ significantly from slender column failure patterns. The concrete and steel in short columns will be stressed when they are axially loaded. The yield stress will be reached by the concrete and steel, and failure will begin without any further deformation. The material, not the entire column, fails in this form of failure. It's also called material failure pattern. In the other hand, when the slender column axially loaded, the load-carrying capacity of the column decreases very much. Even under low loads, the columns become unstable and buckle to the side. This means that even minor loads cause the concrete and steel to achieve their yield stress and begin to fail due to lateral buckling. This pattern also

called stability failure. In addition to the previous two types of columns failure, shear failure pattern may be occurred when a force that tends to cause a sliding failure on a material in a plane parallel to the force's direction [21], [22], [23], [24]. Figure 1-8 Column Failure Patterns[25-27]. shows different types of column failure patterns.

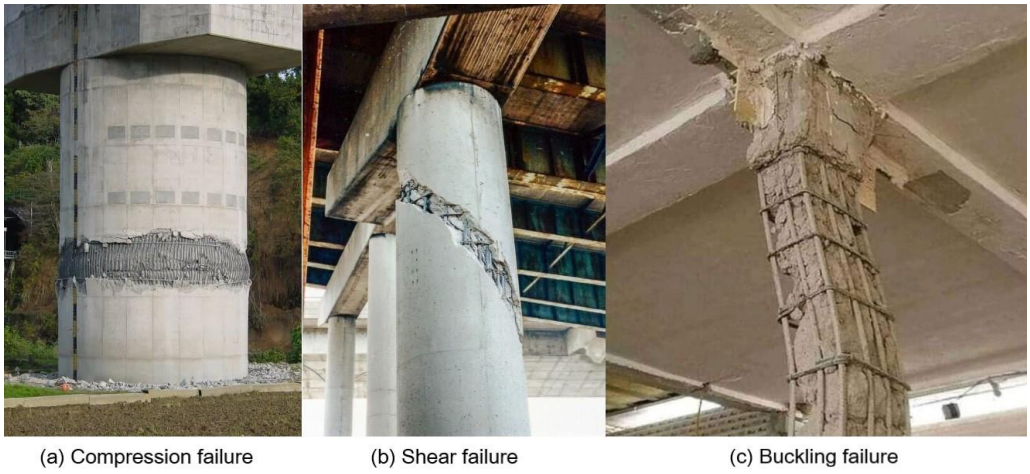

Figure 1-8 Column Failure Patterns[25-27].

1.5 Steel Fiber Reinforced Concrete Columns (SFRCC)

Concrete is a brittle material with a low tensile strength. When short steel fibers are combined with hydrated cement paste in concrete, they occupy the interparticle gaps that exist around coarse aggregates. Steel fibers improve the toughness, ductility, and energy absorption capacity of concrete under impact. The addition of fibers considerably increases the concrete strength's quasi-brittle properties and tensile straining performance. Nonetheless, the fiber inclusion in the concrete mix increases the concrete's tension straining capability several times over its crushing strain. Steel

fibers are made in a variety of ways and come in a variety of shapes and sizes. They may be deformed or straight. The majority, on the other hand, have a circular cross-section with diameters ranging from 0.4 to 1.3mm and lengths ranging from 25 to 60mm [28], [29], [30]. Fig. 1.9 shows the steel fiber reinforced concrete column (SFRCC).

Figure 1-9 Steel Fiber Reinforced Concrete Column (SFRCC).

1.6 Nonlinearity

A nonlinear structural problem is one in which the structure's stiffness changes as it deforms. All physical structures exhibit nonlinear behavior. Linear analysis is a convenient approximation that is often adequate for design purposes. The possible sources of nonlinearity in nonlinear stress analysis problems listed below [31]:

1. Material nonlinearity: Since the flow stress (stress versus strain curve) in the plastic domain is fundamentally nonlinear, material nonlinearity is related to the inelastic behavior of deformation beyond the yield stress of the material. Material nonlinearity involves the nonlinear behavior of a material based on a current deformation, deformation history, rate of deformation, temperature, pressure, and so on. Examples of nonlinear material models are large strain (visco) elasto-plasticity and hyperelasticity (rubber and plastic materials) as shown in Figure 1-10.

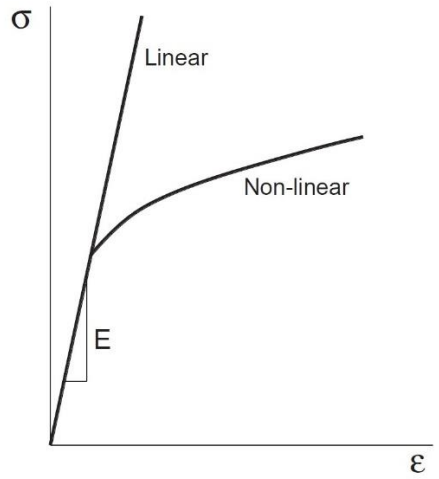

Figure 1-10 Material Nonlinearity [32].

2. Geometric nonlinearity: Due to deformation, the final (current) geometry differs from the initial (initial) geometry, which leads to geometric nonlinearity. Only stretching contributes to the buildup of strain and changes in stress state during the deformation of a vector (or line) embedded in the

material, as opposed to rigid-body rotation and translation. Rotation and translation of rigid bodies have no impact on shape (or size) changes, strain accumulation, or alterations in the stress state. When adjacent vectors (or lines) contained in the material are deformed, shearing occurs as shown in Figure 1-11.

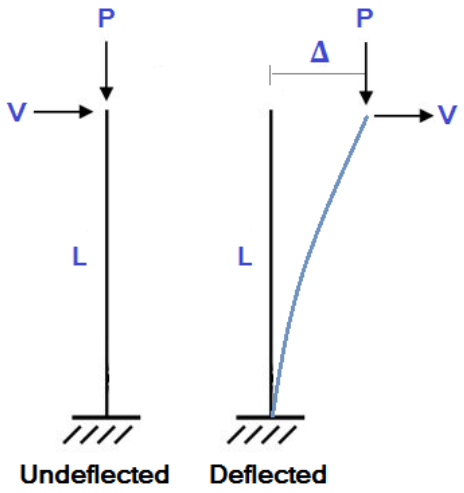

Figure 1-11 Cantilever column, undeflected and deflected shape [33].

3. Boundary nonlinearity: The interaction between workpieces and tools or between various workpieces, such as contact with friction at the material-tool interfaces, is a source of nonlinearity resulting from changes in static and kinematic boundary conditions [32]. The kinematic degrees-of-freedom of a model can be constrained by imposing restrictions on its movement as shown in Figure 1-12.

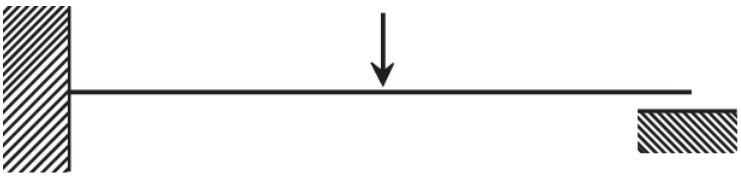

Figure 1-12 Cantilever Beam Hitting a Stop [34]

1.7 Nonlinear Finite Element Analysis.

Large deformation and material behavior are the two sources of nonlinearity. When a material's stress-strain curve isn't linear, it's called material nonlinearity, plasticity and damage in steel and concrete, as well as nonlinear elasticity in soils and concrete under certain conditions, are examples. Because the strain cannot be represented as a linear function of the gradient of the displacement, as is anticipated in linear elasticity, geometric nonlinearity arises [35]. Also, if the boundary conditions vary through the analysis, it’s called boundary nonlinearity. An analyst must be familiar with a variety of solution strategies as well as the physical problem. A single strategy will not always work well, and in certain cases, it may not work at all. It may take numerous attempts to achieve an acceptable result. Nonetheless, nonlinear analysis is being used more frequently than in the past. This is due in part to the fact that computing costs have decreased and capable software has become available [36]. As example ABAQUS software which used in this research.

1.8 Objective of Research

The aim and objective of this study was to validate a nonlinear 3D finite element model based on experimental reference columns tests conducted at the Amara Technical Institute, which used mean material attributes to analyze the behavior of slender RC columns affected by buckling. These goals are summarized below:

1. Investigating numerically the behavior of solid and hollow slender RC columns subjected to concentric or eccentric loads using finite element software ABAQUS by comparing the analysis outputs with experimental results.
2. The effect of the imperfection value of the columns on the finite element model response was studied.
3. Developing a second order equation represents the relationship between imperfection factor and SFR distribution through the RC slender column.
4. Studying the influence of different parameters, like slenderness ratio, column section shape, concrete strength, etc. on the ultimate load.

1.9 Thesis Layouts

The present thesis content is divided in to five chapters, as follows:

1. Chapter one (Introduction): This chapter presents an overview of slender columns and explains second- order effects, nonlinearity, buckling and imperfection.

2. Chapter two (Literature Review): This chapter literature reviews and the previous studies and present the experimental benchmark researches for this work.

3. Chapter three (Finite Element Modeling): Presents the main focus of this research which was finite element modeling, and the setting up of model's geometry, materials properties, boundary conditions and meshing according to the finite element theory.

4. Chapter four (Numerical Analysis and Results): This chapter illustrates the finite element analyses and their discussions. In addition, a parametric study is carried out to investigate the impact of various parameters.

5. Chapter five (Conclusions and Recommendations): Includes the conclusions and recommendations for future research.

CHAPTER TWO: LITERATURE REVIEW

2.1 General

Relatively slender columns have recently become popular in many building constructions, either throughout the structure or in specific areas, such as the frontispiece of buildings and the inside of corridors, due to their architectural style and efficiency in the use of space.

This chapter presents a brief review of the previous researches related to this study for both solid and hollow reinforced concrete column, also display the adopted reference studies for this work.

2.2 Reinforced Concrete Columns

2.2.1 Solid Columns

[37] studied a nonlinear finite element analysis using ABAQUS for an axial loaded slender reinforced concrete column (1300x150x150) mm subjected to biaxial load that took into account second-order effects. The difference was between experimental and numerical results was 21-34%, which was significant. Conclusions based on the results of parametric studies found that the concrete column with a higher compressive strength, a smaller load eccentricity, and a larger cross-section

had a higher maximum load, and with higher slenderness, lower elasticity and fracture energy, and lower tensile strength had a smaller peak load as shown in Figure 2-1.

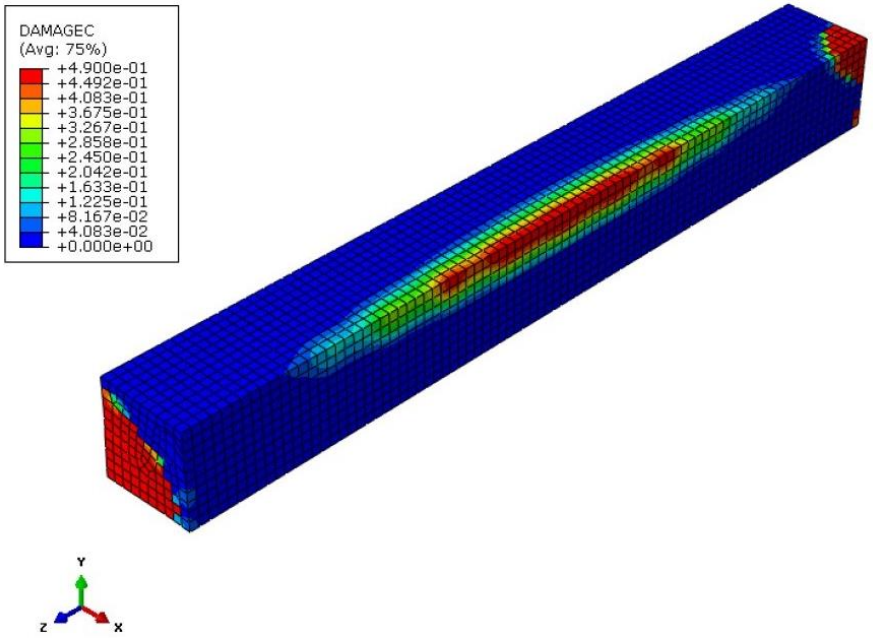

Figure 2-1 Crack Pattern of The FE Model by [37].

[38] investigated the behavior of 10-slender reinforced concrete columns strengthened with carbon fiber-reinforced polymers (CFRPs) subjected to eccentric loads using ANSYS. Several characteristics, including three distinct ways to improve axial and flexural rigidity, are explored. The first method is to use CFRP sheet wrapping columns; the second method is to use CFRP sheets in the longitudinal direction of columns; and the third method is to use a new retrofitting method of near surface mounted (NSM) CFRP strips. Ten full-scale specimens with

rectangular cross sections (210 x 150 mm) were subjected to eccentric compressive force until they failed. All specimens had a total length of 3000 mm, with different slender ratios of 73, 60, and 50, and characteristic strengths of 25, 35, and 45 MPa, respectively.

The conclusions of this investigation were that the ultimate loads of specimens increased by 111% and 113% when longitudinal direction CFRP sheets and NSM-CFRP strips was used instead of control specimens. While, the maximum deflection is increased by 105 and 132% when transverse direction CFRP sheets were combined with longitudinal direction NSM-CFRP strips. Also, the use of longitudinal NSM-CFRP strips was more effective in preventing CFRP strip debonding in compression and ensuring the epoxy adhesive's stability.

[39] discussed the behavior of slender concrete filled steel tube column subjected to eccentric loading using finite element analysis. Finite element package ABAQUS 6.13-1 is used to analyze the load carrying capacity of the composite columns. A total of 144 square concrete filled steel tube composite columns with large slenderness ratios (L/D>15, 27.41-57.92) were investigated. The results revealed that a composite column with a smaller eccentricity, a big cross-sectional area, and a large steel tube thickness may supported a larger maximum load. The load carrying capacity decreased as eccentricity increased to 157 mm at 32.71%. While length

increased (from 4.5 to 9m) the mid height displacement increased from 0 to 48% as shown in Figure 2-2.

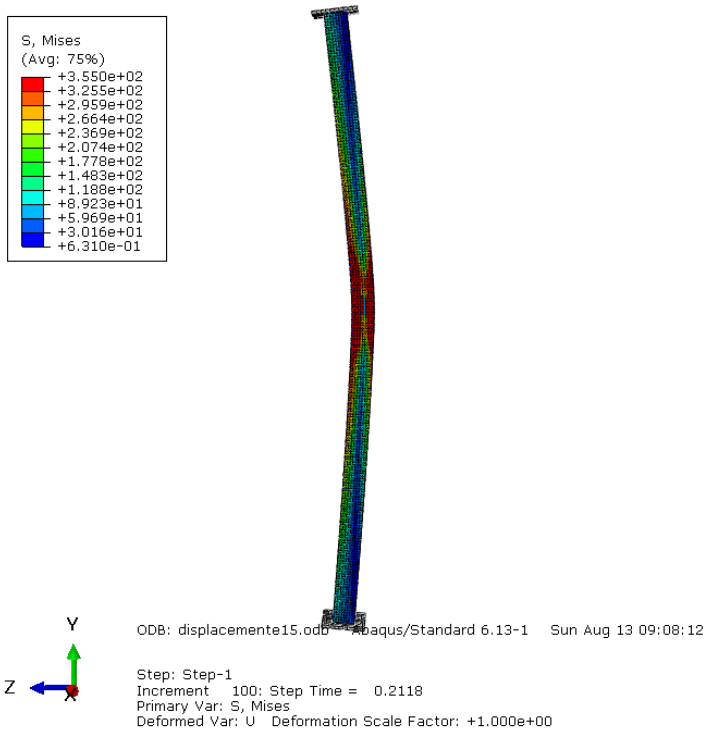

Figure 2-2 Stress Components and Invariants by [39].

[40] demonstrated the structural performance of special shaped reinforced concrete (SSRC) columns. Using experimental and numerical methods (+ shaped, T shaped and L shaped) columns were studied. The research is based on nine RC specimens that were tested to failure, also eighteen FE models that were examined using ABAQUS. When compared to equivalent square-shaped columns, the usage of SSRC columns increased strength by about 12% and reduced deformations by 40%. When special shaped reinforced concrete columns are compared with the equivalent

square-shaped columns, the results showed that they perform well structurally as shown in Figure 2-3.

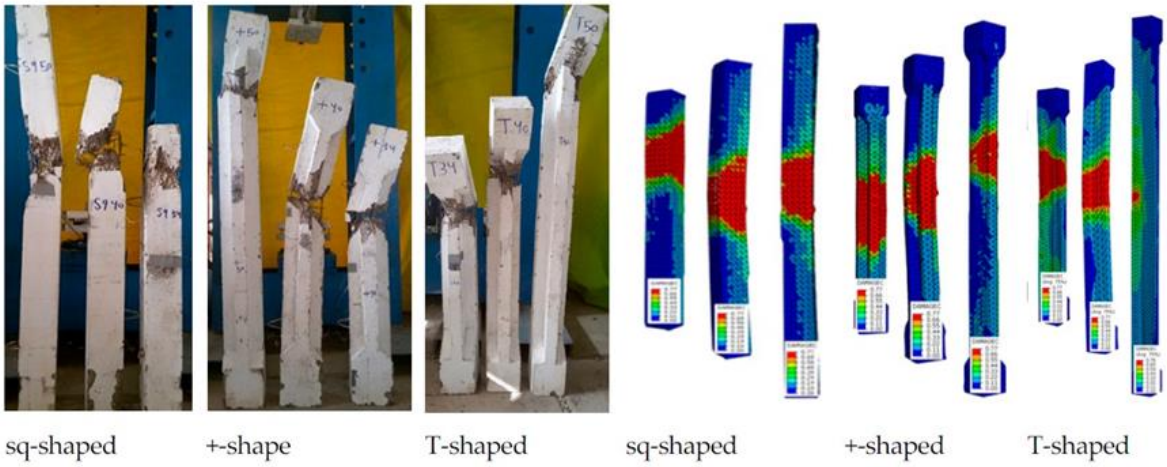

Figure 2-3 Results of the Experimental Test and Finite Element Analysis by [40].

[41] studied the load capacity and failure modes of thin-walled steel tubular slender columns filled with concrete under axial and eccentric loads. For the slender columns, various concrete compressive strengths and length/diameter (width) ratios are used. ABAQUS, a finite element program, is used to model and analyze the columns. The load capacity of the slender columns was found to be reduced when the load eccentricity was increased to 50 mm by (40-56%). The circular columns outperformed their square and rectangular counterparts in terms of performance. The confinement effect of the steel tube on the concrete core was increased as the steel tube become thicker, resulting in a higher load capacity of the slender columns. The

axially loaded square and rectangular slender columns also buckled more than their axially loaded circular counterparts.

[42] investigated numerically the jacketing method of slender reinforced concrete column. The experimental testing focused on 8 columns with a cross section of 0.25 x 0.37 m and height of 2.50 m. ABAQUS software was used to carry out the simulation as shown in Figure 2-4.

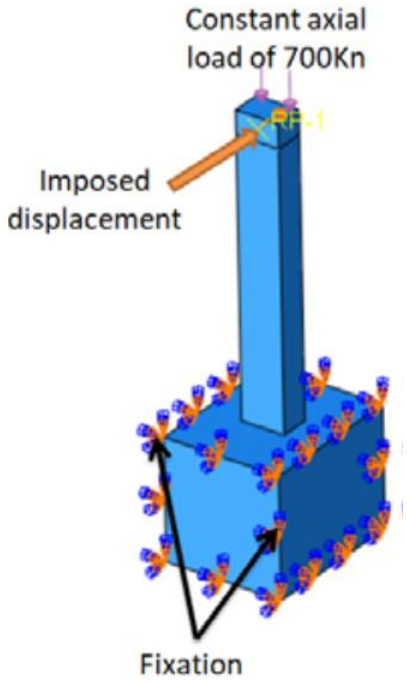

Figure 2-4 Loading and Boundary Conditions by [42]

Five models were tested in this study, first unjacketed model was the reference, second model was jacketed with perfect contact and the other three models used a friction coefficient of 0.1, 0.3 and 0.5. In comparison between the unjacketed model and the models with friction interface, it was found that the jacketed model with

perfect contact had the best column performance by 63% of ultimate load. In the other hand the comparison between the unjacketed model and the friction models, it was found that the ultimate load for the friction models increased by 35%, also the model with perfect contact had an ultimate load by 21% in comparison to the friction models. It's worth noting that the friction models produced similar results.

[43] presents the using a layer of the fiber concrete for a slender columns' strengthening. Based on the experiments, the basic dimensions of the column were determined to be 160 mm 160 mm and a height of 2500 mm, the eccentricity was determined to be equal to e = 100 mm. The 3D models were built in the nonlinear application ATENA 3D to check the samples from the experimental program. It was found that the strengthening column with steel fiber carried out 258.19% more than the unreinforced column, while the strengthening column by reinforcement concrete caried out an average of 144.71% compared to the steel fiber reinforced concrete column.

[44] investigated the strengthened column subjected to axial force using steel-fiber-reinforced (SFR) and carbon fiber-reinforced polymer (CFRP) on a portion or the entire length of the column to determine the effective length, which is responsible for increasing the column's ability to resist buckling. Seven samples were made as

slender reinforced columns with cross-sections of 120 mm x 60 mm and a length of 2000 mm as shown in Figure 2-5.

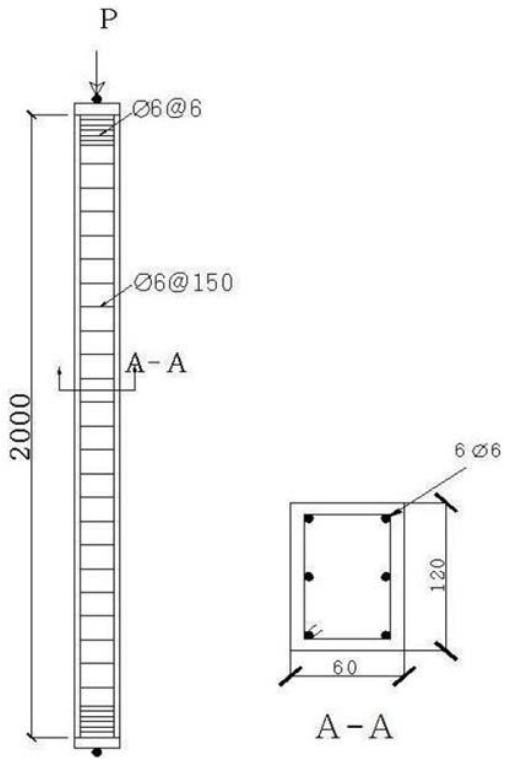

Figure 2-5 Geometry of Samples by [44]

It was discovered that strengthening the middle half of the column length with SFR resulted in an ultimate load that was comparable to strengthening the entire column with the same material. In addition, compared to the non-strengthened column, the SFR-enhanced column raised its ultimate load by 42.6%, 42.1%, and 33.3% for strengthened lengths of dimensions L, L/2, and L/3, respectively. For strengthened lengths of L and L/2, respectively, the increase in ultimate load that could be handled by the column strengthened by CFRP was 53.0% and 33.8%. For slender concrete

columns, an interaction diagram was used as a theoretical study. The interaction diagram for the CFRP-strengthened column was larger than the interaction diagram for the SFR-strengthened column, and which was larger than the non-strengthened column as shown in Figure 2-6.

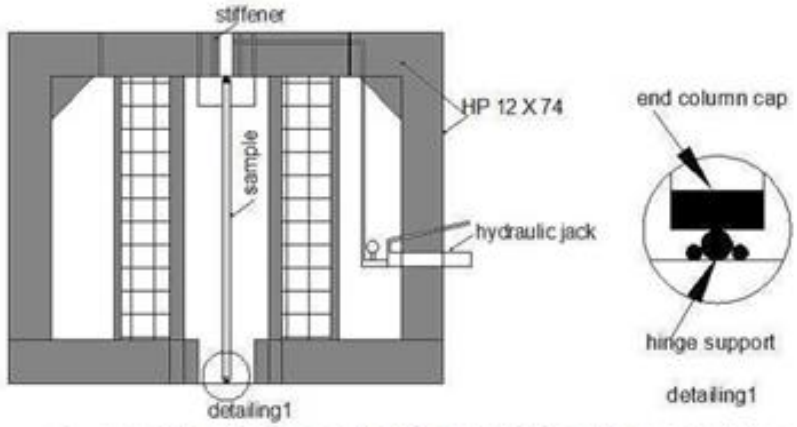

a. Loading frame detailing the hinged connection.

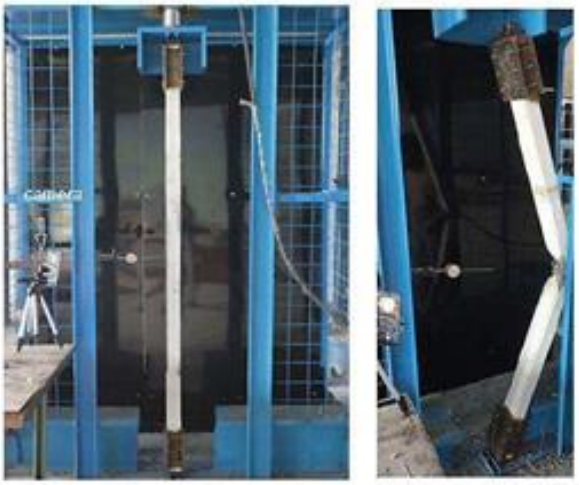

b. Sample in device before and after failure.

Figure 2-6 Experimental Test Details by [44]

It is important to be notice that this study is the first experimental reference study for the present thesis.

2.2.2 Hollow Columns

[45] investigated the behavior of slender RC columns with longitudinal opening subjected to axial compression load and uniaxial bending. The specimens of the research included the analysis of eight slender columns with dimensions of (150x150x1300 mm). To simulate the behavior of reinforced concrete slender columns with longitudinal holes, a nonlinear finite element analysis was performed using the ANSYS as shown in Figure 2-7.

Figure 2-7 Modeling and Meshing of the Analyzed Columns by [45].

Two parameters are considered (longitudinal steel ratio of the column and grade of steel (fy)). The results revealed that the selected four values of steel ratios (1.6%,2.3%,3.2% and 4.2%) led to increase the ultimate load by (0.00%,7.14%, 17.59% and 35.51%) respectively. Finally, it can be concluded that, the selected four grades of steel (350, 450, 550 and 650) MPa led to increase the ultimate load by (0.00%,19.98%, 31.97%, 41.12%) respectively.

[46] studied numerically the strength, stiffness, ductility, cracking patterns, and modes of failure of hollow RC columns with square cross-section with various load eccentricity as shown in Figure 2-8. Models were analyzed by nonlinear finite element method using ATENA v.2.1.10 software.

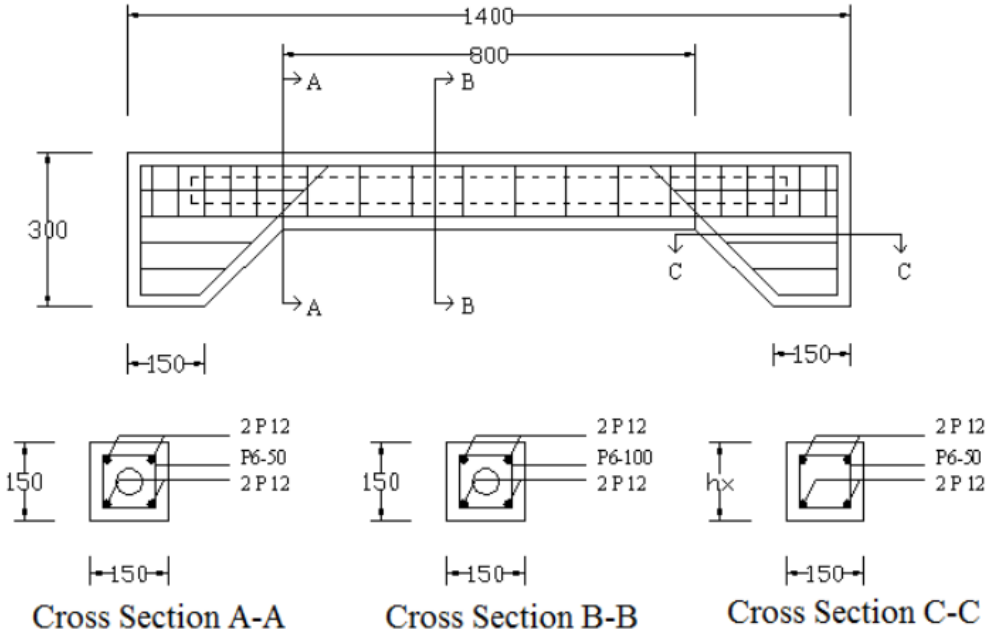

Figure 2-8 Details Columns Dimensions by [46].

The numerical results showed that the different ultimate load strength of the columns was 2.3% average, while the different stiffens was 21% average, and the different ductility was 28.5% average. From the analysis show that the numerical results were approaching the experimental results that has been done before as shown in Figure 2-9.

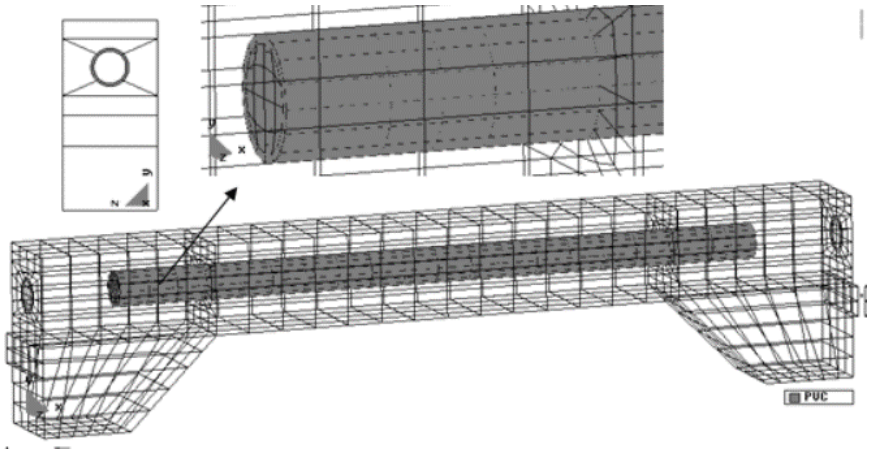

Figure 2-9 FE Modeling Column by [46].

[47] studied the effect of fibers shape, hollow ratio and cross-sectional shape on the behavior of solid and hollow slurry infiltrated fiber concrete (SIFCON) columns. The height of all columns is 1000 mm and the dimensions are illustrated in Figure 2-10.

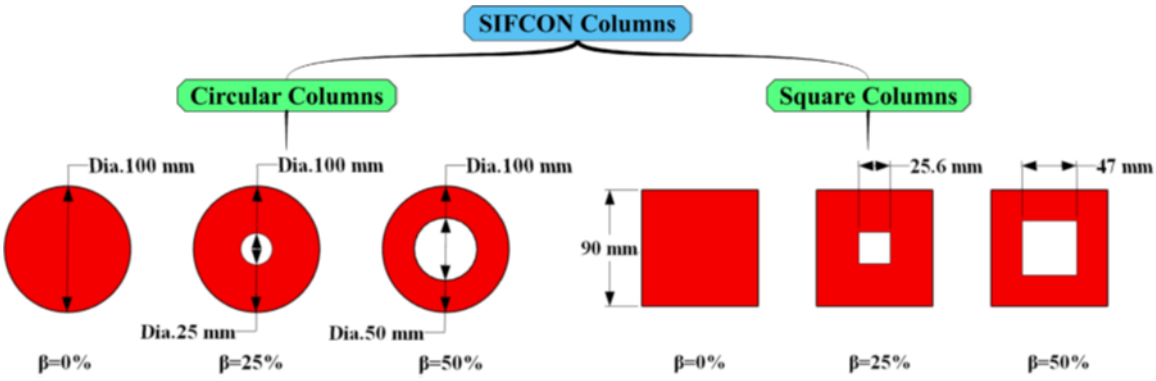

Figure 2-10 Cross Section Shape, Hollow Ratio (β) % and Dimension of SIFCON Column Specimens by [47]

The effect of fiber shape, cross-section shape and the hollow ratio of SIFCON columns was investigated experimentally and these results compared with analytical

predictions from ABAQUS program. Where each solid column has better performance than the same cross section hollow columns. For load carrying capacity, the decreasing ratios were (5.8% and 16.5%) in square hollow hybrid SIFCON column with (β = 25% and 50%) respectively. The hollow columns showed lower energy absorption capacity than similar solid columns, and decreased with increasing in hollow ratio of columns. Where compared with solid columns, the percentage decrease was (23.39 and 78.25) % for circular hooked end columns with hollow ratio (β = 25% and 50%) % respectively.

[48] develops analytical simplified calculation approach that approximates the output results of finite element computations for columns with a complicated hollow square-section under eccentric loads. Constant 500×500 mm external dimensions, variable height H from 3.5 to 4.5 m and variable hollow square-section wall thickness t was taken. 3D numerical model fits the behavior of compression elements and makes it possible to determine ultimate load of column with about 98 % precision, The using of 1D numerical model provides more conservative result than 3D numerical model, the difference of determined ultimate load capacity is up to 3.4 %, but 1D model can significantly reduce the time required for calculations, column bending stiffness and energy absorption, at the time when changes of the column height have negligible impact on the column characteristics, obtained equation for prediction of ultimate load capacity of the column with random chosen parameters

of cross-section from the factors interval on which a function was defined allows to determine it with precision more than 96 %.

[49] studied the analysis of short reinforced concrete columns with variable cross-sections along the column in a linear manner by using the ANSYS V.15 software package. The variables that were studied included the type of section, solid or hollow, the ratio of longitudinal and transverse reinforcement, the ratio of the hollowness as shown in Figure 2-11.

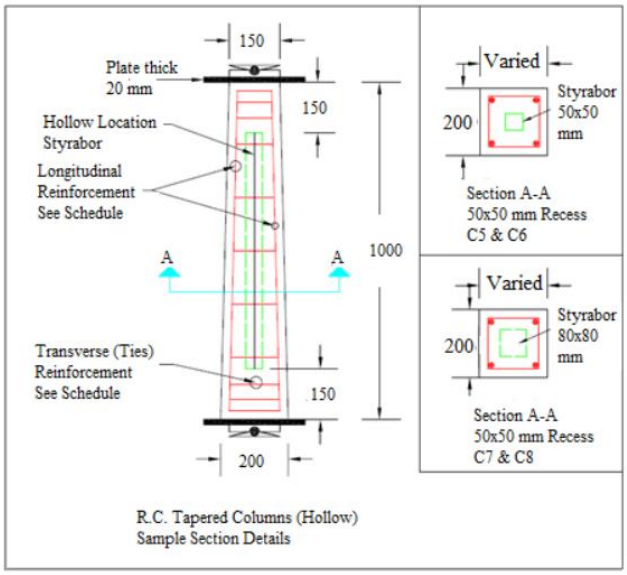

Figure 2-11 Dimension and Details of R.C. Tapered Columns (hollow section) [49]

When increased steel reinforcing ratios i.e. (longitudinal or ties) led to improvement in strength capacity load by about (22-35%) and reduced the lateral displacement by about (15-20%). while the ductility of specimen's enhancement by about (8-13%) for the solid section. while the model with a hollow section (recess), these recesses

led to a decrease in load capacity by about (25-38%) and increased in lateral displacement by about (11- 18%) with the same other property of specimens. also, hollow recess gives a decrease in ductility ratio by about (20-29%) compared with solid specimen's models. It can show clearly that when increased longitudinal reinforcing led to give more in strength capacity of specimens contains hollow recess.

[4] studied experimentally the behavior of hollow reinforced concrete columns under concentric and eccentric loads. It was based on the results of a two-stage casting and testing of fifteen concrete columns. Seven specimens were tested under axial loads in the first stage, and eight specimens were designed with corbels at the ends of the column for testing under eccentric loads in the second stage. With a cross section of (140x80) mm and a length of 2000 mm as shown in Figure 2-12.

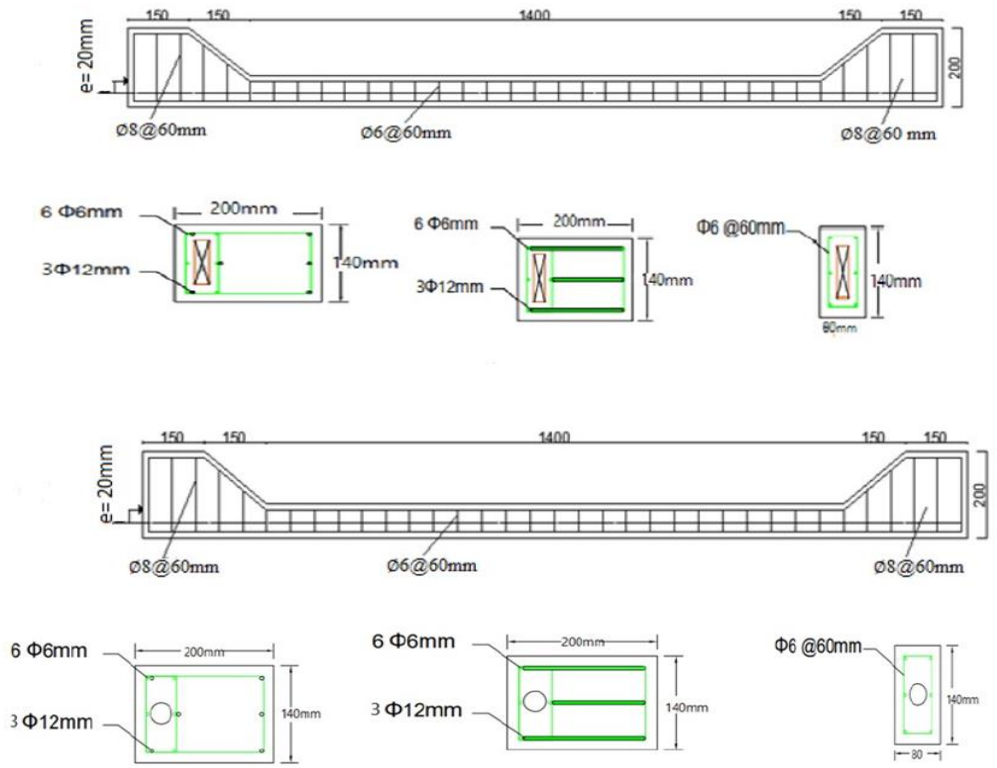

Figure 2-12 Columns Details with Different Hole Shape [4].

For the column's specimens, four experimental parameters were investigated. Lateral reinforcement (ties), carbon fiber reinforced polymer (CFRP) sheet strengthening, opening shape, and eccentric load were the variables. It was found that the columns strengthened by lateral reinforcement (ties) and CFRP from the ends of ties at opposite sides of the width of column for lengths 360 mm,167 mm and 500 mm caused an increase in the ultimate load by ranges of (16.4, 6.9 and 37.9) %, respectively compared with un-strengthened column. Effect of increasing the eccentricity values of reinforced concrete slender columns led to reduce ultimate load capacity by (10.26 and 17.95) % for (e =20 mm and e=40 mm) respectively.

For 20 mm load eccentricity, it was found that the column having circular opening shape caused an increase in the load capacity than column having rectangular by 14.29%. For (40 mm) eccentricity, it was found that the column having circular opening shape gave an increase in the load capacity than column having rectangular by 18.75% as shown in Figure 2-13.

Figure 2-13 Failure Mode of Specimens [4].

This work was the second reference study for the present thesis.

2.3 Summary

From the previous studies, it was found that many numerical and experimental researches had been done on the behavior of slender RC columns. However, it can be noticed the limitation of numerical researches studied the effect of (SFR) strengthening distribution on the geometrical properties according to Eurocode of the solid or hollow slender reinforced concrete columns subjected to concentric or eccentric loads in terms of load-displacement and failure mode.

CHAPTER THREE: FINITE ELEMENT MODELING

3.1 Introduction

Because of its inherent advantages over previous approaches, the finite element method (FEM) quickly became the most valuable numerical analytical tool for engineers and applied mathematicians [50]. Its key benefit is that it may be used on any shape in any number of dimensions. The FEM is a typical method for turning governing energy principles or governing differential equations into a matrix equation system that may be solved for an approximate solution. Finite element analysis (FEA) is the term used when the FEM is applied to a specific field of analysis (such as stress analysis, temperature analysis, or vibration analysis) [51].

Engineering education has changed substantially since the invention of the digital computer. In today's world, everything but the simplest problems are solved using a computer software that not only speeds up computations but also allows for the presentation of results in fancy graphics [52].

There are several types of FE simulation software such as Abaqus, ANSYS, ATINA, ADINA, DIANA, OpenSees, VECTOR2, etc. Abaqus is one of the most powerful software used in finite element analysis [53]. This chapter presents a nonlinear finite element analysis to study the behavior of solid and hollow slender reinforced

concrete columns subjected to concentric and eccentric loads using ABAQUS/CAE/2020.

3.2 ABAQUS Computer Software

The Abaqus software is one of the successful finite element packages which was developed in 1978 and has been used since then for numerical simulation of complex problems in various fields, such as Civil and especially Structural Engineering [54]. Abaqus has a large library of elements that can be used to model almost any geometry. It also offers an extensive number of material models that can simulate the behavior of metals, rubber, polymers, composites, reinforced concrete, crushable and resilient foams, and geotechnical materials like soils and rock. Abaqus offers a wide range of capabilities for simulation of linear and nonlinear applications. Component interactions are modeled by associating the geometry defining each component with the relevant material models and specifying component interactions in problems with numerous components. ABAQUS/Standard, ABAQUS/Explicit and ABAQUS/CFD are the available products. ABAQUS/Standard uses implicit solutions and satisfies equations at each increment for static problems and equations of motion at each step time for dynamic problems. ABAQUS/Explicit uses explicit integration to perform the simulation at current time and extrapolates the equations of motion for the simulation at the next time step [31].

3.3 Slender Column FEA

To use the appropriate type of analysis provided by ABAQUS and obtaining results without errors, it's important to understand some definitions related to the structural behavior of slender columns:

3.3.1 Buckling

Buckling is a physical phenomenon in which a relatively straight, slender element bends laterally (typically suddenly) from its longitudinal position due to compression. Buckling, rather than material failing, is a loss of stability caused by geometric effects. However, if the resulting deformations are not controlled, it might lead to material failure and collapse. In a linear elastic range, most structures can operate. That is, when the load is removed, they return to their original shape. When the elastic range is surpassed, as when matrix cracking develops in a composite, permanent deformations result. There are two types of buckling, according to a comprehensive examination: deflection buckling and bifurcation buckling. In fact, in real-life situations, most, if not all, buckling occurrences are of the deflection type, this type occurs when ought of straightness (geometry) inhomogeneous (material) member to be subjected to compressive force, and it generally occurs before the axial compression stresses can cause failure of the material by yielding or fracture of that compression member. A bifurcation buckling occurs when a completely straight

(geometry) homogenous (material) member is subjected to compressive force, the resultant of which must pass through the member's centroidal axis [55], [56]. Real columns are never perfect, and defects in them have a significant impact on their stability. The real columns buckle before the buckling force because of these defects from the perfect shape or material [57]. The material yielding or the column buckling can both cause a column to fail. The engineer is interested in determining when this changeover takes place [58], [59].

3.3.2 Second-Order Effects

When compared to perfectly axially loaded columns with no initial imperfections, the inevitable lateral deformations associated with eccentrically loaded columns increases the susceptibility to second-order effects [60]. Second-order effects develop when an eccentric axial force (self-weight or applied load) or an axial load and a horizontal load cause a bending moment and an additional displacement develop, also it called P-delta effects. These effects are more noticeable when the column is slender. Second-order effects are unimportant if their impact is small, and codes have set restrictions for slenderness ratios in relation to loads for this reason. As a result, ignoring second-order effects and underestimating deformations may result in an unsafe design in some cases [37]. The sensitivity of a frame to second order effect illustrated simply as shown in Figure 3-1.

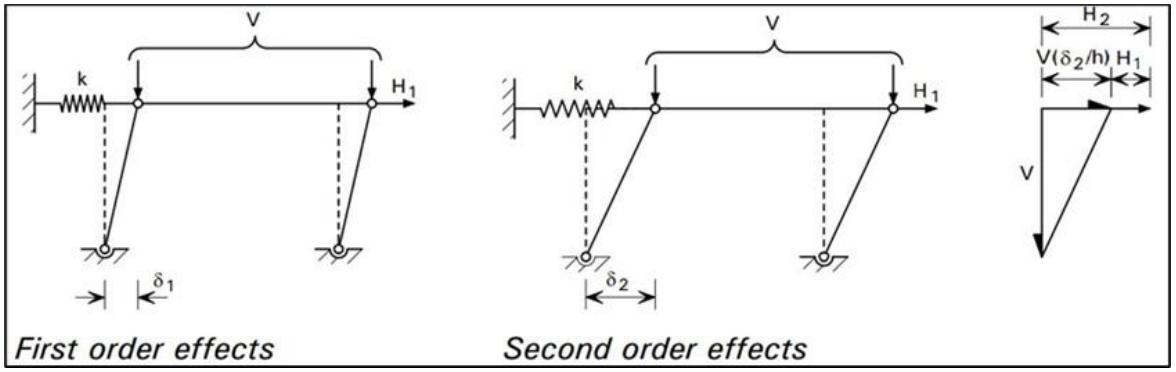

Figure 3-1 First and Second Order Effects in a Pinned Braced Frame [61].

3.3.3 Imperfection

Imperfection refers to the trait or state of being imperfect. These imperfections are divided into geometric imperfection, material imperfection and boundary imperfections [58]. Local and overall (bow, global, or out-of-straightness) geometric imperfections are the two basic categories of initial geometric imperfections. Initial local geometric imperfections can be discovered on the outer or inner surfaces of metal structural members in perpendicular directions to the member surfaces. Initial overall geometric imperfections, on the other hand, are global profiles for the entire structural member throughout its length in any direction [62], [63]. Material imperfections are defined as deviations from the material's parameters, such us the heterogeneity of concrete components (cement, sand, gravel). changing in supports and loading conditions do to increase of loads for example are known as boundary imperfections.

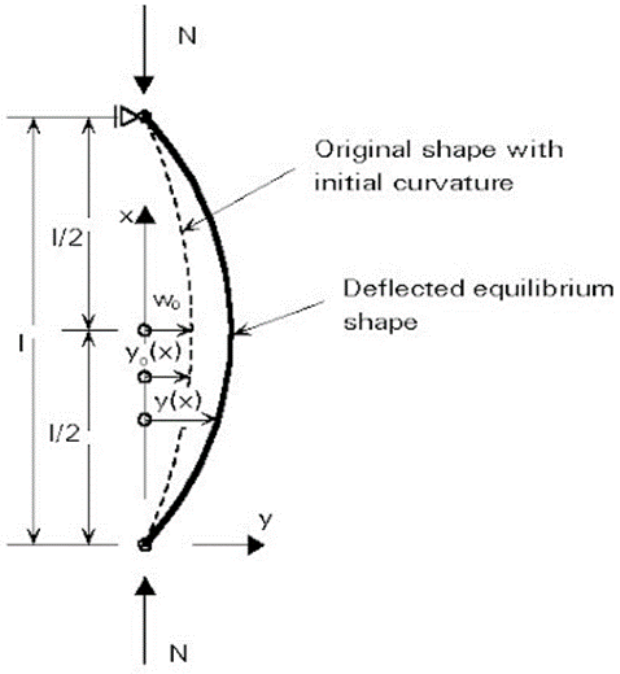

Figure 3-2 Behavior of Imperfect Column.

3.4 ABAQUS Model Design

3.4.1 Geometry Modeling

A physical model is typically created by assembling various components. The assembly interface in Abaqus allows analysts to create a finite element mesh using an organizational scheme that parallels the physical assembly. In Abaqus the components that are assembled together are called part instances. This section explains how to organize an Abaqus finite element model in terms of an assembly of part instances. The mesh is created by defining parts, then assembling instances of each part. Each part can be used (instanced) one or more times, and each part instance has its own position within the assembly. This organization of the model

definition matches the way models are created in Abaqus/CAE, where the assembly can be created interactively or imported from an input file. The three definitions below give more details about geometry modeling in Abaqus:

- Assembly: An assembly is a collection of positioned part instances. An analysis is conducted by defining boundary conditions, constraints, interactions, and a loading history for the assembly.

- Part: A part is a finite element idealization of an object. Parts are the building blocks of an assembly and can be either rigid or deformable. Parts are reusable; they can be instanced multiple times in the assembly. Parts are not analyzed directly; a part is like a blueprint for its instances.

- Part instance: A part instance is a usage of a part within the assembly. All characteristics (such as mesh and section definitions) defined for a part become characteristics for each instance of that part—they are inherited by the part instances. Each part instance is positioned independently within the assembly.

When creating a model, it is often necessary to refer to something outside of the current level; for example, a section definition within a part must refer to a material, which is defined at the model level. Loads defined within a step must refer to sets

within the assembly. But some references between levels are not allowed; for example, a set in one part instance cannot refer to nodes in another part instance.

A model can contain multiple parts, each part exists in a local coordinate system, Assembly module used to create instances of the parts and position those instances relative to each other in a global coordinate system. To simulate the slender RC column specimens, three main parts were created plain concrete column, longitudinal steel bars and ties reinforcing. Plain concrete column modeled as a solid deformable part, both longitudinal and tie reinforcing modeled as a wire deformable part Figure 3-3 shows the Assembly module of slender RC column specimen.

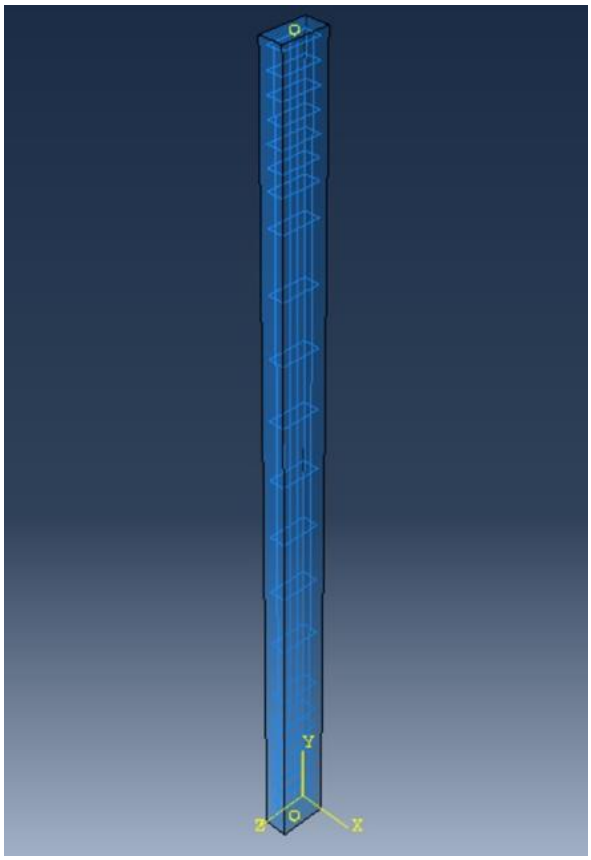

Figure 3-3 Assembly Module of Slender RC Column Specimen.

3.4.2 Material Modeling

The material library in Abaqus is intended to provide comprehensive coverage of both linear and nonlinear, isotropic and anisotropic material behaviors. The use of numerical integration in the elements, including numerical integration across the cross-sections of shells and beams, provides the flexibility to analyze the most complex composite structures. Some of the mechanical behaviors offered are mutually exclusive: such behaviors cannot appear together in a single material definition. Some behaviors require the presence of other behaviors; for example, plasticity requires linear elasticity. Any number of materials can be defined in an analysis. Each material definition can contain any number of material behaviors, as required, to specify the complete material behavior. For example, in a linear static stress analysis only elastic material behavior may be needed, while in a more complicated analysis several material behaviors may be required. A name must be assigned to each material definition. This name allows the material to be referenced from the section definitions used to assign this material to regions in the model. Abaqus requires that the material be sufficiently defined to provide suitable properties for those elements with which the material is associated and for all of the analysis procedures through which the model will be run. Thus, a material associated

with displacement or structural elements must include either a “Complete mechanical” category behavior or an “Elasticity” category behavior as shown in Figure 3-4.

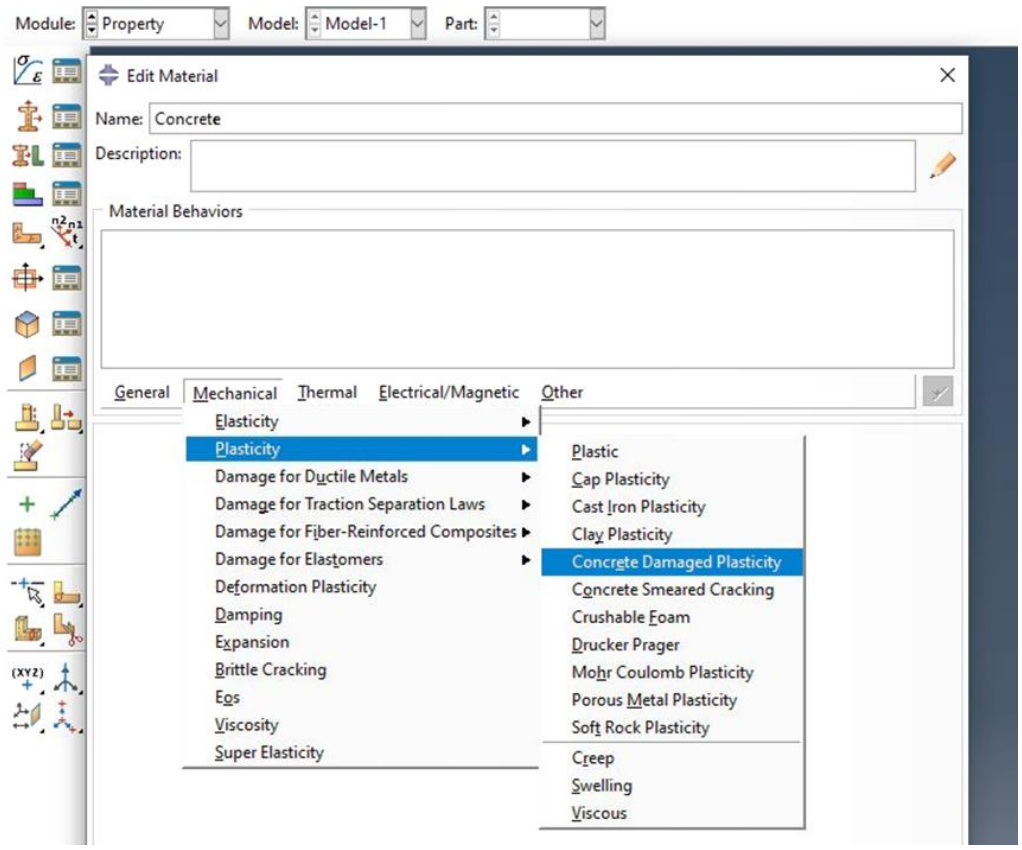

Figure 3-4 Defining Material Behavior.

Due to joint operation of concrete and steel, the structural behavior of RC structures is exceedingly complex. Concrete is brittle, but tensile cracks may close under stress reversal, allowing broken parts to be reassembled. Concrete damaged plasticity (CDP) is a popular concrete model used in FEM analysis since it is primarily intended for reinforced concrete structures. Two main failure mechanisms of the

CDP model are tensile cracking and compressive crushing of the concrete. The model assumes that the uniaxial tensile and compressive response of concrete is characterized by damaged plasticity, as shown in Figure 3.8. It is assumed that the uniaxial stress-strain curves can be converted into stress versus plastic-strain curves. This conversion is performed automatically by Abaqus from the user-provided stress versus inelastic strain data [64], [65], [66], [67], [68], [69].

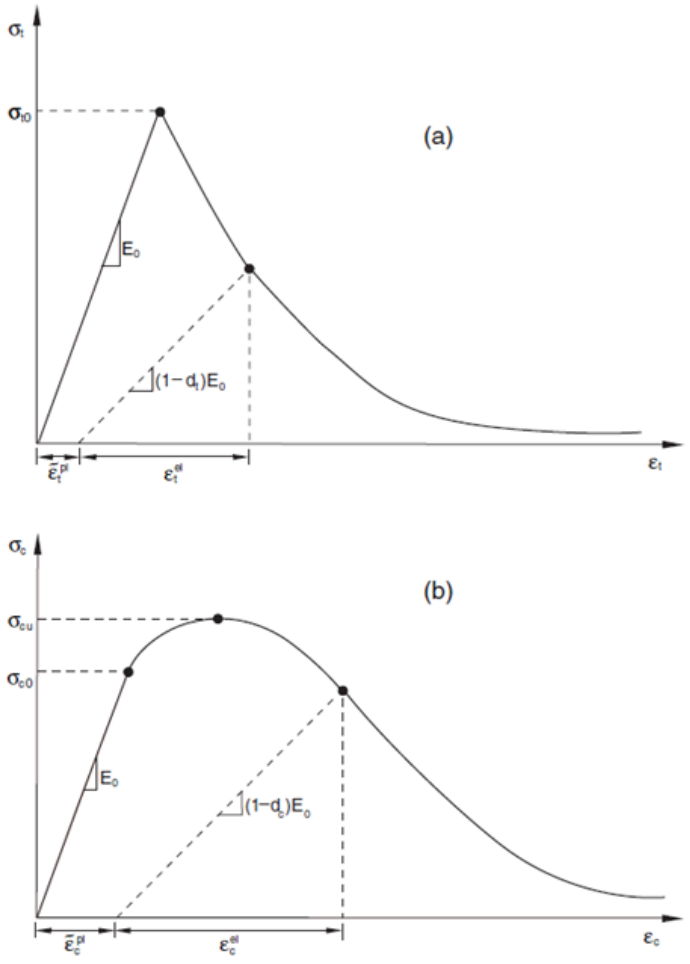

Figure 3-5 Response of Concrete to Uniaxial Loading in Tension (a) and Compression (b) [64]

Under compound stress, the recommended ABAQUS parameters of the concrete damage plasticity model are listed in Table 3-1.

Table 3-1 Recommended Concrete Damage Plasticity Parameters.

Dilation angle	eccentricity	f_{b0}/f_{c0}	stress invariant ratio k	viscosity parameter μ
36	0.1	1.16	0.667	0

The reinforcing steel bars were modeled using Abaqus' plasticity model, a bilinear model characterized the stress–strain relationship of reinforcement (elastic perfectly plastic). The yield strength, plastic strain, elastic modulus and poison ratio were set to 410 MPa, 0, 200 GPa and 0.3 respectively which is the same experimental steel properties as shown in Figure 3-6.

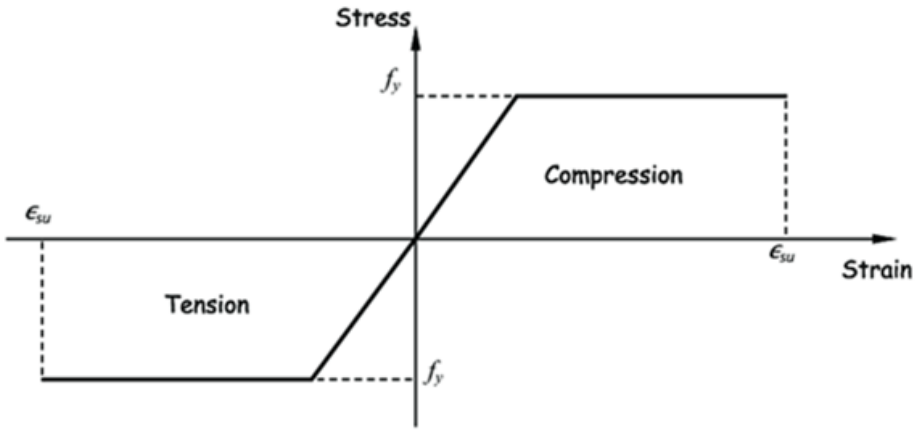

Figure 3-6 Stress-Strain Curve for Steel Reinforcement.

3.4.3 SFR Modeling

In the experimental work, a hooked-end steel wire fibers with a length of 30 mm and a diameter of 0.55 mm were used. This type of steel fiber is classified as Type II, six cubes of the concrete mix were used during the casting of the samples and allowed to cure for 28 days before testing. The results for the compressive strength of concrete were 55 MPa [44]. The concrete damaged plasticity model (CDPM), a continuum plasticity-based damage model, has generated significant concerns due to the increased global adoption of ABAQUS. The model can provide a general capability for modeling the nonlinear deformation and irreversible damage of plain concrete with high accuracy in all structural types and loading paths by adopting the concept of isotropic damaged elasticity in combination with isotropic tensile and compressive plasticity [70]. Since the experimental work adopted the compressive strength of concrete cubes only, a concrete damaged plasticity model (CDPM) will be used without modifying.

3.4.4 Analysis Type

There are two types of analyses methods in Abaqus: linear and nonlinear FE analyses. Because the buckling behavior complexity, nonlinear analysis couldn’t depict axially loaded slender column real behavior, for dynamic analysis produced by Abaqus software which used to solve buckling problems. This development

occurred as a result of two aspects. First, all FEM equations are based on the equilibrium of stresses and strain compatibility, which means that these equations are impossible to solve due to the discontinuous response at the buckling point. Second, until final collapse, a perfect (ideal) column is used to illustrate the FE model. Instead of bifurcation, Abaqus handles the discontinues problem by displaying a geometric imperfection mode in the perfect (ideal) geometry of the model. In Abaqus, there are numerous approaches for defining an imperfection. One of these techniques is to use the *IMPERFECTION keyword to directly apply the imperfection in the input file. This necessitates data like as eigenvalues and buckling modes, which were provided via linear elastic buckling analysis. In a brief, the FE simulation of the provided specimens necessitated the creation of two models for the same mesh size: To determine the likelihood of collapse, an initial model for elastic buckling analysis was developed as shown in Figure 3-7.

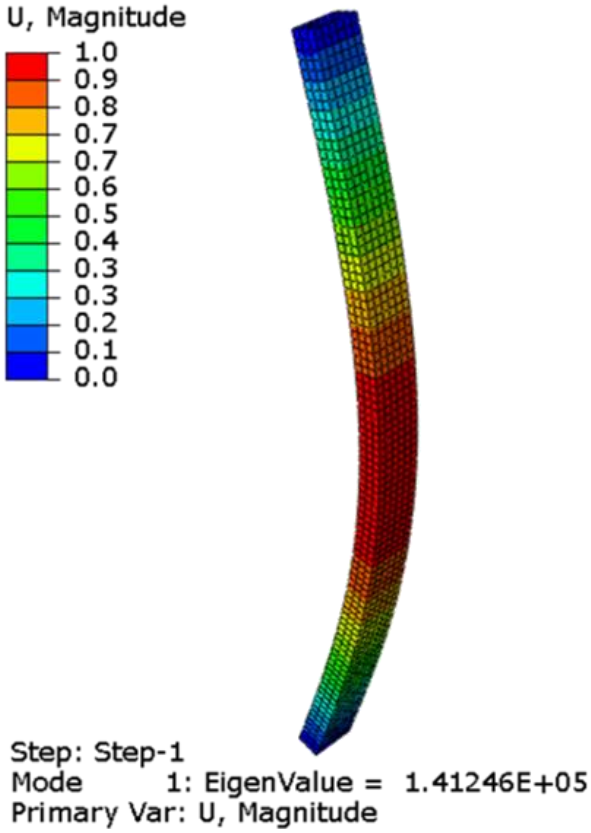

Figure 3-7 Linear Analysis (Buckling Mode).

This model was analyzed with linear elastic buckling to get possible buckling mode and Eigenvalue of this mode which represent the critical load. The plastic model then imports imperfection data (buckling mode, Eigenvalue) from the linear analysis to do the nonlinear analysis of slender RC columns [71]. The input file of both models has been altered as shown in Figure 3-8.

```
**OUTPUT REQUEST
**
*Restart, write, frequency=0
**
**FIELD OUTPUT: F-Output-1
**
*Output, field, variable=PRECELECT
*NODE FILE
U
*End Step
```

Linear analysis

```
**--------------------------
--
*IMPERFECTION, FILE=Job-1,
STEP=1
1,4
**
**STEP: Step-1
**
*Step, name= Step-1, nlgeom= YES
*Dynamic, Explicit
,1.
```

Nonlinear analysis

Figure 3-8 Input File of Imperfection Factor (Highlighted Characters).

3.4.5 Boundary Conditions

Boundary conditions in Abaqus can be used:

1. To specify the values of all basic solution variables displacements and rotations at nodes.
2. can be given as “model” input data (within the initial step in Abaqus/CAE) to define zero-valued boundary conditions.
3. can be given as “history” input data (within an analysis step) to add, modify, or remove zero-valued or nonzero boundary conditions.
4. can be defined by the user through subroutines DISP for Abaqus/Standard and VDISP for Abaqus/Explicit.

Only zero-valued boundary conditions can be prescribed as model data (i.e., in the initial step in Abaqus/CAE). The data could be specified using either “direct” or “type” format. The “type” format is a way of conveniently specifying common types of boundary conditions in stress/displacement analyses. “Direct” format must be used in all other analysis types. For both “direct” and “type” format you specify the region of the model to which the boundary conditions apply and the degrees of freedom to be restrained. Boundary conditions prescribed as model data can be modified or removed during analysis steps.

Both ends of the samples were treated as pinned ends in the nonlinear analysis, identical to the test condition. Reference points (RP) where used to simulate the pin ends conditions. At both ends, the movement were constrained in all axes, except the axial movement at the top end was allowed. Although all rotations in all axes were allowed. Deformation control is often more stable than load control when performing analysis. As a result, in this study, the load was translated to a velocity of 0.01 m/s and applied to the top surface of specimens in RP that produced previously as shown in Figure 3-9.

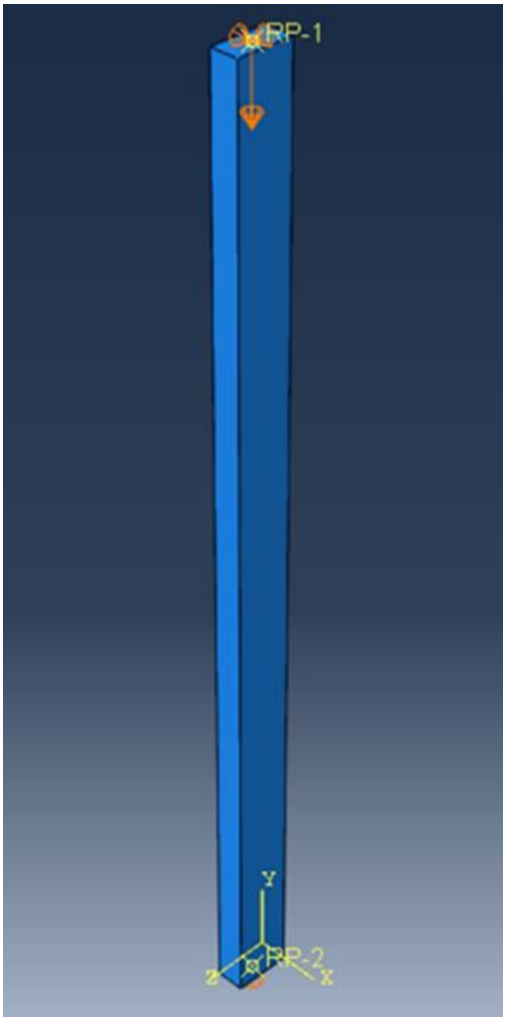

Figure 3-9 Load and Boundary Conditions.

3.4.6 Interaction

Abaqus provided various types of kinematic constraints, two types of constraints were used during the column FE modeling design:

1. Embedded region constraint: An element or a group of elements can be embedded in a group of host elements. Abaqus will search for the geometric relationships between nodes on the embedded elements and the host elements.

If a node on an embedded element lies within a host element, the degrees of freedom at the node will be eliminated by constraining them to the interpolated values of the degrees of freedom of the host element. Host elements cannot be embedded themselves Figure 3-10. the embedded region constraint in solid element.

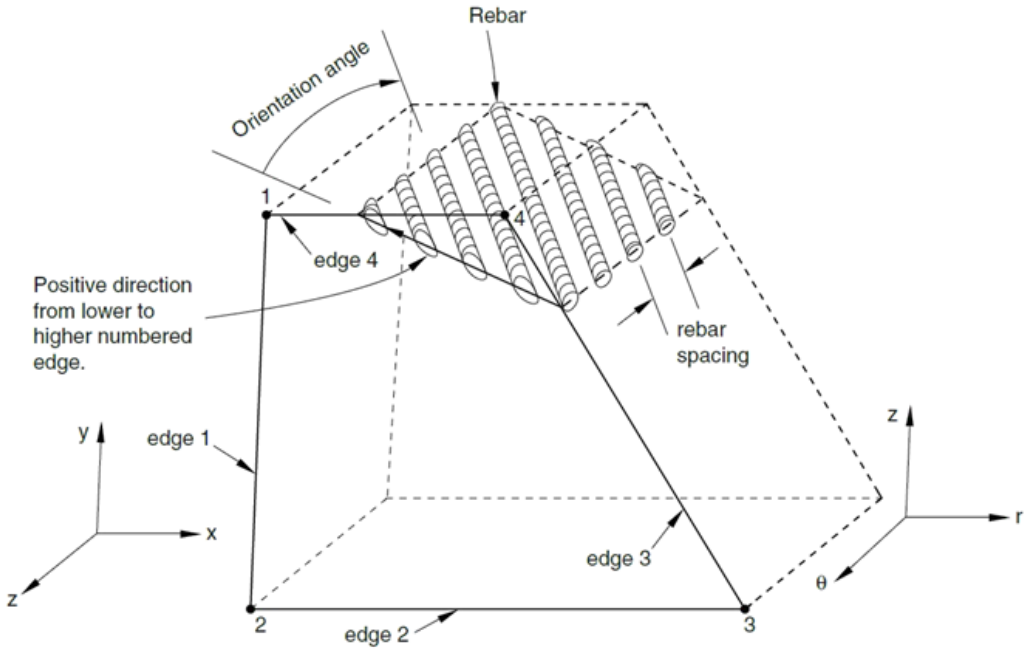

Figure 3-10 Orientation of Rebars in Plane and Axisymmetric Solid Elements [72]

2. Coupling constraint: In Abaqus/Standard a node or group of nodes can be constrained to a reference node. Similar to multi-point constraints, the kinematic coupling constraint allows general node-by-node specification of constrained degrees of freedom as shown in Figure 3-11.

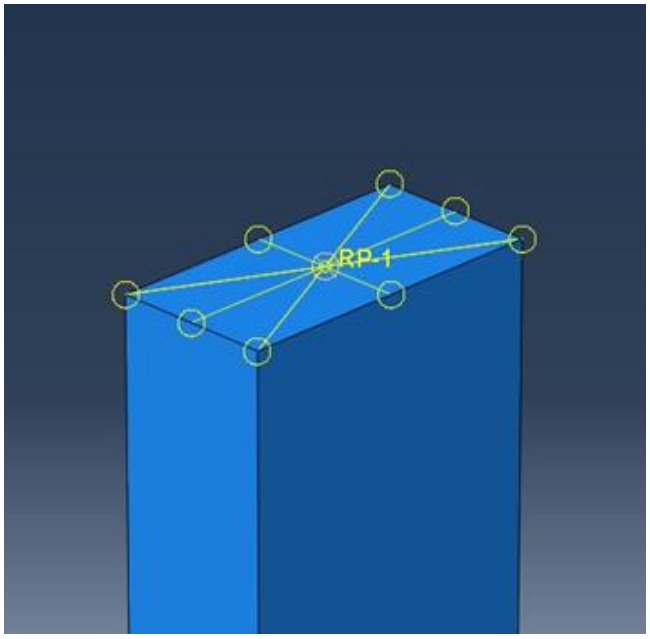

Figure 3-11 Coupling Constraint.

To ensure a complete link between the reinforcing bars and the concrete, the interactions were represented as an embedded region. The motion of the surface can be constrained by applying a coupling constraint on the motion of the reference point as shown in Figure 3-12.

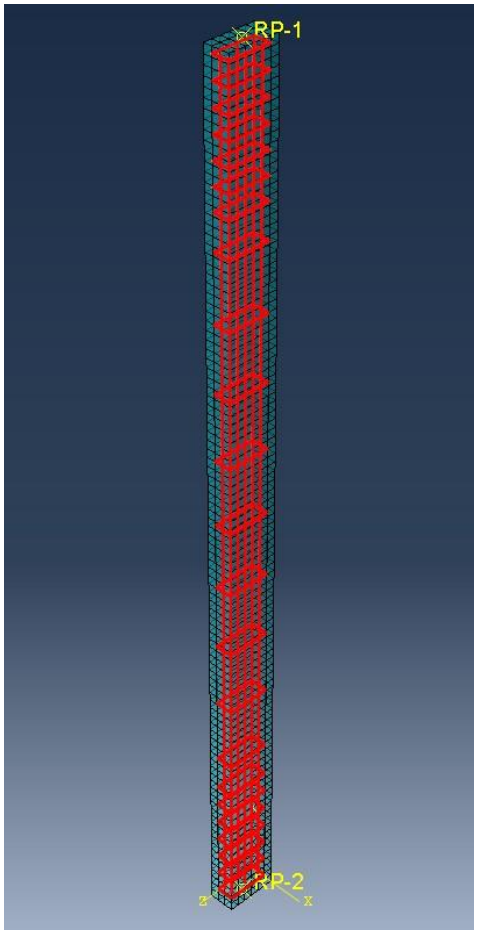

Figure 3-12 Model Constrains.

3.4.7 Meshing

Five aspects of an element characterize its behavior:

- Family.
- Degrees of freedom (directly related to the element family).
- Number of nodes.
- Formulation.

- Integration.

Each element in Abaqus has a unique name, such as T2D2, S4R, C3D8I, or C3D8R. The element name identifies each of the five aspects of an element.

The element families that are used most commonly in a stress analysis is shown in Figure 3-13. One of the major distinctions between different element families is the geometry type that each family assumes.

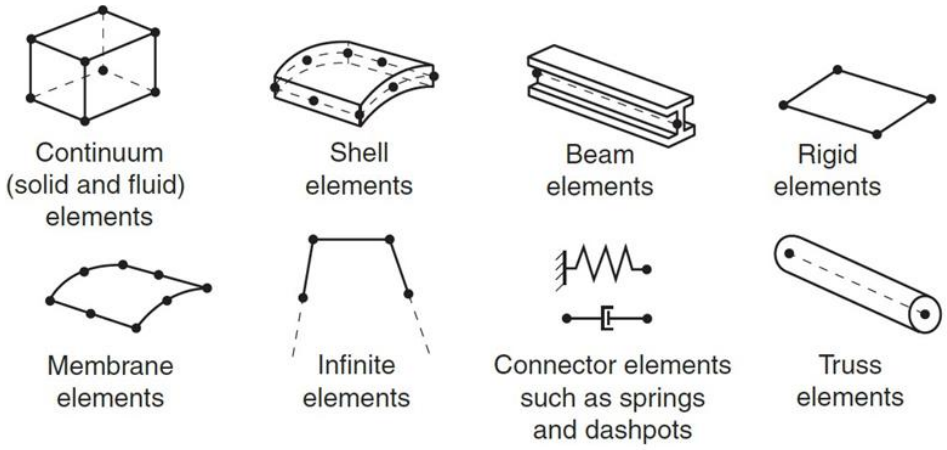

Figure 3-13 Commonly Used Element Families.

The first letter or letters of an element's name indicate to which family the element belongs. For example, S4R is a shell element, CINPE4 is an infinite element, and C3D8I is a continuum element.

The degrees of freedom are the fundamental variables calculated during the analysis. For a stress/displacement simulation the degrees of freedom are the translations and, for shell, pipe, and beam elements, the rotations at each node.

Displacements or other degrees of freedom are calculated at the nodes of the element. At any other point in the element, the displacements are obtained by interpolating from the nodal displacements. Usually, the interpolation order is determined by the number of nodes used in the element.

- Elements that have nodes only at their corners, such as the 8-node brick shown in Figure 3-14(a), use linear interpolation in each direction and are often called linear elements or first-order elements.

- In Abaqus/Standard elements with mid-side nodes, such as the 20-node brick shown in Figure 3-14(b), use quadratic interpolation and are often called quadratic elements or second-order elements.

- Modified triangular or tetrahedral elements with mid-side nodes, such as the 10-node tetrahedron shown in Figure 3-14(c), use a modified second-order interpolation and are often called modified or modified second-order elements.

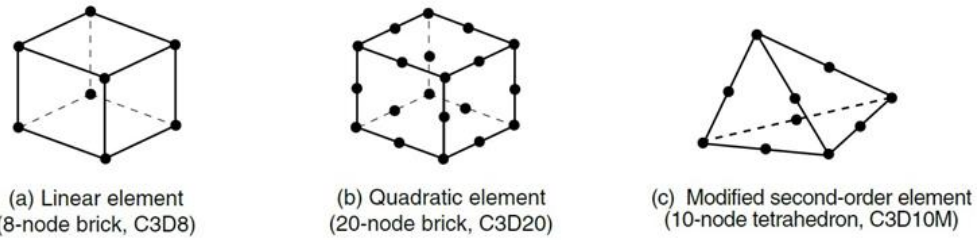

Figure 3-14 Linear Brick, Quadratic Brick, and Modified Tetrahedral Elements.

Typically, the number of nodes in an element is clearly identified in its name. The 8-node brick element is called C3D8, and the 4-node shell element is called S4R.

The beam element family uses a slightly different convention: the order of interpolation is identified in the name. Thus, a first-order, three-dimensional beam element is called B31, whereas a second-order, three-dimensional beam element is called B32. A similar convention is used for axisymmetric shell and membrane elements.

A rectangular mesh was utilized to produce good results from the model. The mesh elements were 20 mm in size. A mesh size of 10 mm might have been chosen, but that would have resulted in a lot more elements and more computational time with the same results. Table 3-2 shows mesh details for each of the column's components.

Table 3-2 Meshing Details.

Part	Type of element	Number of elements	Material type
Concrete column	C3D8 (8-node linear brick)	1800	Concrete
Reinforcement	T3D2 (2-node linear 3-D truss)	910	Steel

The reinforcement nodes line up with the concrete column's nodes. This increases the model's accuracy and, as a result, the quality of the outputs as shown in Figure 3-15.

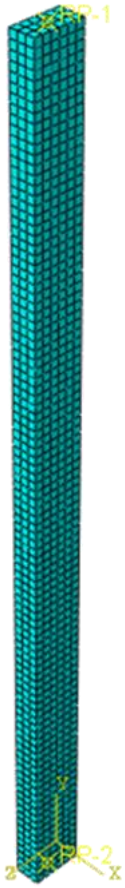

Figure 3-15 Element’s Mesh of Model.

3.5 Mode of Failure

The failure modes of the finite element analysis were compared with the failure modes obtained from tests of the specimens, which results from the compressive and tensile loads. The new versions of ABAQUS, 2019 and above, provided two methods of concrete damage failure patterns visualization, the standard method and element deletion method.

3.5.1 Standard Method

When the analysis completed, ABAQUS represents the results in the visualization viewport and the maximum compression or tension damage elements presented in red color as shown in Figure 3-16.

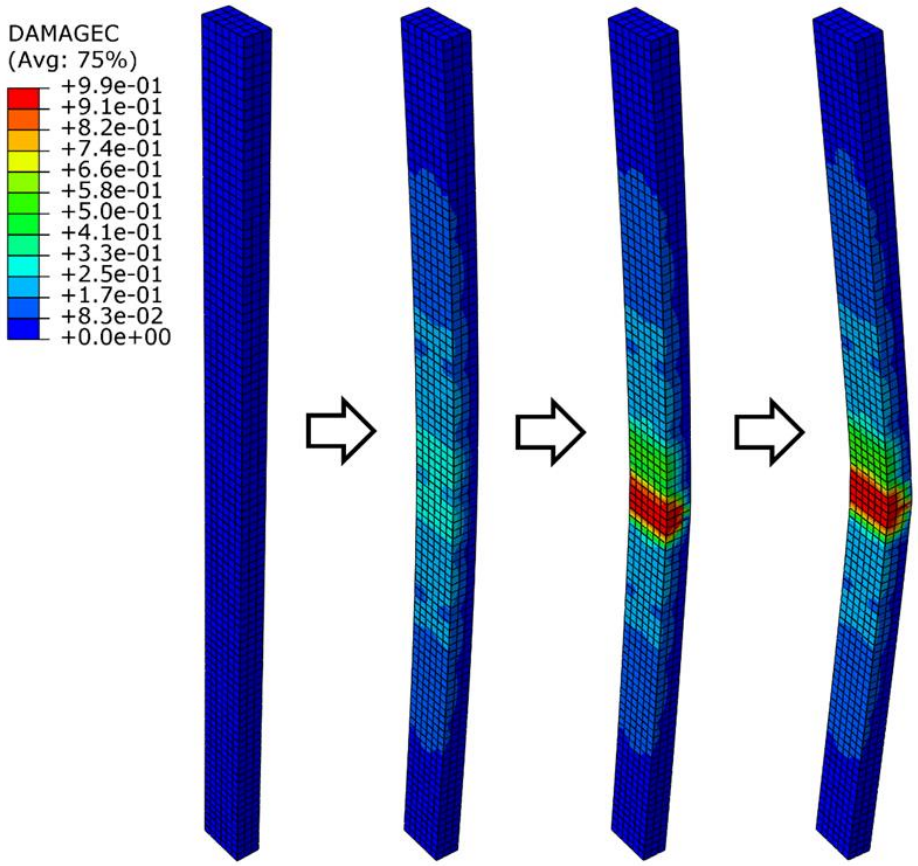

Figure 3-16 Failure damage progress visualized using standard method.

3.5.2 Element Deletion Method

In this method, any element exceeds the compression or tension damage parameter value, will be deleted automatically. Therefore, the failure pattern will be more realistic. This method depending on the maximum inelastic strain parameters and the maximum damage parameters of tension or compression, which were entered to the concrete property module as a concrete damage plasticity model, by using

*Concrete Failure keyword and the maximum values directly in the script file as shown in Figure 3-17.

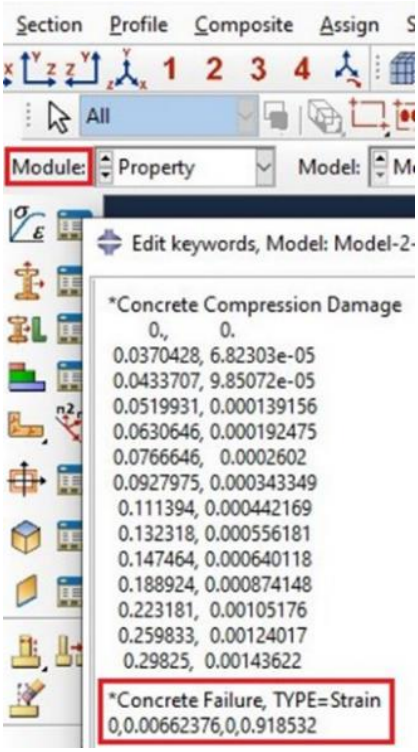

Figure 3-17 Element Deletion Keyword (highlighted in Red).

When the analysis completed, the results obtained and the failure patterns presented as shown in Fig 4.10.

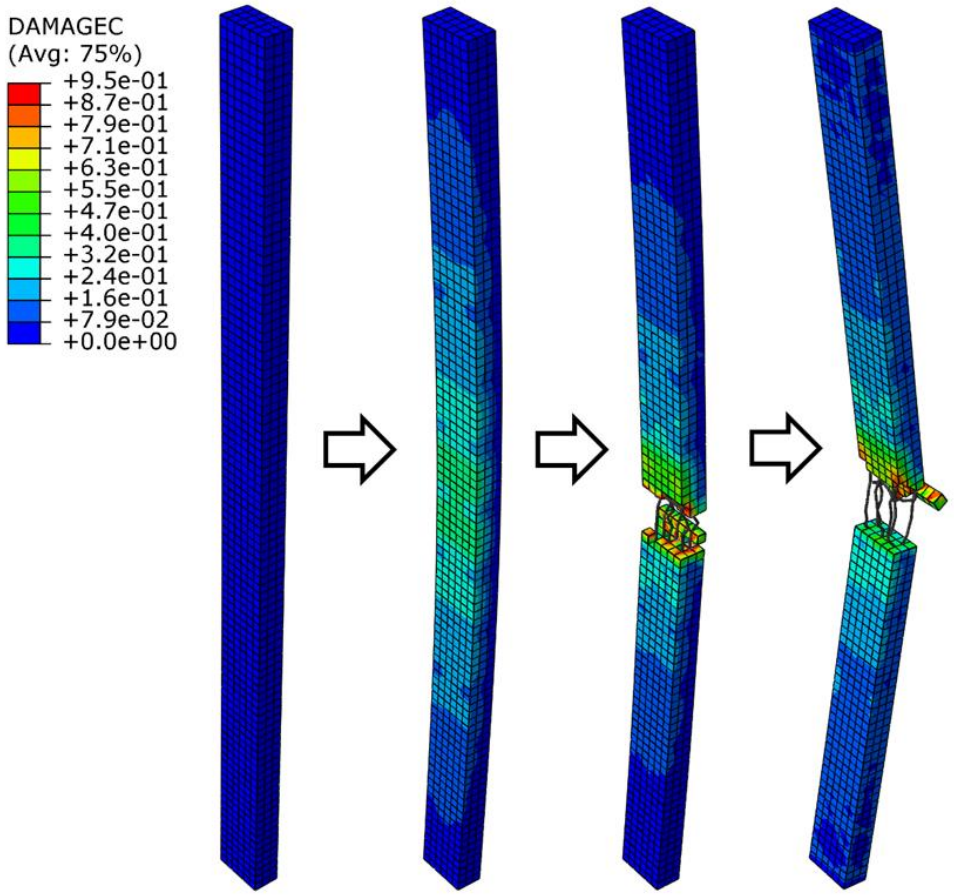

Figure 3-18 Failure Damage Progress Visualized using Element Deletion Method.

Since ABAQUS/2020 version used in this study, then the second method can be adopted. However, both FE and tested specimens, showed identical modes of failure.

CHAPTER FOUR: NUMERICAL ANALYSIS AND RESULTS

4.1 Introduction

In this chapter, the experimental results obtained from previous studies of solid and hollow slender reinforced concrete columns will be compared with the theoretical results obtained from the finite elements method simulation using ABAQUS/Standard 2020 software in terms of load-deflection relationship and failure mode. Also, some important variables that may affect the behavior of such columns will be discussed through a parametric study conducted to determine the ultimate load and deflection.

4.2 Details of Study

This work studied the structural behavior of two types of slender RC columns, solid and hollow, depending on the available experimental results tested by Mohammed Al Helfi & Ali Al Lami [44] for solid columns, and Alaa & Mohammed Al Helfi [4] for hollow columns.

Four columns from the first study and five columns from the second study, were selected and simulated using ABAQUS software.

4.2.1 Solid Column Details

The length of all columns was 2000 mm and 120 mm x 60 mm in cross-section, column top and bottom ends were supported by load plate working as a hinge, and the major longitudinal reinforcement was symmetrically 2 × 3Ø6. The stirrups were Ø6 @ 50 mm along distance of 300 mm from each end of column, and 150 mm in the remaining length as shown in Figure 4-1.

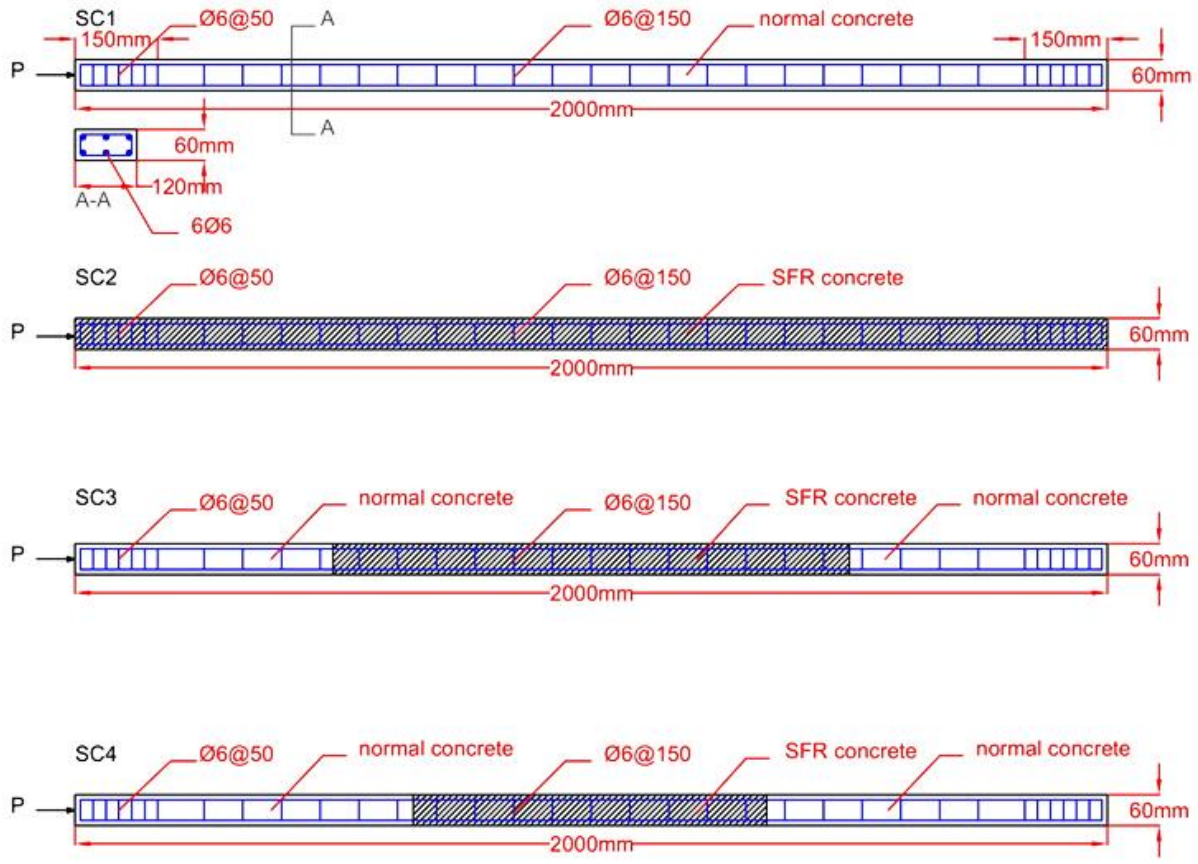

Figure 4-1 Solid Column Details [44].

First normal concrete column SC1 of (f´c=28 MPa) was the reference, while the other three columns SC2, SC3, and SC4 were strengthened using SFR along the whole length of the column, in the middle half (L/2) and the middle third (L/3) of column length, respectively. The compressive strength of strengthened concrete was (f´c=44 MPa). All columns were axially loaded. Table. 4.1. demonstrate the details of columns.

Table 4-1 Details of Solid Slender RC Column Specimens [44].

Column ID	Strengthening material	SFR Strengthening length	Ultimate load test result (kN)
SC1	Non	Non	182
SC2	SFR	L	261
SC3	SFR	L/2	260
SC4	SFR	L/3	244

4.2.2 Hollow Column Details

The length of all columns was 2000 mm and 140 x 80 mm in cross-section, also, column top and bottom ends were supported by load plate working as a hinge, and the major longitudinal reinforcement was symmetrically 2 × 3Ø6. The stirrups were Ø6 @ 30 mm along distance of 500 mm from each end of column, and 60 mm in the remaining length as shown in Figure 4-2.

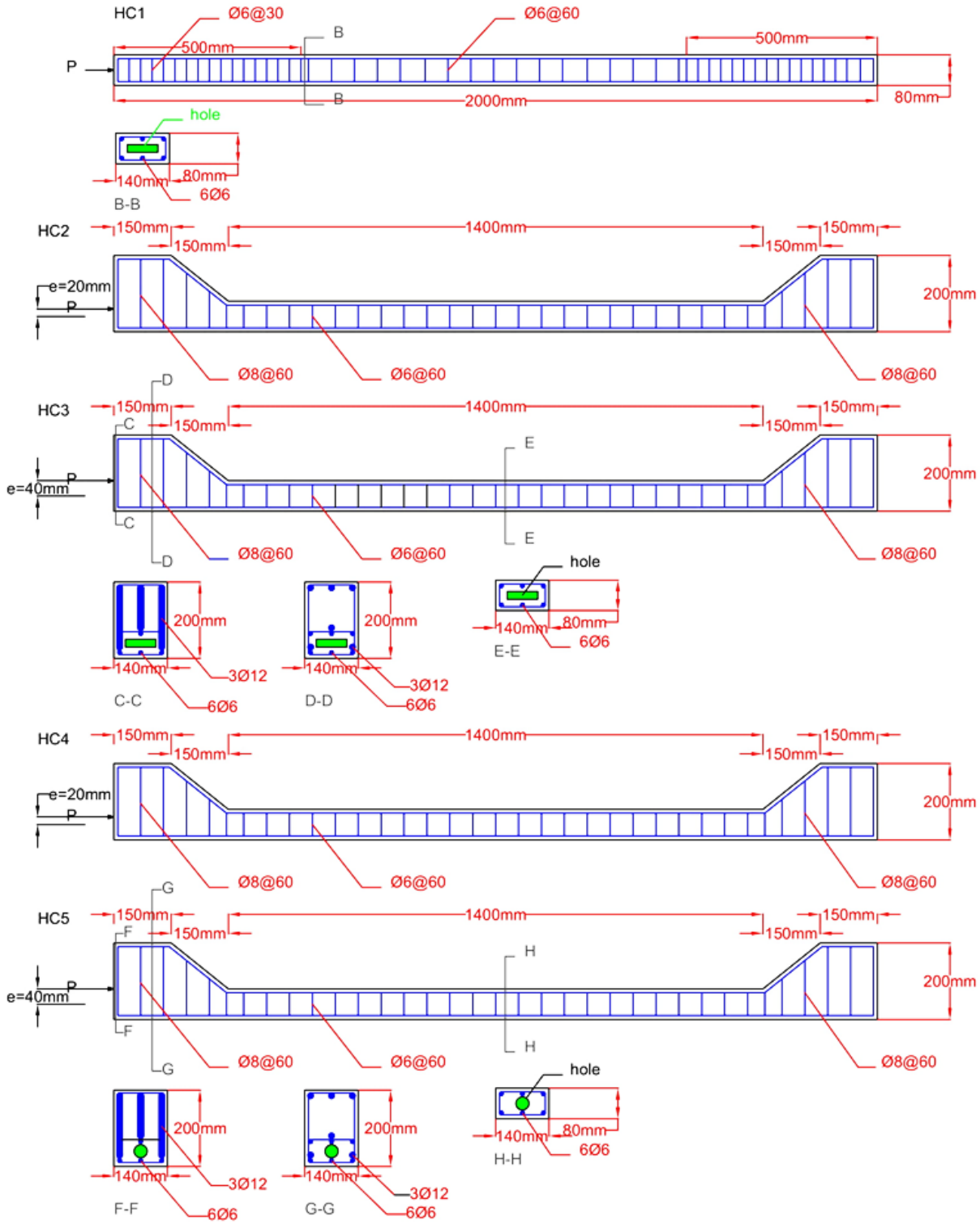

Figure 4-2 Hollow Column Details [4].

First column HC1 were concentrically loaded and the other four columns HC2, HC3, HC4, and HC5 were designed with a corbel at the ends for testing under eccentric load as shown in Figure 4-2. The compressive strength of normal concrete for all columns was 35 MPa. Table 4-2. demonstrate the details of columns.

Table 4-2 Details of Hollow Slender RC Column Specimens [4].

Column ID	Shape of opening	Dimension of opening (mm)	Eccentricity (mm)
HC1	Rectangular	20×80	0
HC2	Rectangular	20×80	20
HC3	Rectangular	20×80	40
HC4	Circular	D45	20
HC5	Circular	D45	40

4.3 Verification of Imperfection Factor

The steel or concrete column which carries the load in pure compression with no moments presented in it, called Euler's column. In ideal conditions, the Euler buckling load is reached instantly, and failure occurs immediately, but this is not the situation in the actual world, where deflections are noticed as the load increases until it reaches a critical load as shown in Fig. 4.3.

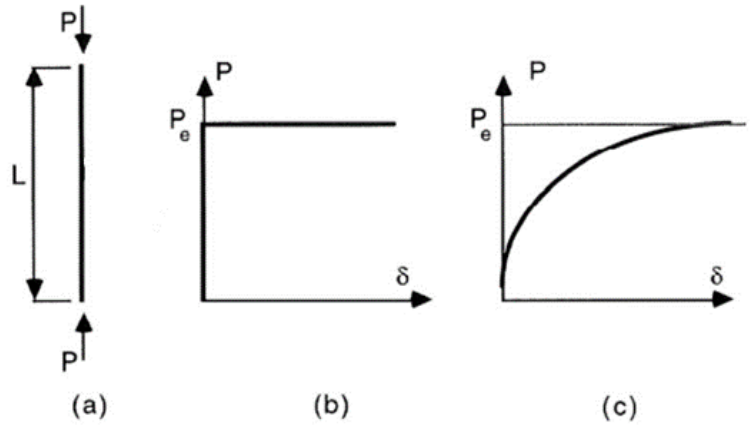

Figure 4-3 (a) Column Under a Load, (b) Ideal Euler Load-Deflection Curve, (c) Actual Load-Deflection Curve.

The FE model is illustrated as a perfect column up to complete failure. Abaqus deals a discontinuous problem by turn it into a problem with a regular (continuous) response instead of bifurcation, which can be solved by presenting a geometric imperfection pattern in the ideal (perfect) geometry of the model. In order to specify the suitable value of column imperfection factor, it's necessary to review civil engineering codes. Eurocodes, is the most important sources for obtaining the value of the imperfection factor.

In this section two verification are presented: the first verification to see which imperfection factors provided by Eurocodes gives satisfying results for the reference model, and the second verification by choosing different imperfection factor values in addition to reference model imperfection factor to investigate SFR strengthened distribution effect on the geometrical properties according to Eurocode.

4.3.1 First Verification

According to Eurocode 2 [9], an eccentricity (e_o) may be used as a simplified alternative for walls and isolated columns in braced systems to cover imperfections associated to normal execution variations.

$$e_o = \frac{l_o}{400} \quad (4\text{-}1)$$

where;

l_o: the effective length of the column.

or, according to Eurocode 3 (Eurocode 3), the eccentricity equal of:

$$e_o = \alpha_m \frac{L}{500} \quad (4\text{-}2)$$

$$\alpha_m = \sqrt{0.5(1 + \frac{1}{m})} \quad (4\text{-}3)$$

where;

L: the span of the bracing system.

α_m: the reduction factor for the number of columns in a row.

m: the number of columns in a row including only those columns which carry a vertical load.

Since all solid columns in this study were subjected to concentric load, other than hollow columns with variable load eccentricity except first hollow column, these solid columns will be verified.

clear length of column = 2000 mm

from equation 4-1, imperfection $e_o = \frac{l_o}{400} = \frac{2000}{400} = 5$ mm

from equation 4-2, imperfection $e_o = \alpha_m \frac{L}{500} = 1 \times \frac{2000}{500} = 4$ mm

These two values, in addition to zero imperfection (Euler's perfect column), will be used in FE simulation and compared with reference column SC1 experimental results.

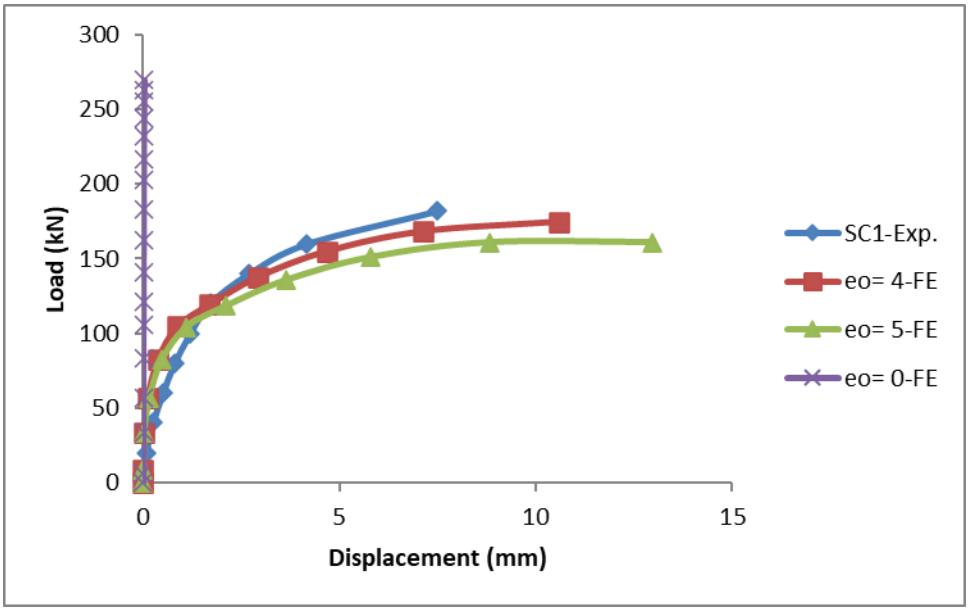

Figure 4-4 Load-Displacement Curves for Column SC1.

As illustrated in Figure 4-4 imperfection factor $e_o = 4$ is considered to be satisfactory, in the other hand the column with $e_o = 0$ will behave as Euler's perfect column by crashing at the middle as shown in Figure 4-5.

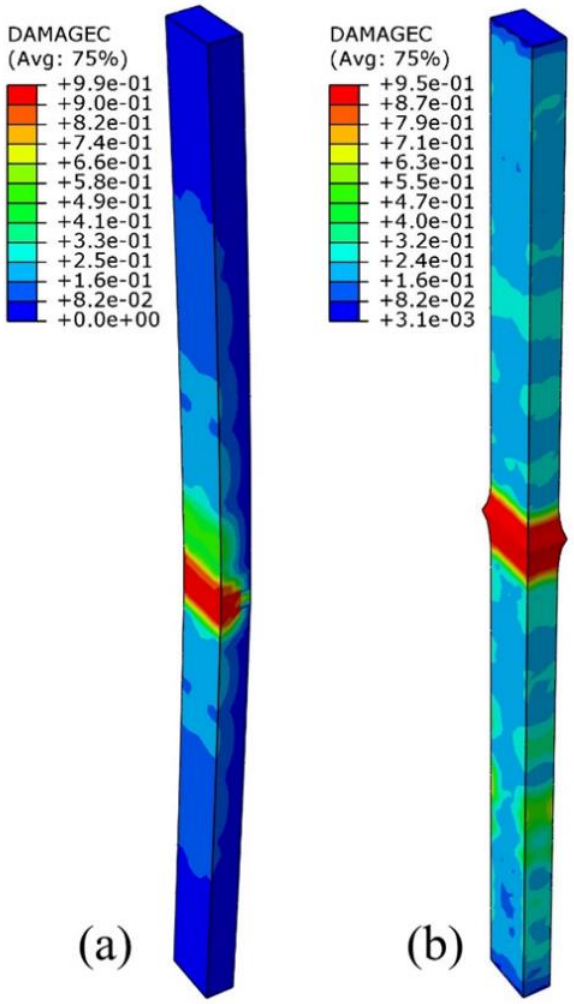

Figure 4-5 Column Failure; (a) Imperfection $e_o = 4$; (b) Imperfection $e_o = 0$.

4.3.2 Second Verification

This verification based on the effect of SFR on the slender RC column imperfection factor obtained from the Eurocode. Two values will be tested in addition to reference column imperfection factor value (1.5, 2.5, 4) to see how well the results match the experimental work as shown in Figure 4-6.

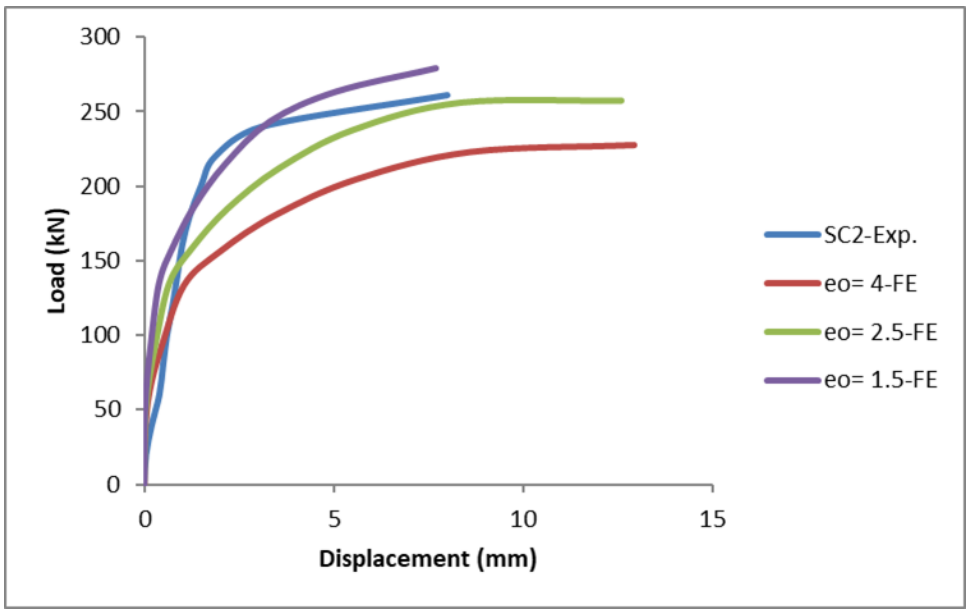

SFR strengthened column along the whole length.

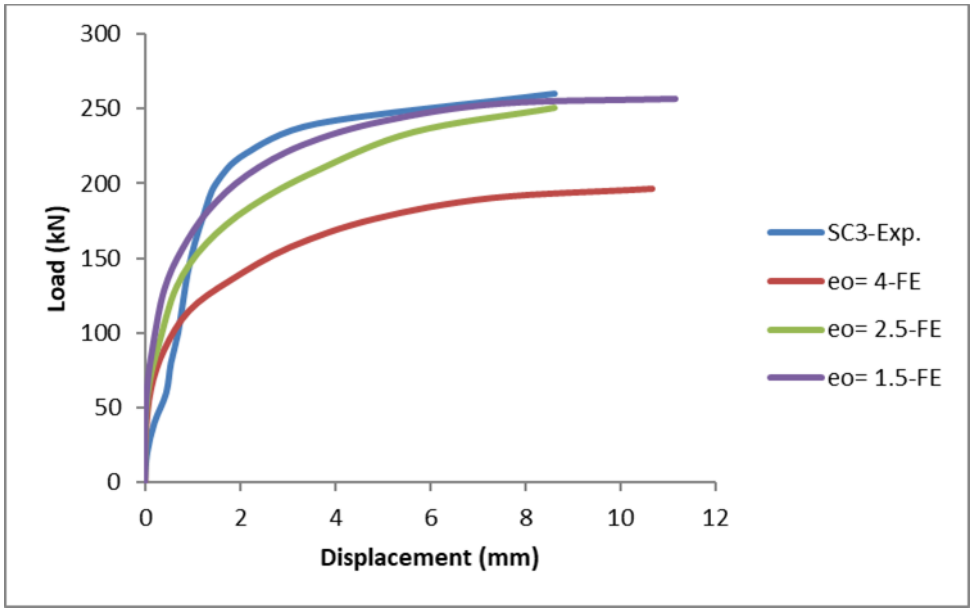

SFR strengthened column in the middle half (L/2).

Figure 4-6 Load-Displacement Curves of Solid Column Specimens with Various Imperfection Factor.

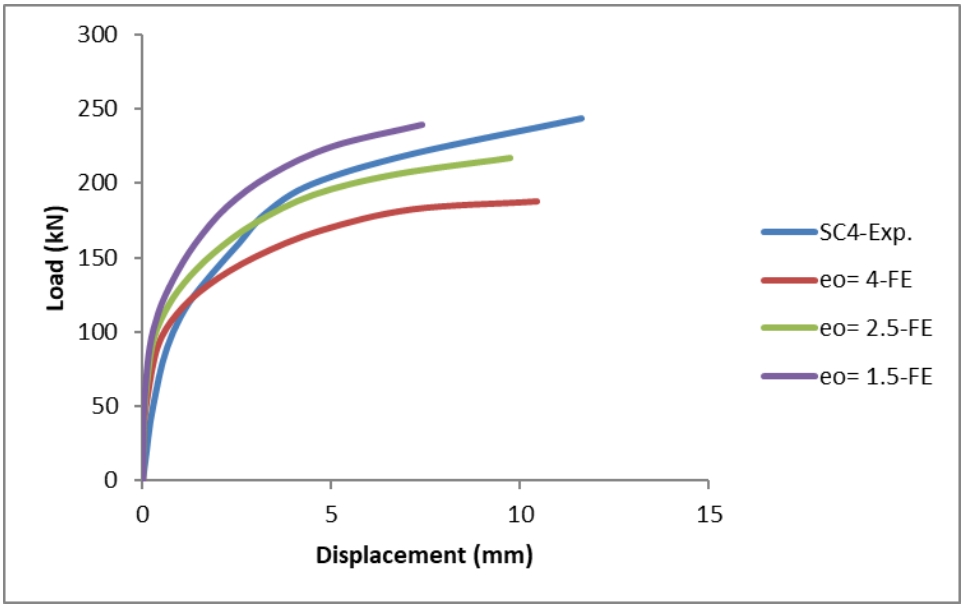

SFR strengthened column in the middle third (L/3).

Figure 4-6 Continued.

The use of steel fibers causes the variation in imperfection values. These fibers prevent concrete from spalling and boost the deformation capacity of concrete columns subjected to compressive axial load, allowing the ultimate load to vary in accordance with the SFR distribution [73]. As a result of the previous curves from Figure 4-6, the best values of imperfection factor that simulate the behavior of the real columns tested in the laboratory could be summarized as shown in Table 4.3.

Table 4-3 Column's Imperfection (e_o).

Column	SFR strengthening	Imperfection (e_o)
SC1	Non	4
SC2	L	1.5
SC3	L/2	1.5
SC4	L/3	2.5

The previous verification can be represented as a relationship between imperfection factor and SFR distribution length by curve showing different values for this factor which give a clear idea about concrete composite material deviation imperfection factor as shown in Figure 4-7.

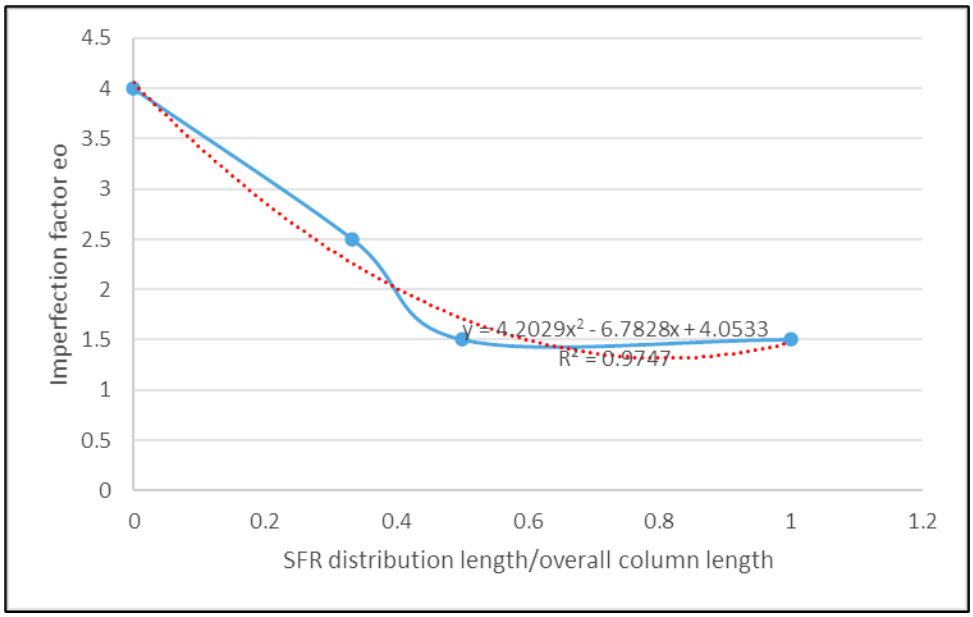

Figure 4-7 Imperfection-SFR Curve.

Although, by getting a graphical relationship it's easy to convert to mathematical equation that can be used to determine imperfection factor for RC slender column strengthened with SFR of any distribution length.

Since;

y = imperfection factor e_o

x = SFR (steel fiber reinforcement distribution length)

the suggested equation will be

$$e_o = 4.2029ySFR^2 - 6.7828\,SFR + 4.0533 \qquad 4\text{-}4$$

Noticed that the slender RC columns imperfection sensitivity is also included the hollow columns if they were concentrically loaded.

4.4 Finite Element Models Validation

The results of ultimate loads of the numerical RC column models ($P_{Ana.}$) were compared with the results of experimental tests ($P_{Exp.}$). A good agreement can be seen between these values as the ratio of ($P_{Ana.}$ / $P_{Exp.}$) as shown in Table 4-4. These ratios between FEA and experimental results showed an acceptable convergence. Therefore, the use of a program like ABAQUS is powerful in such cases.

Table 4-4 Numerical and Experimental Ultimate Load Results.

Column ID	$P_{Exp.}$ (kN)	$P_{Ana.}$ (kN)	$P_{Ana.}$ / $P_{Exp.}$
SC1	182	174.5	0.96
SC2	261	282	1.08
SC3	260	256.8	0.99
SC4	244	219	0.90
HC1	290	291.7	1.00
HC2	175	170.7	0.97
HC3	160	150.9	0.94
HC4	200	181	0.90
HC5	190	171	0.90

Also, the load-displacement curves obtained from the numerical study curves along with the experimental curves are presented and compared in Figure 4-8 and Figure 4-9. These figures show good agreement between the experimental and finite

element load-deflection results. These results prove the validation of the finite element models in the analysis of solid and hollow slender RC columns.

4.4.1 Load- Displacement Curves of Solid Column

The SFR-enhanced columns have a larger ultimate load than the reference column. Table 4-4 shows that the increases in ultimate load for SC2, SC3, and SC4 were 61.6%, 47.1, and 25.5, respectively. The inclusion of the SFR increases the compressive, tensile, and flexural strength of concrete, and consequently the strength of buckling. SFR added a significant increase in peak stress, a significant increase in the strain corresponding to peak stress, and a significant improvement in toughness. SFR in concrete columns subjected to compressive axial load, or combinations of axial load with fixed eccentricity, delay concrete spalling and increase deformation capacity.

For the three models SC2, SC3, and SC4 the increase in the length of the SFR along the column, caused an increase in the buckling load of the columns, as shown in the Figure 4-8. This leads to the fact that the overall length of the column controls the buckling capacity.

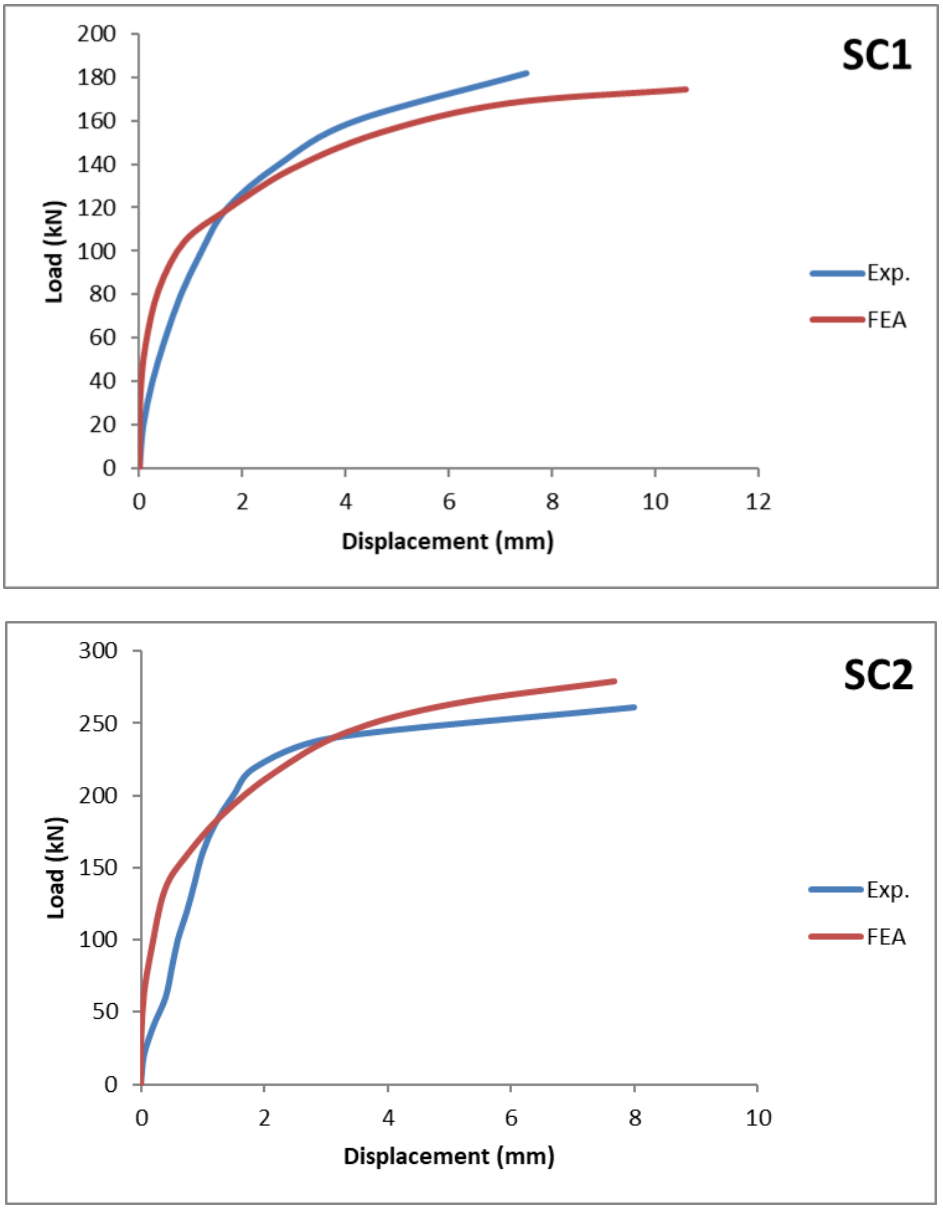

Figure 4-8 Experimental and Numerical Load-Displacement Curve of Solid Columns.

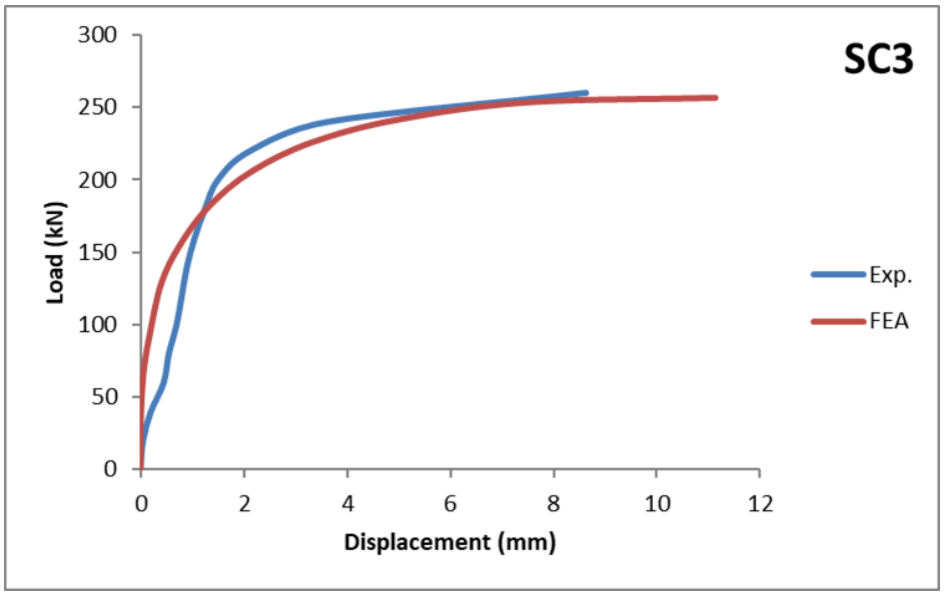

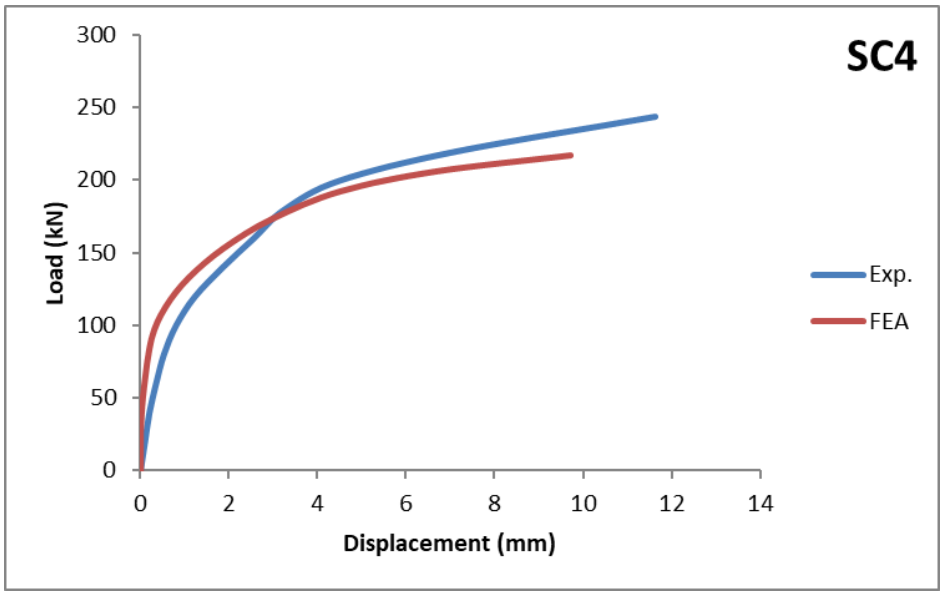

Figure 4-8 Continued.

4.4.2 Load- Displacement Curves of Hollow Column

The effect of the eccentricity and opening shape on slender hollow columns were studied, where the HC2 column was tasted by loading it with an eccentric distance perpendicular to the column's width, equal to one fourth of the column's thickness, which was 20 mm. In addition, the HC3 column was tested with an eccentric distance half the column thickness, which was 40 mm, columns HC4 and HC5 have the same details and loading conditions with respect to columns HC2 and HC3, except the opening shape was circular. The reference column HC1, which was evaluated under axial load, was compared to all four columns.

The load carrying capacity of columns HC2 and HC3 was reduced by 41.6% and 48.3%, respectively, when eccentricity values of 20 mm and 40 mm compared with the column HC1, as shown in the Figure 4-9.

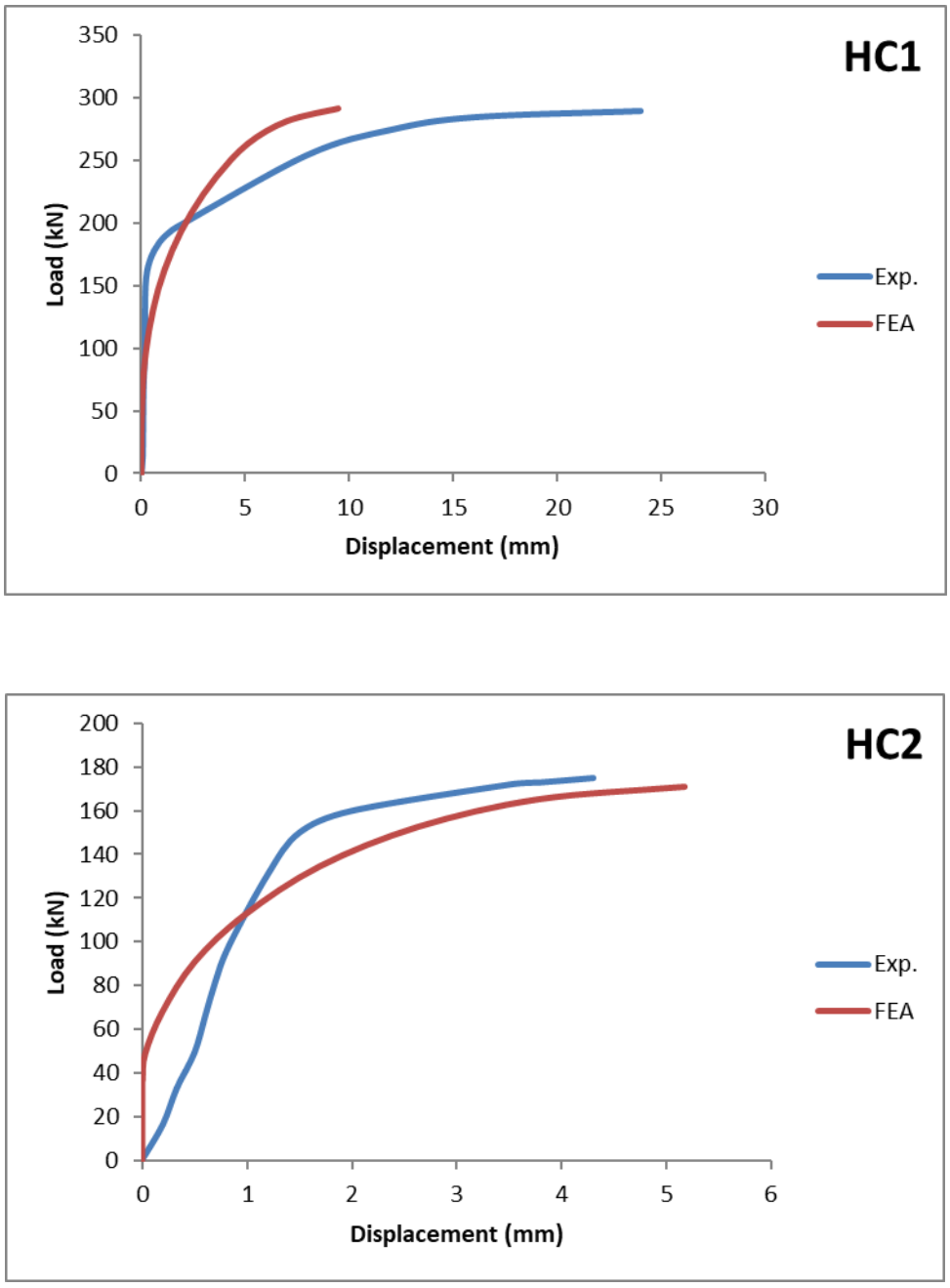

Figure 4-9 Experimental and Numerical Load-Displacement Curve of Hollow Columns.

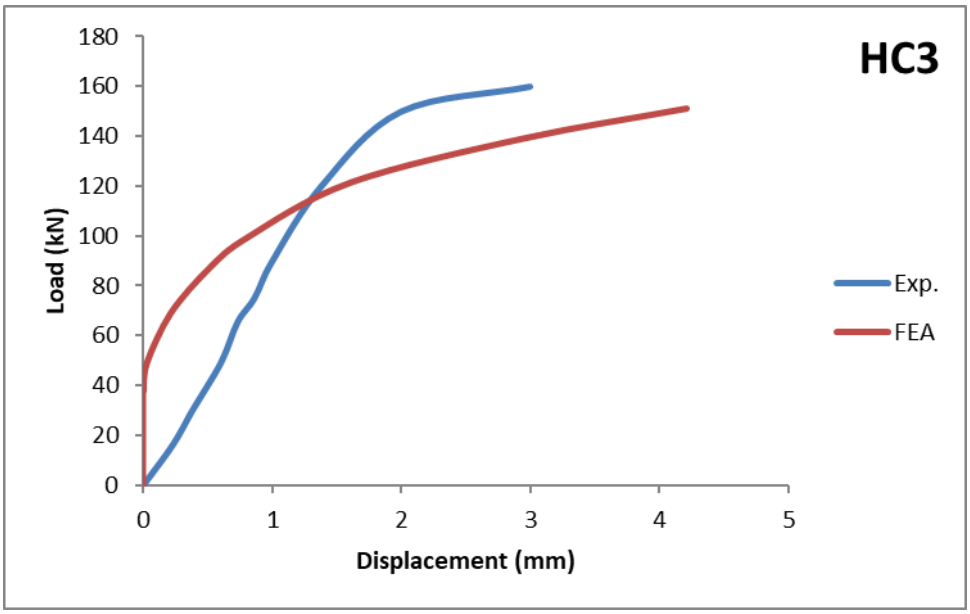

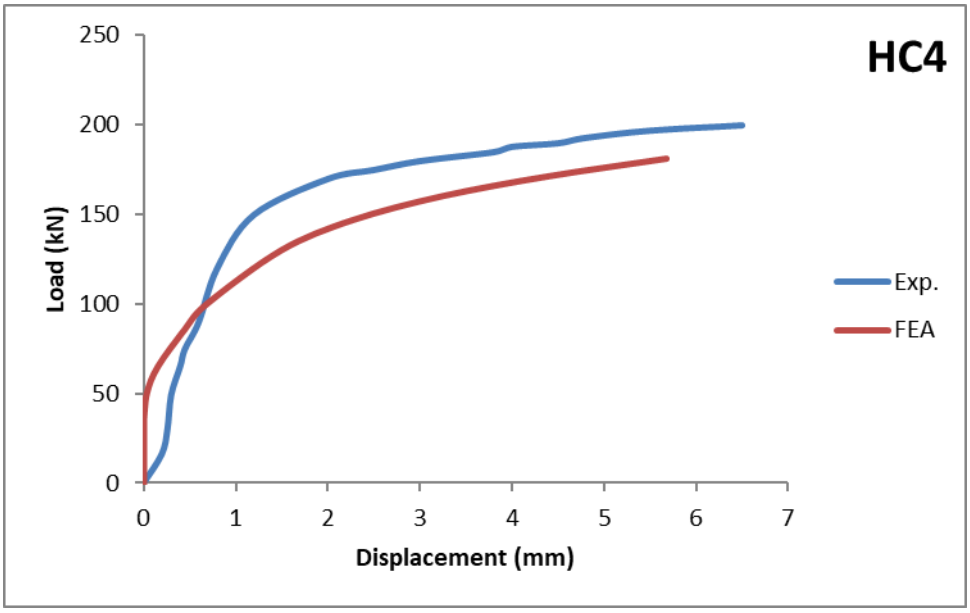

Figure 4-9 Continued.

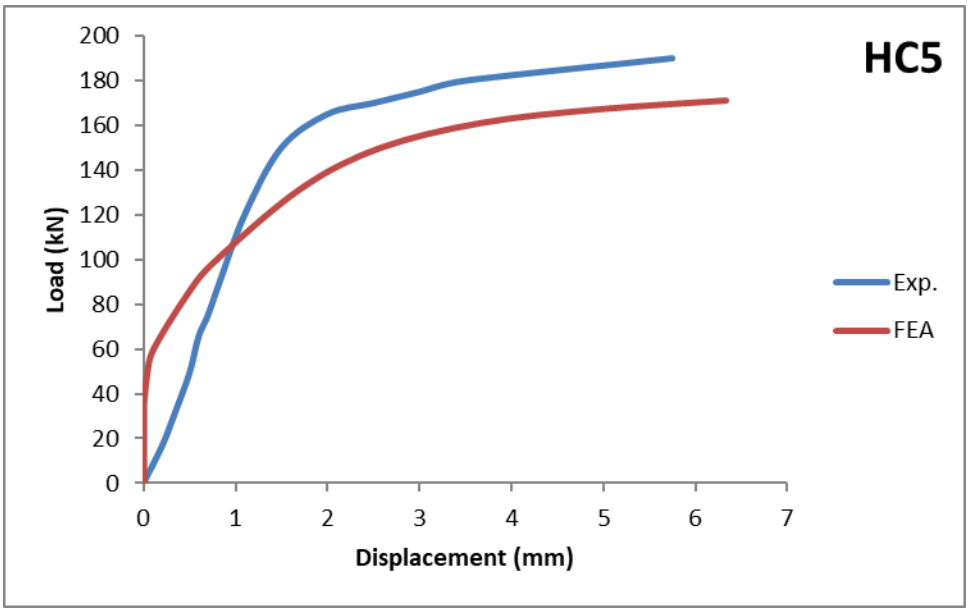

Figure 4-9 Continued.

4.5 Failure Mode

The failure mode of all models was buckling at the midpoint, as shown in Figure 4-10 and Figure 4-11, When the columns are loaded, they buckle in the middle and cracks occur in the areas of tension and compression in the middle of the column without causing the concrete to peel away, and the column subsequently fails in the form of crashing in the middle.

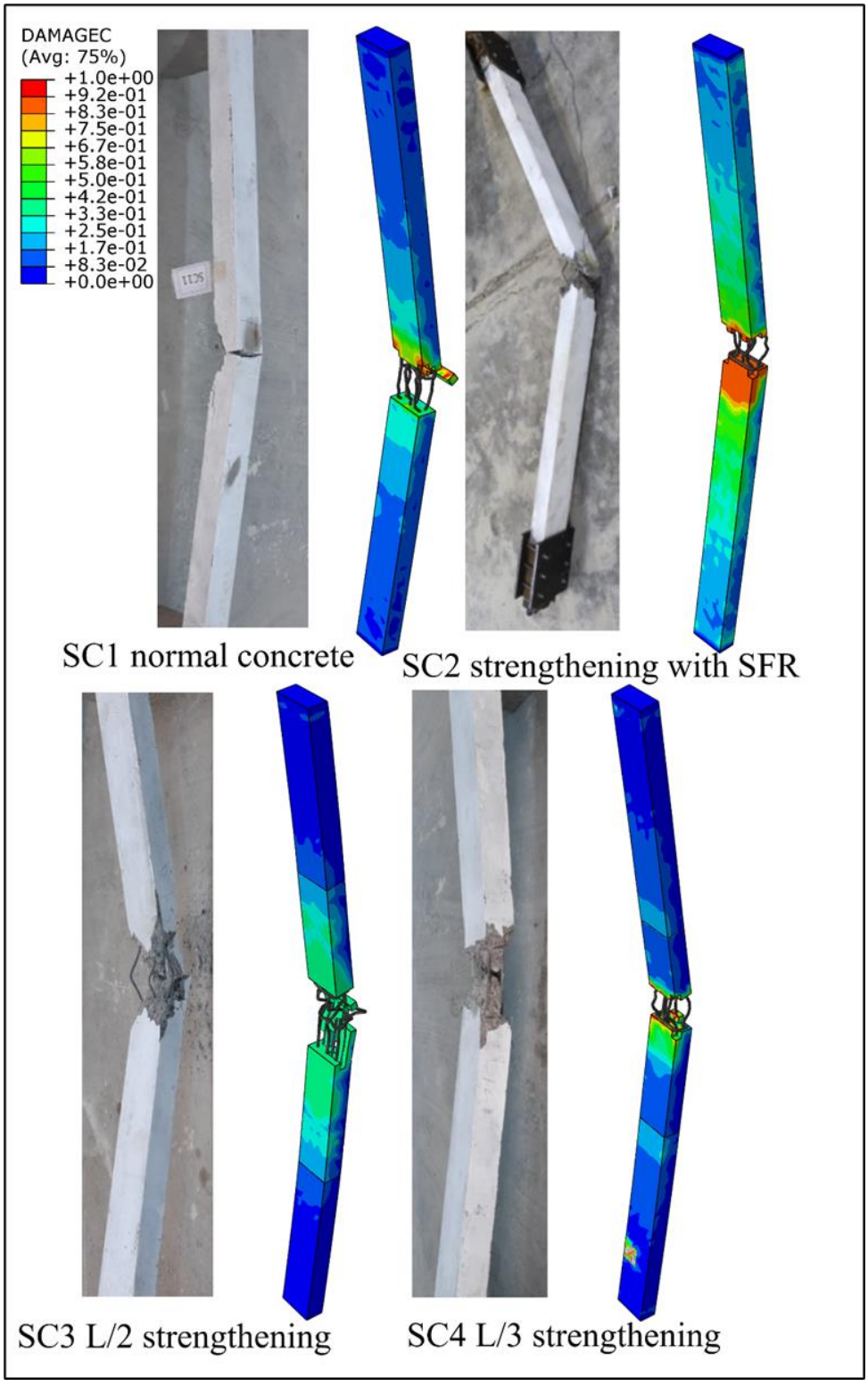

Figure 4-10 Numerical and Experimental Failure Modes of Solid Column Specimens.

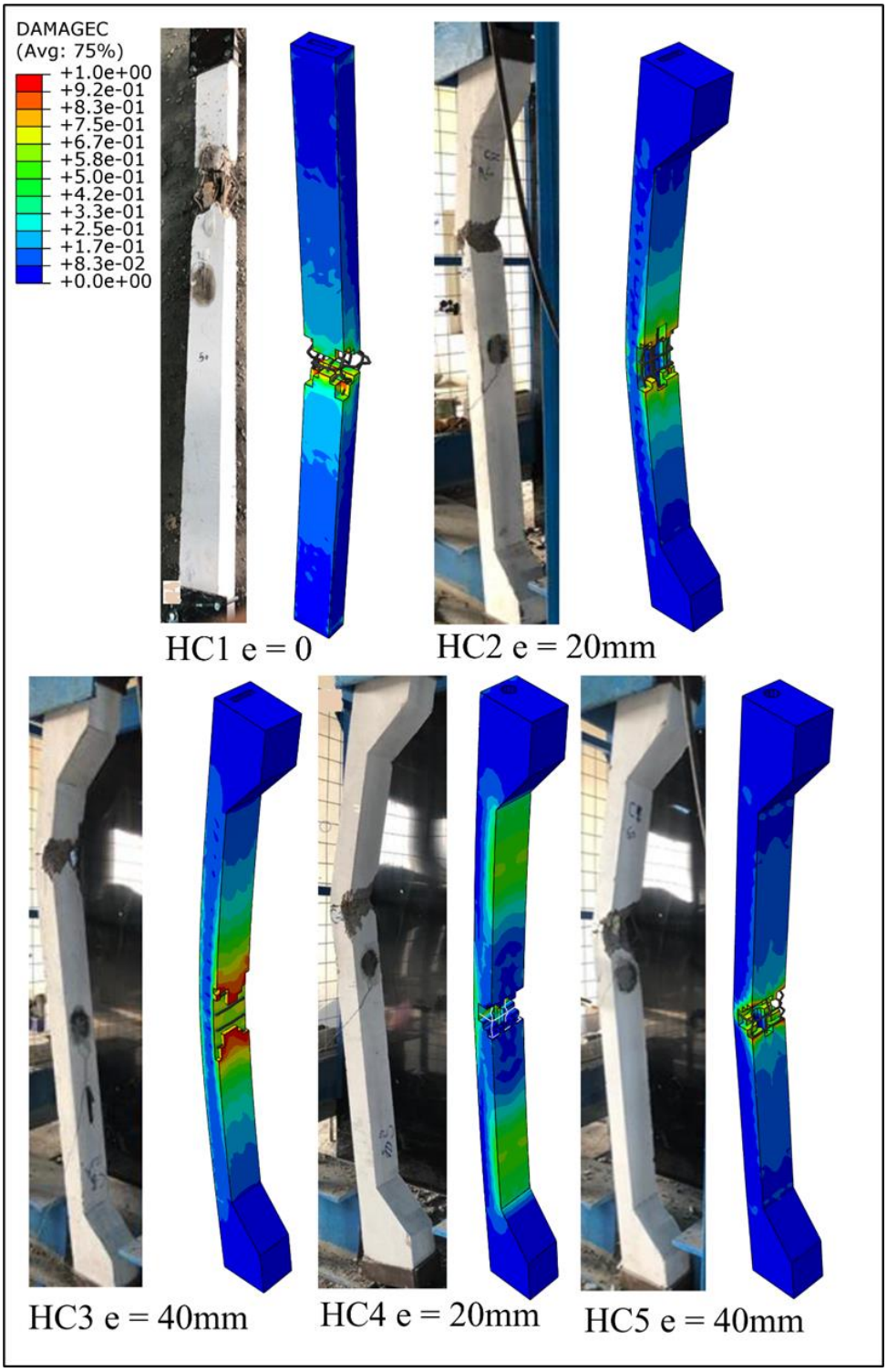

Figure 4-11 Numerical and Experimental Failure Modes of Hollow Column Specimens.

4.6 Parametric Study

Laboratory tests provide results without covering a large number of variables since it necessitates the use of expensive equipment and tools, as well as a specialized laboratory with qualified staff to complete the experiments and the finite element technique FEM is the most appropriate tool for expanding the range of parameters to be explored. Many parameters were taken into account in this section for solid and hollow columns includes slenderness ratio, concrete strength, section shape, load eccentricity, and strengthening with SFR.

4.6.1 Solid Column

Slenderness ratio, concrete strength, section shape, and load eccentricity are the parameters that were taken into account in this section for solid columns, the FEA model (SC1) was used as a reference as shown in Table 4-5.

Table 4-5 Solid Column Parametric Study Details and Results.

Model	Section shape	Cross section (mm)	Length (mm)	Slenderness ratio	Load eccentricity (mm)	f´c (MPa)	Ultimate load (kN)	UP/UR
SC1	Rectangular	60×120	2	115	0	28	182	1.00
SP1	Rectangular	60×120	1.5	87	0	28	194	1.07
SP2	Rectangular	60×120	2.5	144	0	28	172	0.95
SP3	Rectangular	60×120	3	173	0	28	169	0.93
SP4	Rectangular	60×120	2	115	0	25	160	0.88
SP5	Rectangular	60×120	2	115	0	32	197	1.05
SP6	Rectangular	60×120	2	115	0	36	230	1.26
SP7	Square	85×85	2	115	0	28	191	1.05
SP8	Circular	Ø96	2	115	0	28	185	1.02
SP9	Elliptical	a,b=130,70	2	115	0	28	171	0.94
SP10	Rectangular	60×120	2	115	20	28	57	0.31
SP11	Rectangular	60×120	2	115	30	28	32	0.18
SP12	Rectangular	60×120	2	115	40	28	20	0.11

4.6.1.1 Slenderness Ratio

Three different slenderness ratio parameters were selected (87, 144, and 173), to study and compared to reference column (SC1) of 115 slenderness ratios.

Load- deflection curve comparison of the results showed that higher slenderness ratio means a lower critical stress that will cause buckling, in the other word, increasing the slenderness ratio means decreasing the stiffness of the slender column that means the geometrical parameter controlled the buckling, the decreasing of slenderness ratio of column (SP1) lead to increase the ultimate load by 7% with respect to (SC1), and the increasing of slenderness ratio of columns (SP2) and (SP3) lead to decrease the ultimate load by 5% and 7% with respect to (SC1), as shown in Figure 4-12.

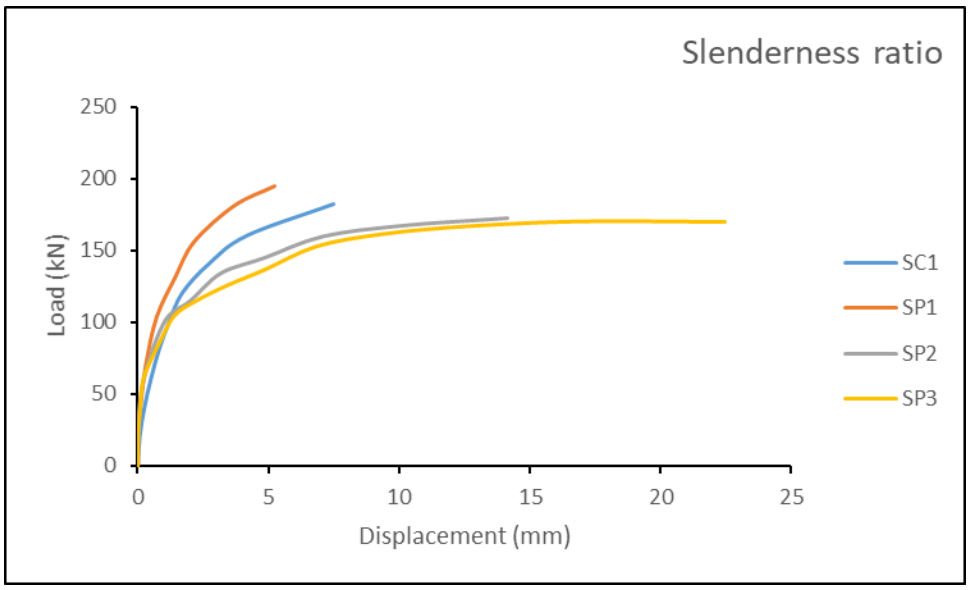

Figure 4-12 Load-Displacement Curves of Slenderness Ratio Parameter.

All three columns fail by buckling at mid-point as shown in Figure 4-13.

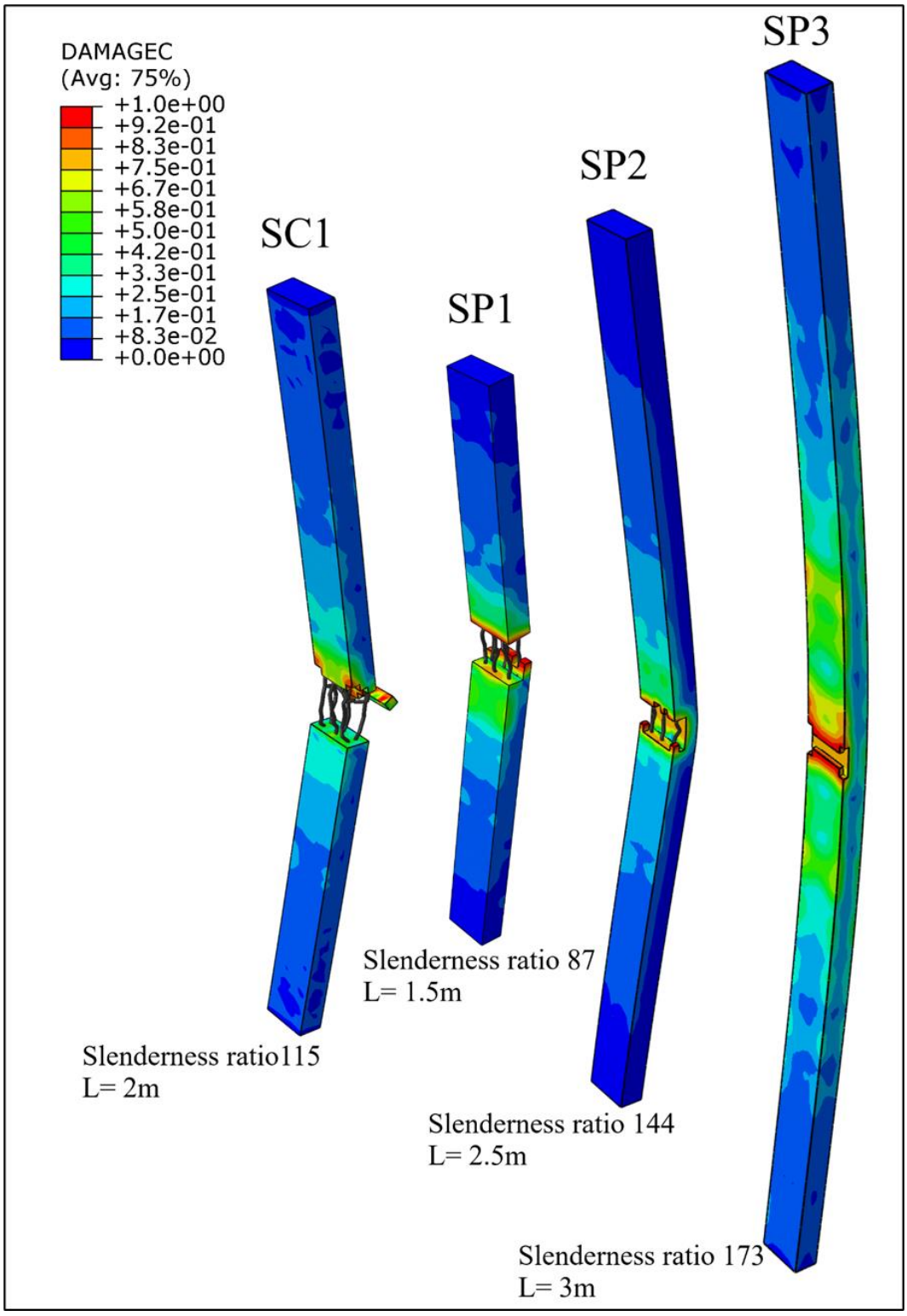

Figure 4-13 Slenderness Ratio Parametric Study Failure Modes.

4.6.1.2 Concrete Compressive Strength

Three different concrete compressive strength parameters were selected (25, 32, and 36 MPa), to study and compared to reference column (SC1) of 28 MPa compressive strength.

Figure 4-14 shows that the increase of concrete strength leads to increase of column buckling resistance, it means that the ultimate failure load of slender column was increased with the increase of concrete strength. The ultimate load of column (SP4) decreased by 12%, whilst columns (SP5) and (SP6) ultimate load increased by 5% and 26% respectively with respect to reference column (SC1). On the basis of the carried out results it can be stated that columns with constant slenderness ratio and same material, buckling strength increase with the increase of material compressive strength.

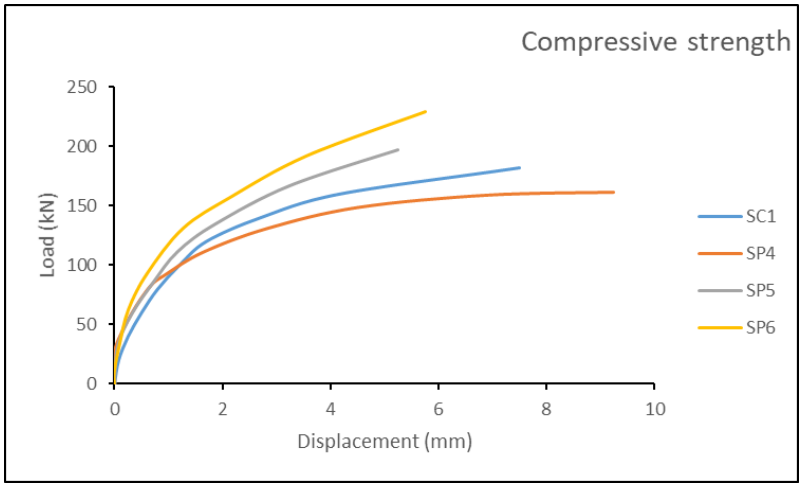

Figure 4-14 Load-Displacement Curves of Concrete Compressive Strength Parameter.

The failure modes are shown in Figure 4-15 below, which shows mid- point buckling for all three columns.

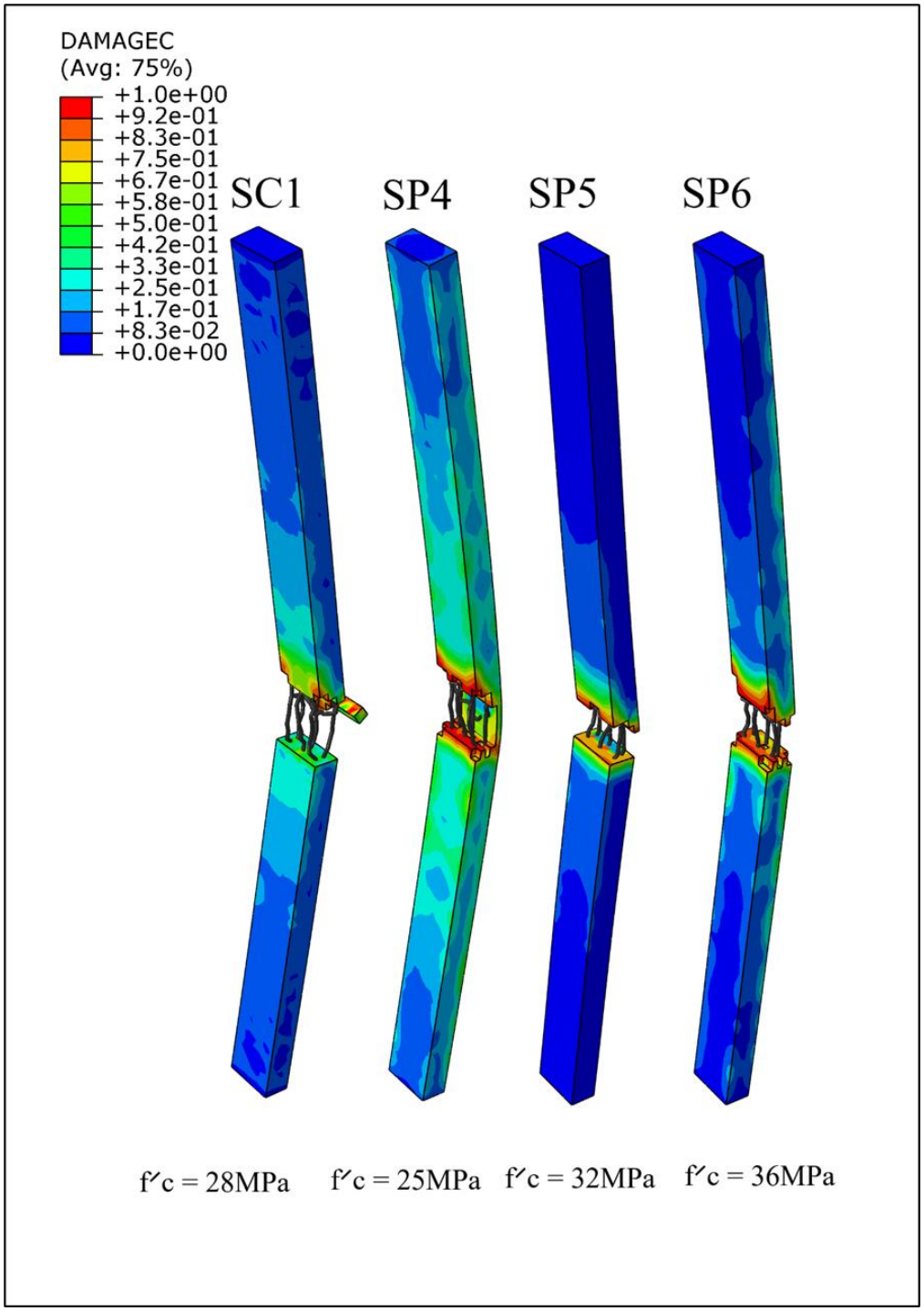

Figure 4-15 Concrete Compressive Strength Parametric Study Failure Modes.

4.6.1.3 Section Shape

The three section shapes of this parameter were selected (square, circular, and elliptical) with equivalent section area of the rectangular reference column, all these columns have a different moment of inertia about the critical buckling axis.

According to the comparison between the obtained results it was found that the square and the circular columns buckling strength increased by 5% and 2% respectively with respect to the reference rectangular column. Square and circular columns are the most effective shapes because the centroid is symmetry about all the axis. Also, the moment of inertia of the circular and square columns will be much higher than that of the rectangular columns, that increase buckling strength. The elliptical column buckling strength decreased by 6% with respect to the reference rectangular column as shown in Figure 4-16.

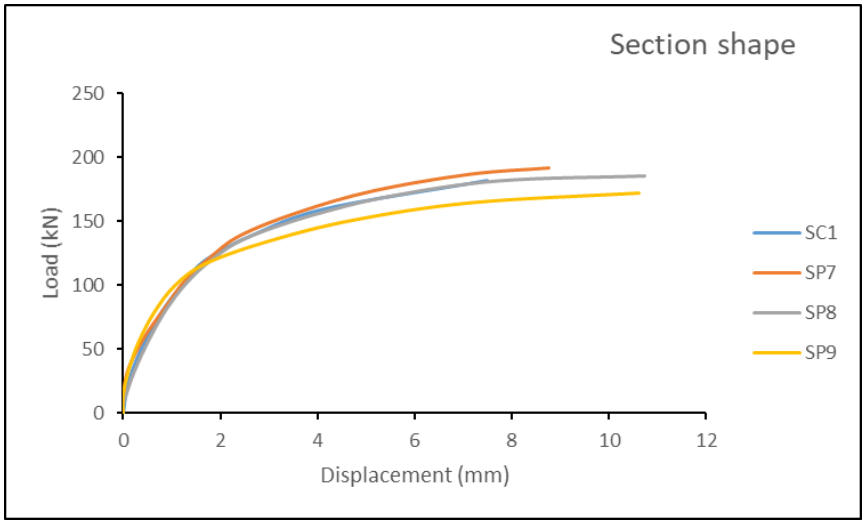

Figure 4-16 Load-Displacement Curves of Section Shape Parameter.

The obtained failure modes of different section shape columns are shown in Figure 4-17 below.

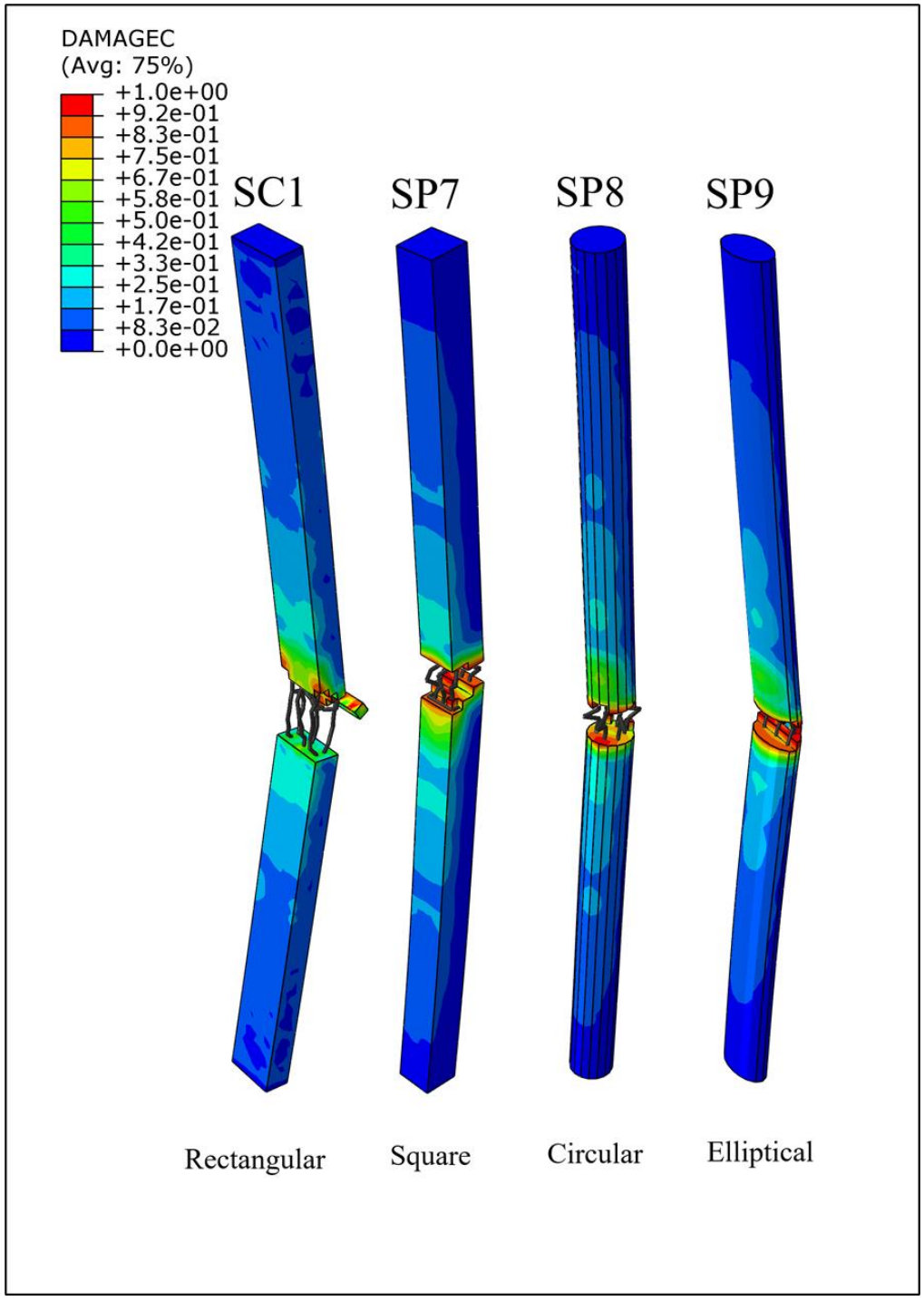

Figure 4-17 Section Shape Parametric Study Failure Modes.

4.6.1.4 Load Eccentricity

Three different load eccentricities were taking (20, 30, and 40 mm) to study and compare with the reference column of zero load eccentricity.

The obtained results shows that the eccentric loads will cause moment in column that led to earlier buckling failure, compare to reference column (SC1), the load eccentricity of (SP10), (SP11), and (SP12) show that the ultimate load decreased by 69%, 82%, and 89% respectively as shown in Figure 4-18. The buckling strength of slender column with concentric load depends on the yield strength the material before reaching the buckling point but with increasing the load eccentricity decreases this stage and causes earlier moments that led column to buckle.

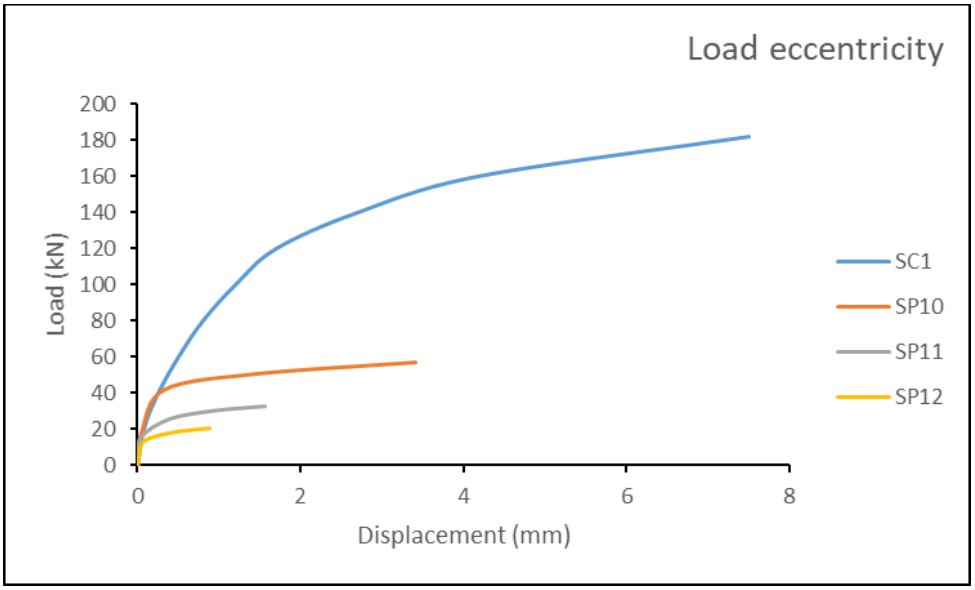

Figure 4-18 Load-Displacement Curves of Load Eccentricity Parameter.

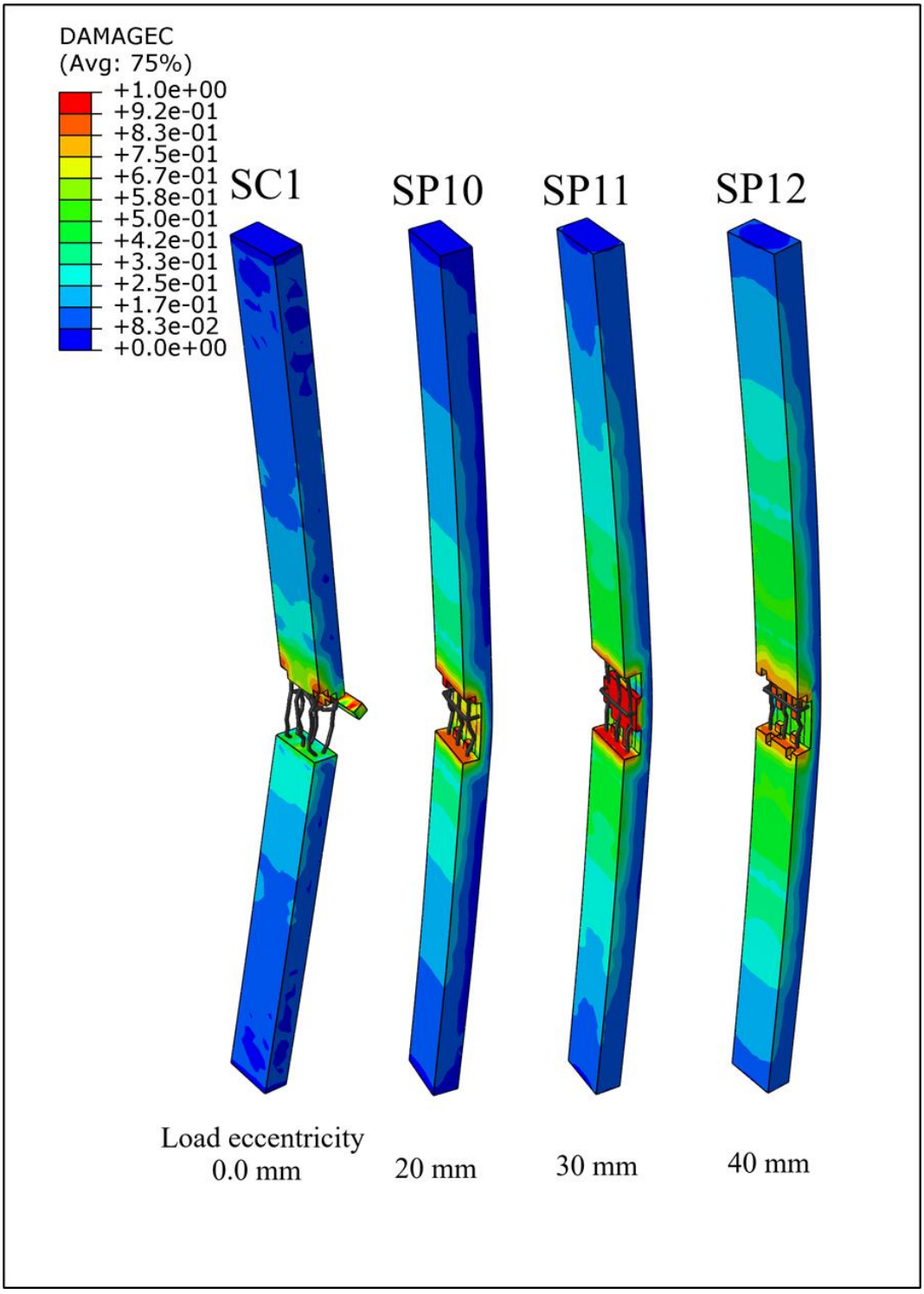

Figure 4-19 Load Eccentricity Parametric Study Failure Modes.

4.6.2 Hollow Column

Slenderness ratio, section shape, concrete strength, and strengthening with SFR are the parameters that were taken into account in this section for hollow columns, the FEA model (HC1) was used as a reference as shown in Table 4-6.

Table 4-6 Hollow Column Parametric Study Details and Results.

Model	Section shape	Cross section (mm)	Length (mm)	Slenderness ratio	SFR strengthening	f´c (MPa)	Ultimate load (kN)	UP/UR
HC1	Rectangular	80×140	2	80	Non	35	291.69	1.00
HP1	Rectangular	80×140	1.5	60	Non	35	316.99	1.09
HP2	Rectangular	80×140	2.5	100	Non	35	273.75	0.94
HP3	Rectangular	80×140	3	120	Non	35	261.86	0.90
HP4	Square	106×106	2	80	Non	35	327.48	1.12
HP5	Circular	Ø119	2	80	Non	35	326.66	1.12
HP6	Elliptical	a,b=80,44	2	80	Non	35	290.53	0.99
HP7	Rectangular	80×140	2	80	Non	25	231.98	0.79
HP8	Rectangular	80×140	2	80	Non	40	320.05	1.09
HP9	Rectangular	80×140	2	80	Non	45	349	1.2
HP10	Rectangular	80×140	2	80	L	35	349	1.2
HP11	Rectangular	80×140	2	80	L/2	35	388.68	1.33
HP12	Rectangular	80×140	2	80	L/3	35	326.82	1.12

4.6.2.1 Slenderness Ratio

Three different slenderness ratio parameters were selected (60, 100, and 120), to study and compared to reference column (HC1) of 80 slenderness ratio.

Load- deflection curve comparison of the results showed that higher slenderness ratio means a lower critical stress that will cause buckling, in the other word, increasing the slenderness ratio means decreasing the stiffness of the slender column,

the decreasing of slenderness ratio of column (HP1) lead to increase the ultimate load by 9% with respect to (HC1), and the increasing of slenderness ratio of columns (HP2) and (HP3) lead to decrease the ultimate load by 6% and 10% with respect to (HC1), as shown in Figure 4-20.

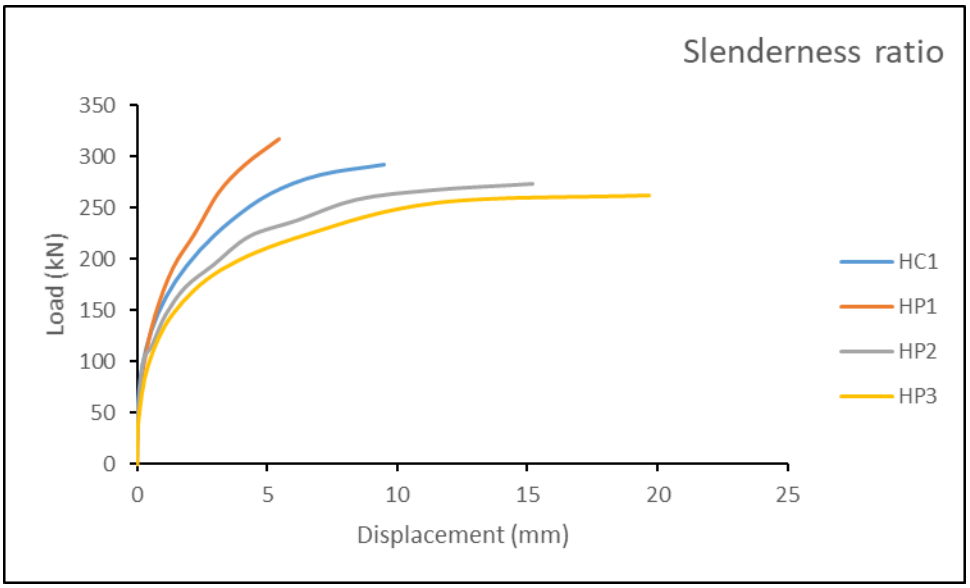

Figure 4-20 Load-Displacement Curves of Slenderness Ratio Parameter.

Figure 4-21 shows the failure modes of the three different slenderness ratio columns.

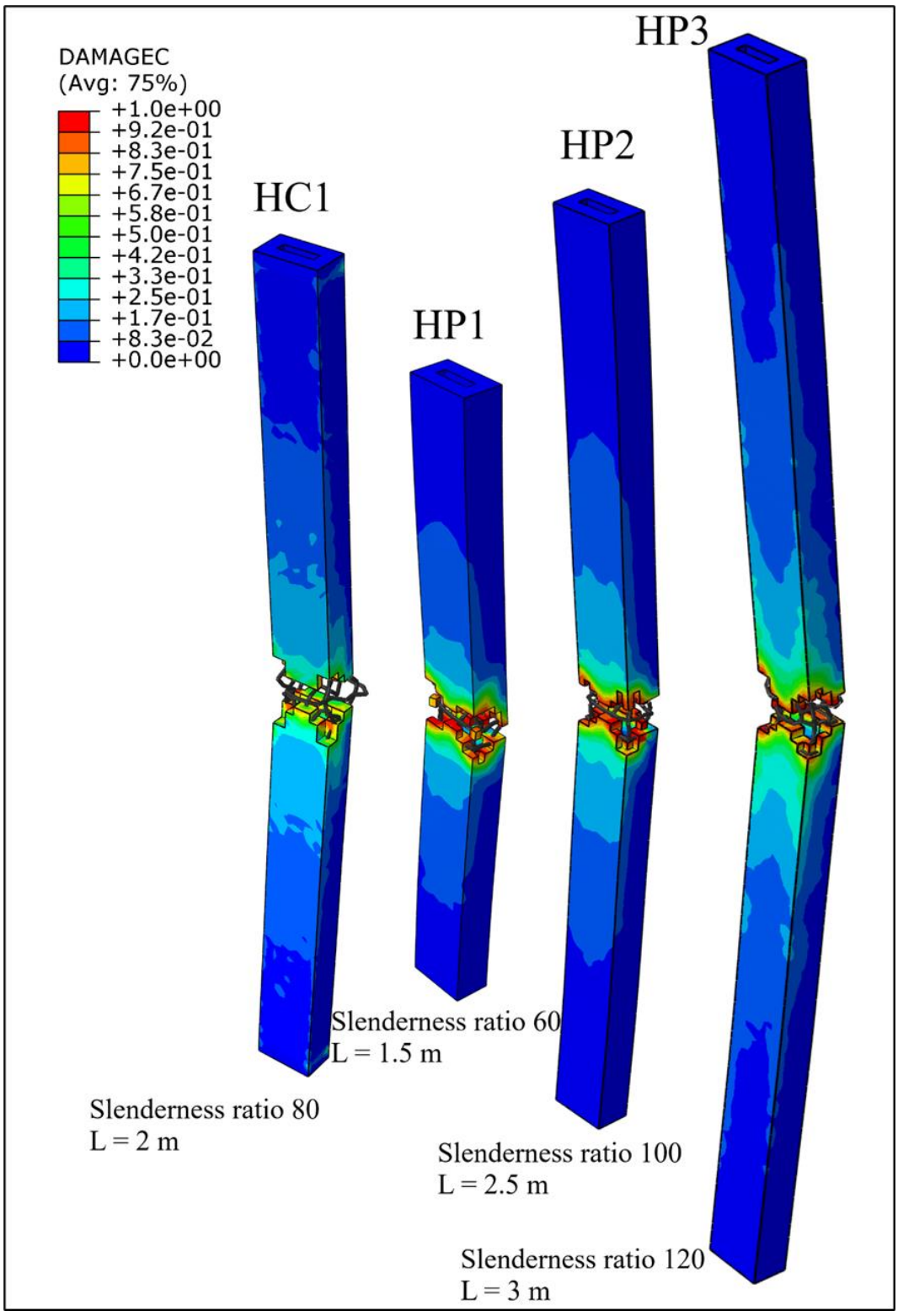

Figure 4-21 Slenderness Ratio Parametric Study Failure Modes.

4.6.2.2 Section Shape

Same as solid column, three section shapes of this parameter were selected (square, circular, and elliptical) with equivalent section area of the rectangular reference column, all these columns have a different moment of inertia about the critical buckling axis.

According to the comparison between the obtained results it was found that the square and the circular columns buckling strength increased by 12% both with respect to the reference rectangular column. Square and circular columns are the most effective shapes because the centroid is symmetry about all the axis. Also, the moment of inertia of the circular and square columns will be much higher than that of the rectangular columns, that increase buckling strength. The elliptical column buckling strength decreased by 1% with respect to the reference rectangular column as shown in Figure 4-22.

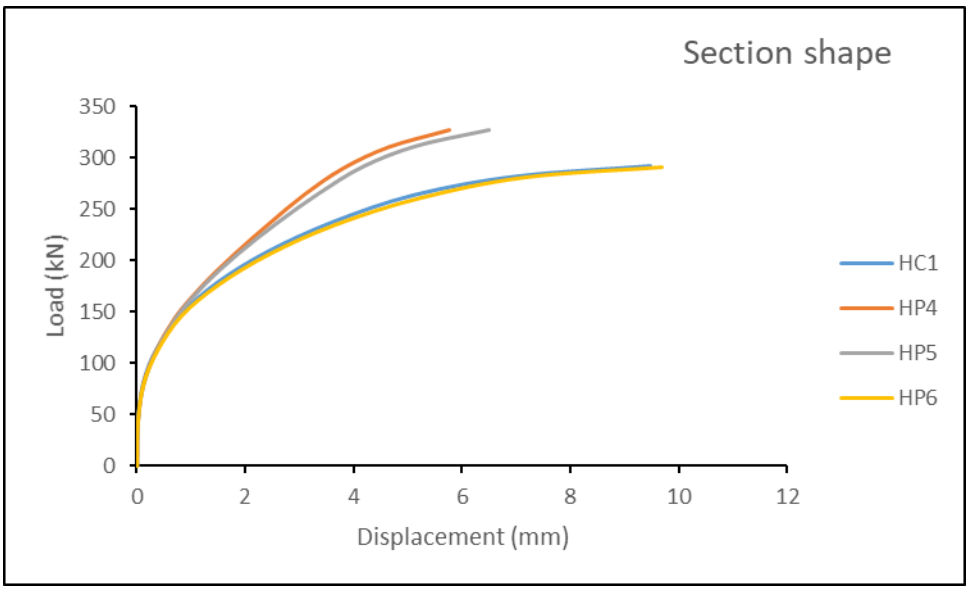

Figure 4-22 Load-Displacement Curves of Section Shape Parameter.

The obtained failure modes of different section shape columns are shown in Figure 4-23 below.

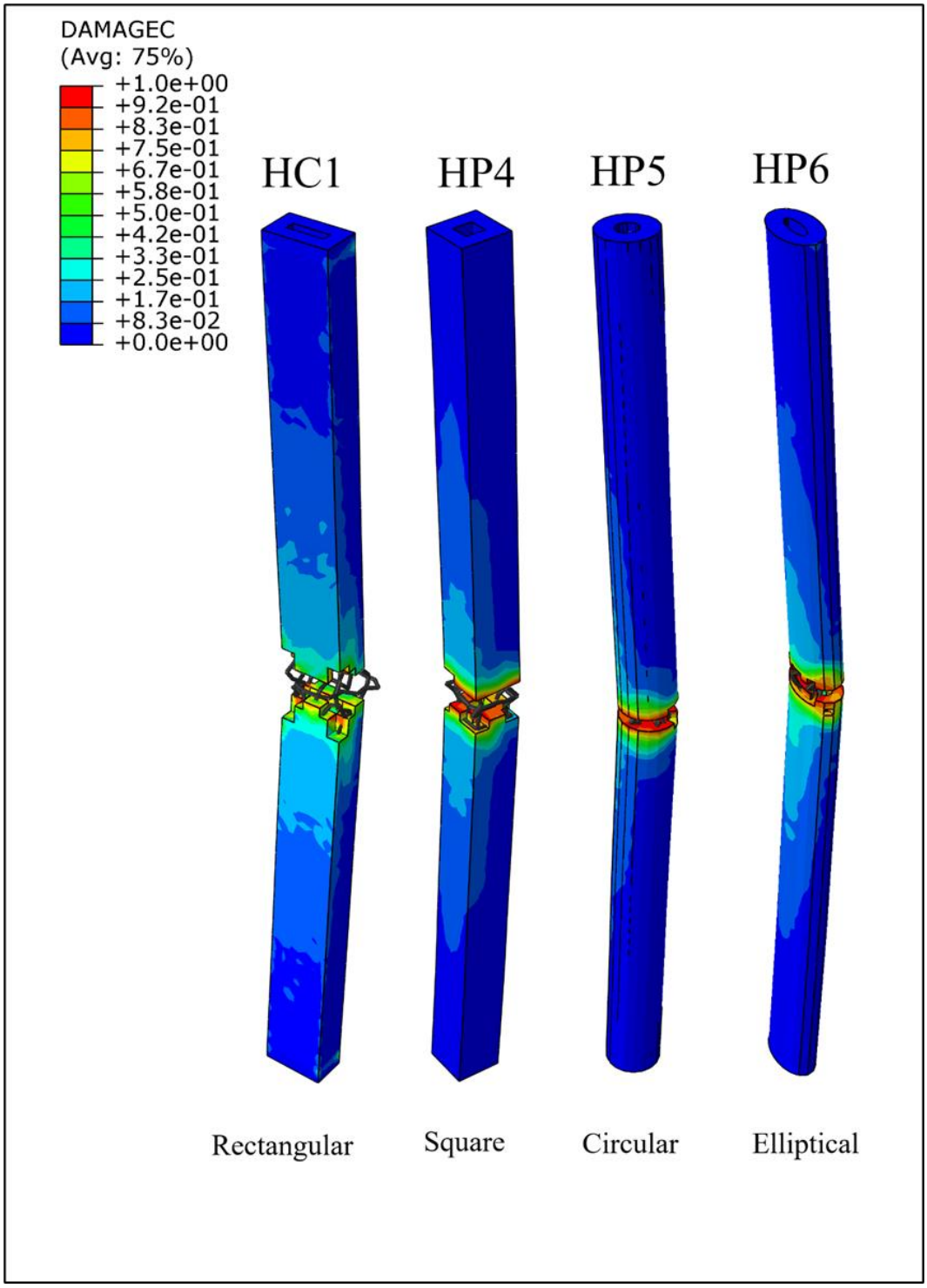

Figure 4-23 Section Shape Parametric Study Failure Modes.

4.6.2.3 Concrete Compressive Strength

Three different concrete compressive strength parameters were selected (25, 40, and 45 MPa), to study and compared to reference column of 35 MPa. Figure 4-24 shows that the increase of concrete strength led to increase of column buckling strength, it means that the ultimate failure load for a slender column was increased with the increase of concrete strength. The ultimate load of column (HP7) decreased by 21%, while columns (HP8) and (HP9) ultimate load increased by 9% and 20% respectively with respect to reference column (HC1). From the obtained results it's found that columns with constant slenderness ratio and same material, buckling strength increase with the increase of material compressive strength.

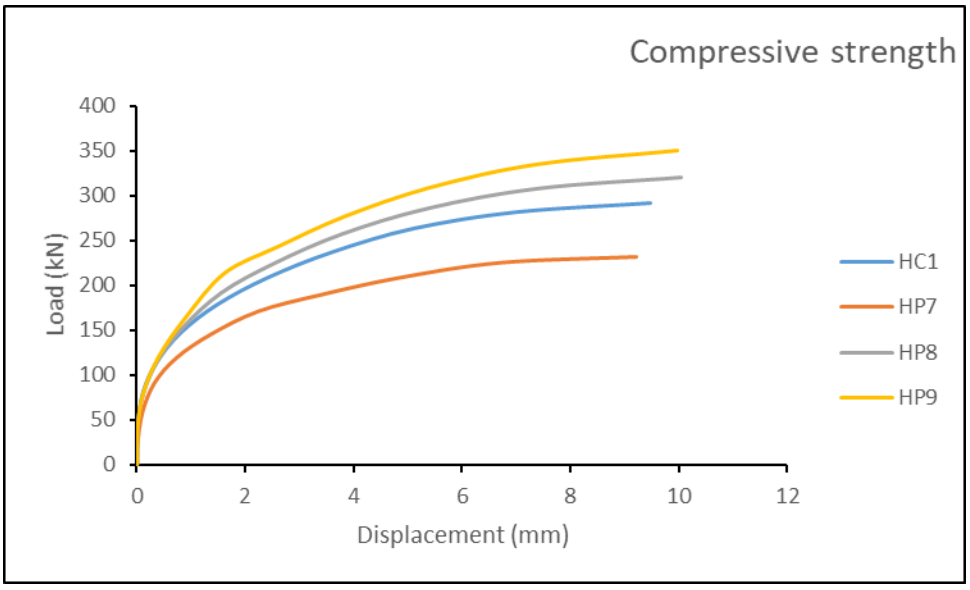

Figure 4-24 Load-Displacement Curves of Concrete Compressive Strength Parameter.

The failure modes are shown in Figure 4-25 below, which shows mid- point buckling for all three columns.

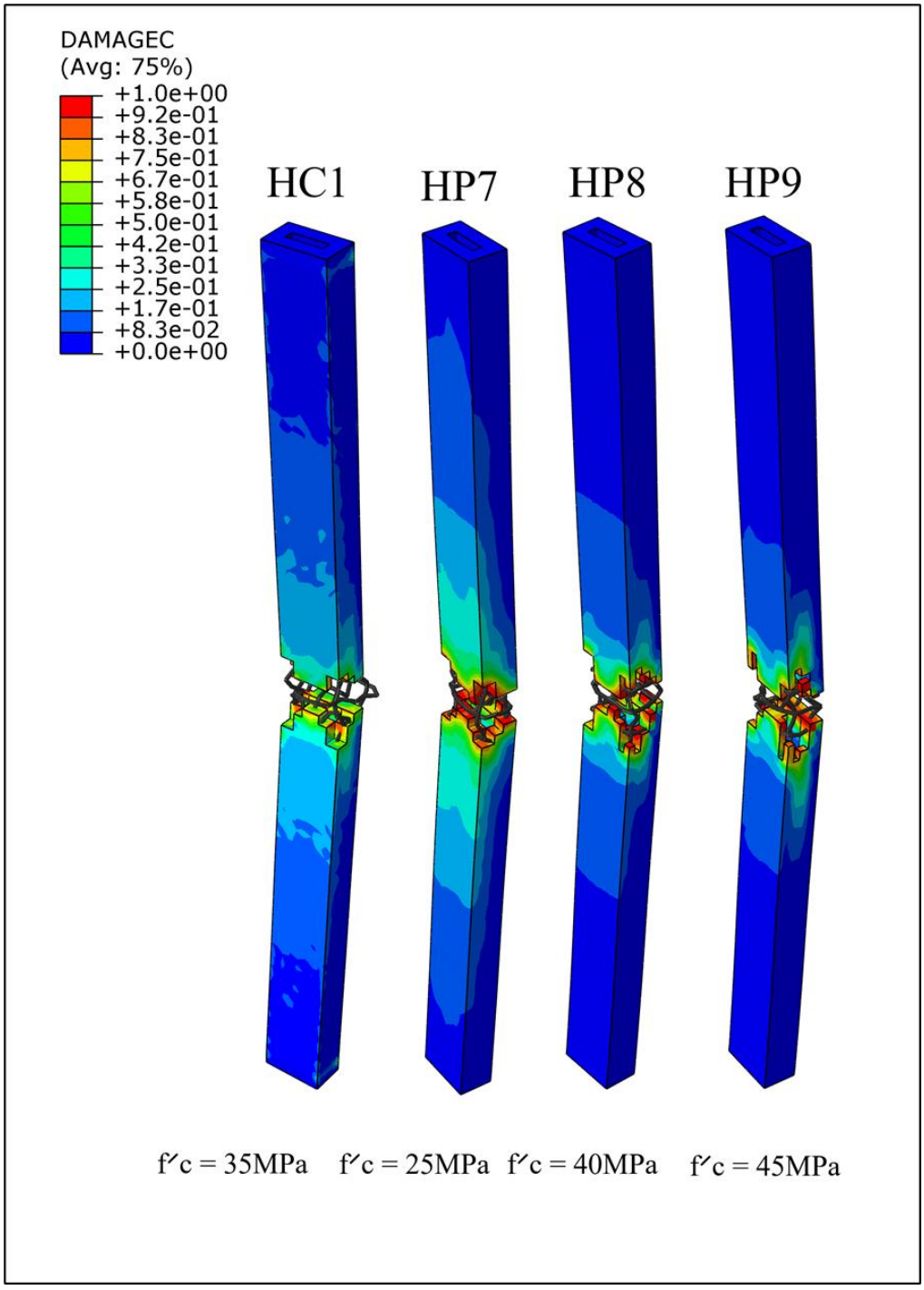

Figure 4-25 Concrete Compressive Strength Parametric Study Failure Modes.

4.6.2.4 Strengthening with SFR

The three different lengths of SFR strengthening that used on the experimental solid columns. All length strengthened with SFR (L), half of length strengthened with SFR (L/2), and one third strengthened with SFR (L/3), to study and compare with the reference column of normal concrete.

The obtained results shows that the ultimate load of column (HP10) with all length strengthened with SFR, (HP11) with L/2 strengthened with SFR, and (HP12) with L/3 strengthened with SFR were 20%, 33%, and 12% respectively compared to the reference column with normal concrete as shown in Figure 4-26.

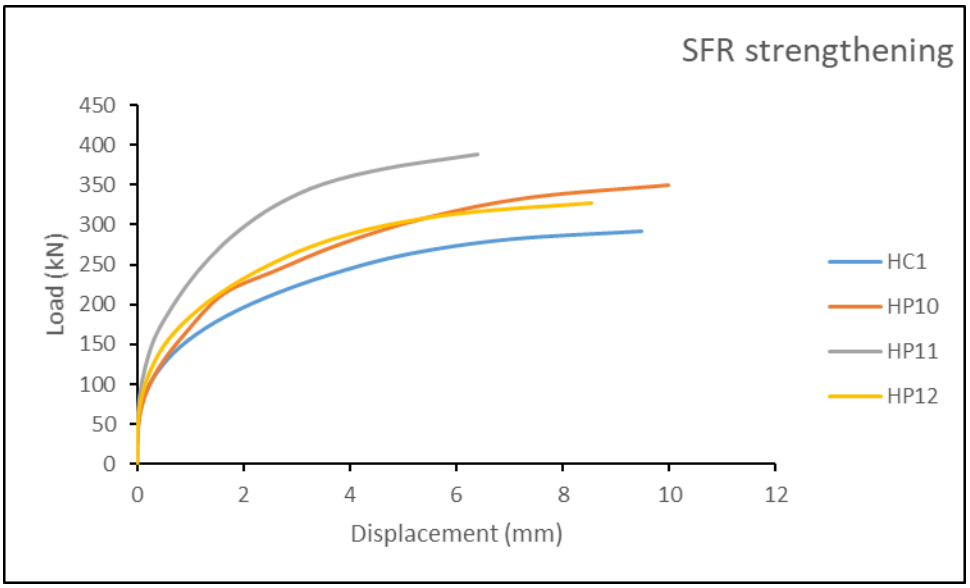

Figure 4-26 Load-Displacement Curves of SFR Strengthening Parameter.

The failure modes of this parameter shows that the column fails by buckling at the mid- point as shown in Figure 4-27.

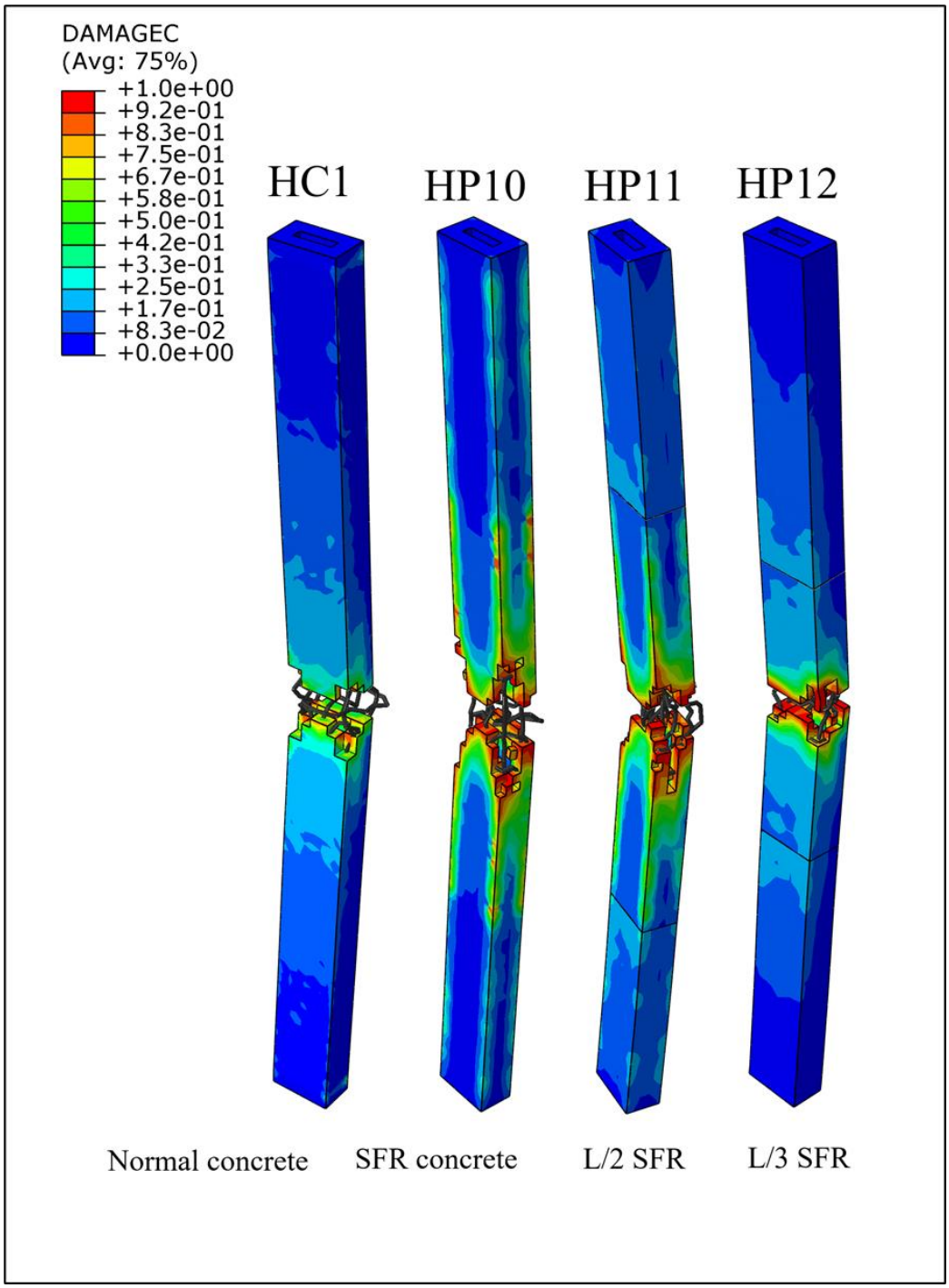

Figure 4-27 Strengthening Parametric Study Failure Modes.

CHAPTER FIVE: CONCLUSIONS AND RECOMMENDATIONS

5.1 Conclusions

The main objective of the present study is to accomplished a nonlinear finite element analysis is employed to simulate the solid and hollow slender RC columns to investigate the columns buckling behavior under concentric and eccentric loading including various parameters.

The following are conclusions that may be drawn from the numerical work:

1. In real life, there is no perfect column, and this imperfection represented in the form of a variable value (factor) according to the Eurocode, this imperfection factor depends on the length of the slender RC column, and it is necessary for numerical calculations of RC columns and cannot be neglected.
2. If the RC slender columns strengthened with SFR in different proportions from its length, the imperfection factor will not depend on RC columns length only, but also on the distribution of SFR.
3. An equation can be derived that represents the relationship between the imperfection factor variance and SFR at any distribution percentage in the middle length of the RC slender column based on the comparison between experimental and numerical results.

4. The new element deletion method of analyses included in ABAQUS 2019 version and above provides more realistic failure visualization especially for crash (damage) analyses than the standard method.
5. Although the slender column material is concrete, Eurocode 3 provides the closest imperfection values even though it is for designing the steel structures than Eurocode 2, that means RC slender column with high reinforcement ratio (ϱ) will behave more likely steel column at buckling.
6. Decreasing columns length will decrease slenderness ratio and led to increase the ultimate load, in the other hand the increasing in columns length will increase the slenderness ratio and led to decrease the ultimate load.
7. When the concrete compressive strength (f´c) of the column decreased the ultimate load will decreased, in the other hand when the concrete compressive strength (f´c) increased that will increase the ultimate load.
8. Increasing column load eccentricity to 20mm, 30mm, or 40mm decreasing the ultimate load by 69%, 82%, and 89% respectively with respect to concentrically loaded reference column.
9. The use of SFR strengthening along the whole length, half length, and third length of the hollow column will change on the imperfection factor, as the solid column.

5.2 Future research recommendation

In order to get a better understanding of the structural behavior of solid and hollow slender RC columns, the following recommendations can be made for further research:

1. In order to obtain a more accurate equation governing the relationship between imperfection factor an SFR distribution length, laboratory tests must be carried out on more specimens with finer variation in SFR distribution ratios, which enhances reducing costs when using SFR with slender RC columns.

2. When simulating SFR strengthened slender RC columns, it is necessary to obtain full detailed readings of laboratory tests for tensile and compressive strength of SFR strengthened concrete samples, in order to modify the equations of the concrete damage plasticity model, which gives a more realistic behavior of the SFR strengthened RC column.

3. Investigate the effects of fatigue and dynamic loads on solid and hollow slender RC columns.

4. Study the effect of bi-axial eccentricity load on the solid and hollow slender RC columns.

5. Other shapes and different boundary condition could be investigated.

APPENDIX: INPUT FILES FOR THE REFRENCE SOLID COLUMN SC1

The input file of the linear followed by nonlinear analysis model is presented in this appendix. Since the text of the input file was very long (136 pages), the parts including the nodes were removed.

1. Linear analyses:

```
*Heading
** Job name: Job-1 Model name: Model-1
** Generated by: Abaqus/CAE 2020
*Preprint, echo=NO, model=NO, history=NO, contact=NO
**
** PARTS
**
*Part, name=concrete
*End Part
**
*Part, name=fullsteel
*End Part
**
**
** ASSEMBLY
**
```

```
*Assembly, name=Assembly
**
*Instance, name=concrete-1, part=concrete
      30.,       2000.,          90.
      30.,       2000.,          90., 30.5773502691896, 1999.42264973081, 90.5773502691896,
120.
** Section: rebar
*Solid Section, elset=_PickedSet2_#2, material=steel
27.28,
** Section: stirrup
*Solid Section, elset=_PickedSet2_#3, material=steel
27.28,
*End Instance
**
*Node
     1,          30.,       2000.,          60.
*Node
     2,          30.,          0.,          60.
*Nset, nset=load
 1,
*Nset, nset=_PickedSet69, internal, instance=fullsteel-1, generate
   1,  916,    1
*Elset, elset=_PickedSet69, internal, instance=fullsteel-1, generate
   1,  910,    1
*Nset, nset=_PickedSet70, internal, instance=concrete-1, generate
```

1, 2828, 1

*Elset, elset=_PickedSet70, internal, instance=concrete-1, generate

1, 1800, 1

*Nset, nset=_PickedSet71, internal, instance=concrete-1

401, 402, 403, 404, 805, 806, 807, 808, 1209, 1210, 1211, 1212, 1613, 1614, 1615, 1616

2017, 2018, 2019, 2020, 2421, 2422, 2423, 2424, 2825, 2826, 2827, 2828

*Elset, elset=_PickedSet71, internal, instance=concrete-1

298, 299, 300, 598, 599, 600, 898, 899, 900, 1198, 1199, 1200, 1498, 1499, 1500, 1798

1799, 1800

*Nset, nset=_PickedSet72, internal

1,

*Nset, nset=_PickedSet73, internal, instance=concrete-1

1, 2, 3, 4, 405, 406, 407, 408, 809, 810, 811, 812, 1213, 1214, 1215, 1216

1617, 1618, 1619, 1620, 2021, 2022, 2023, 2024, 2425, 2426, 2427, 2428

*Elset, elset=_PickedSet73, internal, instance=concrete-1

1, 2, 3, 301, 302, 303, 601, 602, 603, 901, 902, 903, 1201, 1202, 1203, 1501

1502, 1503

*Nset, nset=_PickedSet74, internal

2,

*Nset, nset=_PickedSet79, internal

2,

*Nset, nset=_PickedSet80, internal

1,

*Nset, nset=_PickedSet81, internal

1,

*Surface, type=NODE, name=_PickedSet73_CNS_, internal

_PickedSet73, 1.

*Surface, type=NODE, name=_PickedSet71_CNS_, internal

_PickedSet71, 1.

** Constraint: co-bottom

*Coupling, constraint name=co-bottom, ref node=_PickedSet74, surface=_PickedSet73_CNS_

*Kinematic

** Constraint: co-top

*Coupling, constraint name=co-top, ref node=_PickedSet72, surface=_PickedSet71_CNS_

*Kinematic

** Constraint: embeded

*Embedded Element, host elset=_PickedSet70

_PickedSet69

*End Assembly

**

** MATERIALS

**

*Material, name=concrete

*Density

2.4e-09,

*Elastic

24870., 0.2

*Concrete Damaged Plasticity

35., 0.1, 1.16, 0.667, 1e-05

*Concrete Compression Hardening

10.0631, 0.

13.2336, 6.82303e-05

16.2111, 9.85072e-05

18.9307, 0.000139156

21.3352, 0.000192475

23.3814, 0.0002602

25.0439, 0.000343349

26.3168, 0.000442169

27.2118, 0.000556181

27.6113, 0.000640118

28., 0.000874148

27.3134, 0.00105176

26.3581, 0.00124017

25.2128, 0.00143622

22.1726, 0.00190846

19.0926, 0.00238231

16.2909, 0.00284496

13.8755, 0.00329208

11.8473, 0.00372363

10.1637, 0.00414133

8.77048, 0.00454735

7.61593, 0.00494377

6.65524, 0.0053324

5.85151, 0.00571472

5.17499, 0.00609192

4.38323, 0.00662376

*Concrete Tension Stiffening

2.94032, 0.

2.16471, 8.11863e-05

1.67483, 0.000150884

1.33019, 0.000214742

1.07284, 0.000275089

0.873639, 0.000333099

0.71586, 0.000389443

*Concrete Compression Damage

0., 0.

0.0370428, 6.82303e-05

0.0433707, 9.85072e-05

0.0519931, 0.000139156

0.0630646, 0.000192475

0.0766646, 0.0002602

0.0927975, 0.000343349

0.111394, 0.000442169

0.132318, 0.000556181

0.147464, 0.000640118

0.188924, 0.000874148

0.223181, 0.00105176

0.259833, 0.00124017

0.29825, 0.00143622

0.391057, 0.00190846

0.482123, 0.00238231

0.565776, 0.00284496

0.639014, 0.00329208

0.701048, 0.00372363

0.752481, 0.00414133

0.794594, 0.00454735

0.828861, 0.00494377

0.856693, 0.0053324

0.879323, 0.00571472

0.897782, 0.00609192

0.918532, 0.00662376

*Concrete Tension Damage

0., 0.

0.358827, 8.11863e-05

0.573437, 0.000150884

0.706656, 0.000214742

0.792797, 0.000275089

0.850511, 0.000333099

0.890326, 0.000389443

*Material, name=steel

*Density

7.85e-09,

*Elastic

```
200000., 0.3
*Plastic
410.,0.
**
** BOUNDARY CONDITIONS
**
** Name: bottom Type: Symmetry/Antisymmetry/Encastre
*Boundary
_PickedSet79, PINNED
** Name: top Type: Displacement/Rotation
*Boundary
_PickedSet80, 1, 1
_PickedSet80, 3, 3
_PickedSet80, 4, 4
_PickedSet80, 5, 5
** ----------------------------------------------------------------
**
** STEP: Step-1
**
*Step, name=Step-1, nlgeom=NO, perturbation
*Buckle
3, , 6, 300
**
** BOUNDARY CONDITIONS
**
```

```
** Name: bottom Type: Symmetry/Antisymmetry/Encastre
*Boundary, op=NEW, load case=1
_PickedSet79, PINNED
*Boundary, op=NEW, load case=2
_PickedSet79, PINNED
** Name: top Type: Displacement/Rotation
*Boundary, op=NEW, load case=1
_PickedSet80, 1, 1
_PickedSet80, 3, 3
_PickedSet80, 4, 4
_PickedSet80, 5, 5
*Boundary, op=NEW, load case=2
_PickedSet80, 1, 1
_PickedSet80, 3, 3
_PickedSet80, 4, 4
_PickedSet80, 5, 5
**
** LOADS
**
** Name: Load   Type: Concentrated force
*Cload
_PickedSet81, 2, -1.
**
** OUTPUT REQUESTS
**
```

```
*Restart, write, frequency=0
**
** FIELD OUTPUT: F-Output-1
**
*Output, field, variable=PRESELECT
*NODE FILE
U
*End Step
```

---

2. Nonlinear analyses:

```
*Heading
** Job name: Job-DDD-ED Model name: Model-DDD-ED
** Generated by: Abaqus/CAE 2020
*Preprint, echo=NO, model=NO, history=NO, contact=NO
**
** PARTS
**
*Part, name=concrete
*End Part
**
*Part, name=fullsteel
*End Part
**
```

```
**
** ASSEMBLY
**
*Assembly, name=Assembly
**
*Instance, name=concrete-1, part=concrete
      30.,      2000.,      90.
      30.,      2000.,      90., 30.5773502691896, 1999.42264973081, 90.5773502691896,
120.
** MATERIALS
**
*Material, name=concrete
*Density
 2.4e-09,
*Elastic
24870., 0.2
*Concrete Damaged Plasticity
35.,   0.1,  1.16, 0.667, 1e-05
*Concrete Compression Hardening
 10.0631,          0.
 13.2336, 6.82303e-05
 16.2111, 9.85072e-05
 18.9307, 0.000139156
 21.3352, 0.000192475
 23.3814,   0.0002602
```

25.0439, 0.000343349

26.3168, 0.000442169

27.2118, 0.000556181

27.6113, 0.000640118

28., 0.000874148

27.3134, 0.00105176

26.3581, 0.00124017

25.2128, 0.00143622

22.1726, 0.00190846

19.0926, 0.00238231

16.2909, 0.00284496

13.8755, 0.00329208

11.8473, 0.00372363

10.1637, 0.00414133

8.77048, 0.00454735

7.61593, 0.00494377

6.65524, 0.0053324

5.85151, 0.00571472

5.17499, 0.00609192

4.38323, 0.00662376

*Concrete Tension Stiffening

2.94032, 0.

2.16471, 8.11863e-05

1.67483, 0.000150884

1.33019, 0.000214742

1.07284, 0.000275089

0.873639, 0.000333099

0.71586, 0.000389443

*Concrete Compression Damage

0., 0.

0.0370428, 6.82303e-05

0.0433707, 9.85072e-05

0.0519931, 0.000139156

0.0630646, 0.000192475

0.0766646, 0.0002602

0.0927975, 0.000343349

0.111394, 0.000442169

0.132318, 0.000556181

0.147464, 0.000640118

0.188924, 0.000874148

0.223181, 0.00105176

0.259833, 0.00124017

0.29825, 0.00143622

0.391057, 0.00190846

0.482123, 0.00238231

0.565776, 0.00284496

0.639014, 0.00329208

0.701048, 0.00372363

0.752481, 0.00414133

0.794594, 0.00454735

```
 0.828861,  0.00494377
 0.856693,   0.0053324
 0.879323,  0.00571472
 0.897782,  0.00609192
 0.918532,  0.00662376
*Concrete Failure, TYPE=Strain
0,0.006623755,0,0.918532084
*Concrete Tension Damage
      0.,          0.
 0.358827, 8.11863e-05
 0.573437, 0.000150884
 0.706656, 0.000214742
 0.792797, 0.000275089
 0.850511, 0.000333099
 0.890326, 0.000389443
*Material, name=steel
*Density
 7.85e-09,
*Elastic
200000., 0.3
*Plastic
410.,0.
**
** BOUNDARY CONDITIONS
**
```

```
** Name: bottom Type: Symmetry/Antisymmetry/Encastre
*Boundary
_PickedSet79, PINNED
** ----------------------------------------------------------------
*IMPERFECTION, FILE=Job-1, STEP=1
1,4
**
** STEP: Step-1
**
*Step, name=Step-1, nlgeom=YES
*Dynamic, Explicit
, 1.
*Bulk Viscosity
0.06, 1.2
**
** BOUNDARY CONDITIONS
**
** Name: load Type: Displacement/Rotation
*Boundary, amplitude=Amp-1
_PickedSet80, 1, 1
_PickedSet80, 2, 2, -100.
_PickedSet80, 3, 3
**
** OUTPUT REQUESTS
**
```

*Restart, write, number interval=1, time marks=NO

**

** FIELD OUTPUT: F-Output-1

**

*Output, field, time interval=0.0025

*Node Output

A, RF, U, V

*Element Output, directions=YES

DAMAGEC, EVF, LE, PE, PEEQ, PEEQVAVG, PEVAVG, S, STATUS, SVAVG

*Contact Output

CSTRESS,

**

** HISTORY OUTPUT: H-Output-1

**

*Output, history, time interval=0.0025

*Node Output, nset=load

RF2,

*End Step

REFERENCES

1. Nikolajs Toropovs, D.B., Genadijs Shakhmenko, Aleksandrs Korjakins, Janis Justs, *Effect of Thermal Treatment on Properties of High Strength Concrete.* Latvia_CivilEngineering, 2013. **4**(1): p. 129-133.
2. Aalta. Available from: https://www.aaltadesign.com/microcementcolumns.
3. Unsplash. Available from: https://unsplash.com/photos/5Epo4Osp1ts
4. Alaa Mohammed Sahi, M.S.A.A., *Experimental Study of Hollow Slender Reinforced Concrete Columns Subjected to Eccentric Loads.* Civil and Environmental Engineering, 2021. **17**(1): p. 303-317.
5. Imad, S., Mohammed Ahmed, Jasim,Sardasht, S. Weli, *High Rise Buildings: Design, Analysis, and Safety.* International Journal of Architectural Engineering Technology, 2021. **8**: p. 1-13.
6. Vconthai. Available from: https://www.vconthai.com/products/prestressed-concrete-pile.
7. Chu-Wang, C.G.S., Jose A. Pincheira, Gustavo J. Parra-Montesinos, *Reinforced Concrete Design* 8th ed. 2018: Oxford University Press.
8. ACI, *Building Code Requirements for Structural Concrete (ACI 318-14).* 2014, American Concrete Institute
9. Eurocode2, *Design of concrete structures - Part 1-1 : General rules and rules for buildings*. 2004, CEN.
10. BS8110, *Structural use of concrete*. 1997, BSI.
11. N Vasanthapragash, T.J.J., A L D N Milinda, K L D O Liyanage, *ComparativeStudyofCodeLimitationsonSlendernessinthedesignofcolumns*, in *CECB Symposium, 2019*. 2019.
12. Dailycivil. Available from: https://dailycivil.com/types-of-columns-used-in-construction/.
13. Archiproducts. Available from: https://www.archiproducts.com/en/products/ulma-construction/circular-column-formwork-clr_303349.
14. Wang, T.L., X. Zhao, H., *Experimental study of the seismic performance of L-shaped columns with 500 MPa steel bars.* ScientificWorldJournal, 2014. **2014**: p. 105826.

15. An, J., *Study on Optimization Design of Reinforced Concrete Special-shaped Column Frame Structure.* Chemecal Engineering Transactions 2017. **62**: p. 1075-1080.
16. Liu, J., H. Song, and Y. Yang, *Research on mechanical behavior of L-shaped multi-cell concrete-filled steel tubular stub columns under axial compression.* Advances in Structural Engineering, 2018. **22**(2): p. 427-443.
17. Ferguson, P.M., *Reinforced Concrete Fndamentals*. 2nd ed. 1965: John Wiley & Sons, Inc. 718.
18. Pinterest. Available from: https://in.pinterest.com/pin/types-of-columns-used-in-building-structutres-daily-civil--351351208435059595/.
19. M. Nadim Hassoun, A.A.-M., *Structural Concrete*. 7th ed. 2020: John Wiley & Sons, Inc.
20. Civiltoday. Available from: https://civiltoday.com/construction/building/384-what-is-column-types-of-columns.
21. Preetha.V, K.K., Navaneetha.S, Senthilkumar.V, *Buckling Analysis of Columns.* IOSR Journal of Engineering, 2019: p. 10-17.
22. López, O.A.H., Julio J. Del Re, Gianina Puig, José Espinosa, Luis, *Reducing Seismic Risk of School Buildings in Venezuela.* Earthquake Spectra, 2007. **23**(4): p. 771-790.
23. Macgregor, J.G., *Reinforced Concrete Mechanics and Design*. 3rd ed. 1997: Prentice-Hall, Inc.
24. Haroun, M.A.E., Hussein M., *Behavior of Cyclically Loaded Squat Reinforced Concrete Bridge Columns Upgraded with Advanced Composite-Material Jackets.* Journal of Bridge Engineering, 2005. **10**(6): p. 741-748.
25. Bkumarauthor. Available from: https://bkumarauthor.wordpress.com/2018/05/27/types-of-structural-failure-in-civil-engineering/.
26. Ardexendura. Available from: https://www.ardexendura.com/repair-maintenance-of-concrete-structures/.
27. Civil4m. Available from: https://civil4m.com/threads/what-type-of-failure-occurred-in-this-column.7482/.
28. Singh, H., *Steel Fiber Reinforced Concrete*. 2017: Springer Science+Business Media Singapore.
29. Waleed Tameemi, R.L., *CORRELATIONS BETWEEN COMPRESSIVE, FLEXURAL, AND TENSILE BEHAVIOR OF SELF-CONSOLIDATING FIBER REINFORCED CONCRETE*. 2015, THE UNIVERSITY OF KANSAS CENTER FOR RESEARCH, INC.: LAWRENCE, KANSAS.
30. Shahad S. Khamees, M.M.K., Nameer A. Alwash, *Effects of Steel Fibers Geometry on the Mechanical Properties of SIFCON Concrete.* Civil Engineering Journal, 2020. **6**(1): p. 21-33.

31. ABAQUS-GetStarted, *ABAQUS 6.14 Getting Started with Abaqus*. 2014, Dassault Systèmes.
32. Chris V. Nielsen, P.A.F.M., *Metal Forming*. 2021. 412.
33. Midasoft. Available from: https://www.midasoft.com/bridge-library/geometric-nonlinearity-explained.
34. Hu, Y., et al., *Multi-Scale Modelling of Flexible End Plate Connections under Fire Conditions~!2009-10-07~!2010-01-21~!2010-04-29~!* The Open Construction and Building Technology Journal, 2010. **4**(2): p. 88-104.
35. Mustafa Mahamid, E.H.G., Charles N. Gaylord, *Structural Engineering Handbook*. 5th ed. 2020: McGraw Hill.
36. Robert D. Cook, D.S.M., Michael E. Plesha, *Concepts and Applications of Finite Element Analysis* 3rd ed. 1989: John Wiley & Sons.
37. Yosef, N., *Second-order FE Analysis of Axial Loaded Concrete Members According to Eurocode 2*, in *Department of Civil Achitectural Engineering* 2015, Royal Institute of Technology (KTH).
38. Lotfy, E.M., *NUMERICAL STUDY OF LONG COLUMNS STRENGTHENED BY FIBER REINFORCED POLYMER (FRP).* INTERNATIONAL JOURNAL OF ENGINEERING SCIENCES & RESEARCH TECHNOLOGY, 2018. **7**(5): p. 257-271.
39. Yonas T.Y., T.W., Senshaw F.W., *Finite Element Analysis of Slender Composite Column Subjected to Eccentric Loading.* International Journal of Applied Engineering Research, 2018. **13**(15): p. 11730-11737.
40. Safaa Qays A., A.H.A.-Z., *A Comparative Study of the Performance of Slender Reinforced Concrete Columns with Different Cross-Sectional Shapes.* Fibers, 2020. **8**(6).
41. Alireza Bahrami, A.M.K., *Load Capacity and Failure Modes of Axially and Eccentrically Loaded Thin-Walled Steel Tubular Slender Columns Filled with Concrete.* International Journal on Emerging Technologies, 2020. **11**(5): p. 517-524.
42. S. Boukais, A.N., N. Khelil, A. Kezmane, *Numerical Investigation of the Jacketing Method of Reinforced Concrete Column.* International Journal of Civil and Architectural Engineering, 2020. **14**(1): p. 26-29.
43. Kotes P., V., M., Jost J., Prokop J., *Strengthening of Concrete Column by Using the Wrapper Layer of Fibre Reinforced Concrete.* Materials (Basel), 2020. **13**(23).
44. Mohammed Al-Helfi, A.A., *Experimental Work to Study the Strengthening Effect of SFR and CFRP on a Part or Whole of the Length of Slender RC Columns.* Civil and Environmental Engineering, 2021. **17**(1): p. 9-22.

45. Ihsan A. S. Al- Shaarbaf, M.J.H., Emad A. Abood Al- Zaidy, *Nonlinear analysis of hollow slender reinforced concrete columns under eccentric loading*. University of Thi-Qar Journal, 2018. **13**(4): p. 109-129.
46. Pingkan Nuryanti, D.S., Bambang Suhendro, *NON-LINEAR ANALYSIS OF HOLLOW REINFORCED CONCRETE COLUMN QUARE CROSS-SECTION WITH VARIOUS LOAD ECCENTRICITY AND CONCRETE STRENGTH*. Langkau Betang, 2018. **5**(1): p. 33-44.
47. Shahad S. Khamees, M.M.K., Nameer A. Alwash, *Experimental and numerical investigation on the axial behavior of solid and hollow SIFCON columns.* SN Applied Sciences, 2020. **2**(6).
48. K. Buka-Vaivade, D.S., J. Sliseris, L. Pakrastins, N. Vatin, *Ultimate load capacity of high-performance fibre-concrete hollow square columns*, in *Magazine of Civil Engineering*. 2021.
49. Al-Maliki, H.N.G., *Nonlinear Simulation Analysis of Tapered Reinforced Concrete Column (Solid and Hollow) Behavior under Axial Load.* International Journal of GEOMATE, 2021. **21**(86).
50. Boulbes, R.J., *Troubleshooting Finite-Element Modeling with Abaqus*. 2020: Springer Nature Switzerland AG.
51. Akin, J.E., *Finite Element Analysis Concepts via Solid Works*. 2009: World Scientific.
52. Khennane, A., *Introduction to Finite Element Analysis Using MATLAB and Abaqus*. 2013: Taylor & Francis Group.
53. Johnson, S., *Comparison of Nonlinear Finite Element Modeling Tools for Structural Concrete*. 2006, University of Illinois
54. Farzad Hejazi, H.M.E., *Solving Complex Problems for Structures and Bridges using ABAQUS Finite Element Package*. 2021: Taylor & Francis Group, LLC.
55. Chai Hong Yoo, S.L., *Stability of Structures*. 2011: Elsevier Inc.
56. Barbero, E.J., *Finite Element Analysis of Composite Materials Using Abaqus*. 2013: Taylor & Francis Group, LLC.
57. Björnsson, T., *Structural ananalysis of columns with initial imperfections*, in *Faculty of Civil and Environmental Engineering*. 2017, University of Iceland: Iceland.
58. J. N. S. Suryanarayana Raju, M.V.R., G. Sabarish,P. Venkateswara Rao, *Effect of Imperfections on Stability of Column and Frame.* International Journal of Engineering Research & Technology, 2016. **5**(11): p. 378-381.
59. Wai-Fah Chen, T.A., *Theory of Beam-Columns*. Vol. 1. 2007: J.Ross Publishing.
60. Waseem Abdelazim, H.M.M., Brahim Benmokrane, *Inelastic Second-Order Analysis for Slender GFRP-Reinforced Concrete Columns: Experimental*

Investigations and Theoretical Study. Journal of Composites for Construction, 2020. **24**(3).
61. Steelconstruction. Available from: https://www.steelconstruction.info/Allowing_for_the_effects_of_deformed_frame_geometry.
62. Ellobody, E., *Finite Element Analysis and Design of Steel and Steel-Concrete Composite Bridges*. 2014: Elsevier Inc.
63. ACI-117, *Specification for Tolerances for Concrete Construction and Materials*. 2015, American Concrete Institute
64. ABAQUS-Materials, *ABAQUS 6.14 Analysis User's Guide Volume III: Materials*. 2014, Dassault Systèmes.
65. GÜNTER HOFSTETTER, G.M., *NUMERICAL MODELING OF CONCRETE CRACKING*. 2011: CISM, Udine.
66. T. Yu, J.G.T., Y. L. Wong, S. L. Dong, *Finite element modeling of confined concrete-II: Plastic-damage model*. Engineering Structures, 2010. **32**(3): p. 680-691.
67. B. Alfarah, F.L.-A., S. Oller, *New methodology for calculating damage variables evolution in Plastic Damage Model for RC structures*. Engineering Structures, 2017. **132**: p. 70-86.
68. S.V.Chaudhari, M.A.C., *Modeling of concrete for nonlinear analysis Using Finite Element Code ABAQUS*. International Journal of Computer Applications, 2012. **44**(7): p. 14-18.
69. FATTAH, A.M.A.E., *BEHAVIOR OF CONCRETE COLUMNS UNDER VARIOUS CONFINEMENT EFFECTS*, in *Department of Civil Engineering*. 2012, Kansas State University.
70. Chi, Y., et al., *Finite element modeling of steel-polypropylene hybrid fiber reinforced concrete using modified concrete damaged plasticity*. Engineering Structures, 2017. **148**: p. 23-35.
71. ABAQUS-Theory, *ABAQUS Theory Manual*. 2014, Dassault Systèmes.
72. ABAQUS-Analysis, *ABAQUS Analysis User Guide*. 2014, Dassault Systèmes.
73. K. E. Caballero-Morrison, J.L.B., Juan Navarro-Gregori, J. R. Martí-Vargas,, *Behaviour of steel-fibre-reinforced normal-strength concrete slender columns under cyclic loading*. Engineering Structures, 2012. **39**: p. 162-175.

الملخص

العمود هو أحد المكونات الهيكلية الأساسية في المبنى. أصبح استخدام الأعمدة النحيفة أكثر انتشارًا نتيجة للاهتمام المتزايد باستغلال الفضاء و المتطلبات المعمارية. الهدف من هذه الدراسة هو التحليل اللاخطي لسلوك الأعمدة الخرسانة المسلحة النحيفة المصمتة والمجوفة المعززة بالياف الحديد و المعرضة لاحمال مركزية و لا مركزية ضمن معايير مختلفة. الأعمدة المصمتة كانت بأبعاد (120 × 60 × 2000) ملم تم تحميلها وتقويتها باستخدام الياف الحديد لكل العمود و نصف طول العمود و ايضا ثلث طول العمود في المنتصف بالإضافة إلى العمود المرجعي غير المكون من الخرسانة العادية ، اما الأعمدة المجوفة فكانت بأبعاد (140× 80× 2000) ملم محملة بشكل مركزي وغير مركزي و بأشكال فتحات مختلفة.

تم إجراء هذا العمل على تسع عينات تم اختبارها تجريبياً (أربعة أعمدة مصمتة ، وخمسة أعمدة مجوفة) باستخدام برنامج ABAQUS 2020 لتحليل العناصر المحددة ثلاثية الأبعاد. تظهر النتائج التي تم الحصول عليها بوضوح أن العمود النحيف الذي تمت محاكاته باستخدام برنامج ABAQUS دون تحديد قيمة اللامثالية لبيانات النمذجة سيُظهر مقاومة تحميل أكبر من نتيجة الفحص المختبري و يكون نمط الفشل مشابها لنمط فشل الاعمدة القصيرة، لذا فالعمود يعتبرعمود مثالي ، وهو غير موجود في الواقع. وفقًا للكود الاوربي، تعتمد قيمة هذه اللامثالية على طول الأعمدة ، والطول الثابت يعني قيمة ثابتة، لكن هذا البحث أظهر أن استخدام الياف

الحديد سيغير هذه القيمة على الرغم من أن طول الأعمدة ثابت. أيضًا ، من هذه النتائج ، يمكن اقتراح معادلة لتمثيل العلاقة بين عامل اللامثالية والتغيير في توزيع الياف الحديد.

كما تم تقييم بعض المعايير المهمة ، مثل نسبة النحافة ، وقوة انضغاط الخرسانة ، وأشكال مقطع العمود، وتوزيع الياف الحديد، باستخدام نماذج تمت محاكاتها في البرنامج.

تبين من النتائج التي تم الحصول عليها من الاعمدة المصمتة أن تقليل طول الأعمدة بنسبة 25٪ سيقلل من نسبة النحافة ويؤدي إلى زيادة الحمل النهائي بنسبة 7٪ ، ومن ناحية أخرى ، فإن الزيادة في طول الأعمدة بنسبة 25٪ و 50٪ سيؤدي إلى زيادة نسبة النحافة وخفض الحمل النهائي بنسبة 5٪ و 7٪ على التوالي. عندما تصل قوة انضغاط الخرسانية للعمود إلى 25 ميجا باسكال ، فإن الحمل النهائي سينخفض بنسبة 12٪ ، ومن ناحية أخرى عندما تزداد قوة انضغاط الخرسانة إلى 32 ميجا باسكال سيزداد الحمل النهائي بنسبة 5٪ ، وأيضًا عندما تزداد قوة انضغاط الخرسانة إلى 36 ميجا باسكال سيؤدي ذلك إلى زيادة الحمل النهائي بنسبة 26٪. زادت قيمة الحمل النهائي للاعمدة ذات المقاطع المربعة والدائرية بنسبة 5٪ و 2٪ على التوالي ، بينما انخفضت قيمة الحمل النهائي للعمود ذي المقطع البيضوي بنسبة 6٪. عند تعرض العمود الى حمل لا مركزي يبعد عن محور العمود بمقدار 20 ملم ، 30 ملم ، و 40 ملم فان الحمل النهائي سيقل بنسبة 69٪ ، 82٪ ، 89٪ على التوالي.

من ناحية أخرى ، أظهرت النتائج التي تم الحصول عليها للعمود المجوف أن تقليل طول الأعمدة بنسبة 25٪ سيقلل من نسبة النحافة ويؤدي إلى زيادة الحمل النهائي بنسبة 9٪ ، بينما تؤدي الزيادة

في طول الأعمدة بنسبة 25٪ و 50٪ إلى زيادة نسبة النحافة مما يؤدي إلى تقليل الحمل النهائي بنسبة 6٪ و 10٪ على التوالي. عندما تصل قوة الضغط الخرسانية للعمود إلى 25 ميجا باسكال ، فإن الحمل النهائي سينخفض بنسبة 21٪ ، بينما عندما تزداد قوة ضغط الخرسانة إلى 40 ميجا باسكال و 45 ميجا باسكال ، فإن ذلك سيزيد من الحمل النهائي بنسبة 9٪ و 20٪ على التوالي. زادت قيمة الحمل النهائي للاعمدة ذات المقاطع المربعة والدائرية بنسبة 12٪ ، بينما انخفضت قيمة الحمل النهائي للعمود ذي المقطع البيضوي بنسبة 1٪. ادى استخدام الياف الحديد لتقوية طول الأعمدة بالكامل أو النصف أو الثلث إلى زيادة الحمل النهائي بنسبة 20٪ و 30٪ و 12٪

جمورية العراق
وزارة التعليم العالي و البحث العلمي
كلية الهندسة / جامعة ميسان
قسم الهندسة المدنية

تحليل لا خطي لاعمدة خرسانية نحيفة ذات مقاطع مصمتة و مجوفة معززة بالياف الحديد معرضة لاحمال مركزية او لا مركزية

اطروحة

مقدمة الى كلية الهندسة / جامعة ميسان كجزء من متطلبات الحصول على درجة الماجستير في علوم الهندسة المدنية / الانشاءات

من قبل

ومیض عیسى بریدي

بكالوريوس هندسة مدنية 2009

باشراف

ا. د محمد صالح عبد علي

تشرين اول 2022